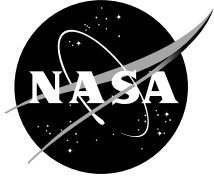


NASA/TM—2002-210006



The First SIMBIOS Radiometric Intercomparison (SIMRIC-1), April–September 2001

*G. Meister, P. Abel, R. Barnes, J. Cooper, C. Davis, M. Godin, D. Goebel, G. Fargion, R. Frouin,
D. Korwan, R. Maffione, C. McClain, S. McLean, D. Menzies, A. Poteau, J. Robertson, and J. Sherman*

National Aeronautics and
Space Administration

Goddard Space Flight Center
Greenbelt, Maryland 20771

The NASA STI Program Office ... in Profile

Since its founding, NASA has been dedicated to the advancement of aeronautics and space science. The NASA Scientific and Technical Information (STI) Program Office plays a key part in helping NASA maintain this important role.

The NASA STI Program Office is operated by Langley Research Center, the lead center for NASA's scientific and technical information. The NASA STI Program Office provides access to the NASA STI Database, the largest collection of aeronautical and space science STI in the world. The Program Office is also NASA's institutional mechanism for disseminating the results of its research and development activities. These results are published by NASA in the NASA STI Report Series, which includes the following report types:

- **TECHNICAL PUBLICATION.** Reports of completed research or a major significant phase of research that present the results of NASA programs and include extensive data or theoretical analysis. Includes compilations of significant scientific and technical data and information deemed to be of continuing reference value. NASA's counterpart of peer-reviewed formal professional papers but has less stringent limitations on manuscript length and extent of graphic presentations.
- **TECHNICAL MEMORANDUM.** Scientific and technical findings that are preliminary or of specialized interest, e.g., quick release reports, working papers, and bibliographies that contain minimal annotation. Does not contain extensive analysis.
- **CONTRACTOR REPORT.** Scientific and technical findings by NASA-sponsored contractors and grantees.
- **CONFERENCE PUBLICATION.** Collected papers from scientific and technical conferences, symposia, seminars, or other meetings sponsored or cosponsored by NASA.
- **SPECIAL PUBLICATION.** Scientific, technical, or historical information from NASA programs, projects, and mission, often concerned with subjects having substantial public interest.
- **TECHNICAL TRANSLATION.** English-language translations of foreign scientific and technical material pertinent to NASA's mission.

Specialized services that complement the STI Program Office's diverse offerings include creating custom thesauri, building customized databases, organizing and publishing research results . . . even providing videos.

For more information about the NASA STI Program Office, see the following:

- Access the NASA STI Program Home Page at <http://www.sti.nasa.gov/STI-homepage.html>
- E-mail your question via the Internet to help@sti.nasa.gov
- Fax your question to the NASA Access Help Desk at (301) 621-0134
- Telephone the NASA Access Help Desk at (301) 621-0390
- Write to:
NASA Access Help Desk
NASA Center for AeroSpace Information
7121 Standard Drive
Hanover, MD 21076-1320



The First SIMBIOS Radiometric Intercomparison (SIMRIC-1), April–September 2001

Gerhard Meister, SIMBIOS Project, Futuretech Corp., Greenbelt, Maryland

Peter Abel and Charles McClain, Goddard Space Flight Center, Greenbelt, Maryland

*Robert Barnes and Giulietta Fargion, SIMBIOS Project, Science Applications International Corp.,
Greenbelt, Maryland*

John Cooper, Raytheon Information Technology and Science Services, Lanham, Maryland

Curtiss Davis and Daniel Korwan, Naval Research Laboratory, Washington, D.C.

Mike Godin and Robert Maffione, HOBI Labs, Watsonville, California

David Goebel and James Robertson, Biospherical Instruments Inc., San Diego, California

*Robert Frouin and Antoine Poteau, Scripps Institution of Oceanography, University of California,
San Diego, California*

Scott McLean and Jennifer Sherman, Satlantic Inc., Halifax, Canada

*David Menzies, Institute for Computational Earth System Science, University of California,
Santa Barbara, California*

National Aeronautics and
Space Administration

Goddard Space Flight Center
Greenbelt, Maryland 20771

Available from:

NASA Center for AeroSpace Information
7121 Standard Drive
Hanover, MD 21076-1320
Price Code: A17

National Technical Information Service
5285 Port Royal Road
Springfield, VA 22161
Price Code: A10

Abstract

This report describes the first SIMBIOS (Sensor Intercomparison and Merger for Biological and Interdisciplinary Oceanic Studies) Radiometric Intercomparison (SIMRIC-1). The purpose of the SIMRIC-1 is to ensure a common radiometric scale among the calibration facilities that are engaged in calibrating *in-situ* radiometers used for ocean color related research and to document the calibration procedures and protocols. SIMBIOS staff visited the seven participating laboratories for at least two days each. The SeaWiFS Transfer Radiometer SXR-II measured the calibration radiances produced in the laboratories. The measured radiances were compared with the radiances expected by the laboratories. Typically, the measured radiances were higher than the expected radiances by 0 to 2 %. This level of agreement is satisfactory. Several issues were identified, where the calibration protocols need to be improved, especially the reflectance calibration of the reference plaques and the distance correction when using the irradiance standards at distances greater than 50 cm. The responsivity of the SXR-II changed between 0.3 % (channel 6) and 1.6 % (channel 2) from December 2000 to December 2001. Monitoring the SXR-II with a portable light source showed a linear drift of the calibration, except for channel 1, where a 2 % drop occurred in summer.

Contents

1	Introduction	1
2	SIMBIOS Devices used During SIMRIC-1	3
2.1	SXR-II	3
2.2	SQM-II	4
2.3	Stability monitoring	7
2.3.1	Method	7
2.3.2	Results	10
2.4	FEL Lamp F-474	11
3	Documentation of Calibration Techniques	16
3.1	Introduction	16
3.2	Laboratories	16
3.2.1	NRL	16
3.2.2	Scripps	19
3.2.3	Biospherical	20
3.2.4	UCSB	21
3.2.5	HOBI Labs	23
3.2.6	NASA GSFC Code 920.1	24
3.2.7	Satlantic	26
3.3	SXR-II Specific Procedures	27
4	Results	28
4.1	Reproducibility	28
4.2	Radiance Calculation	29
4.3	Radiance Comparisons	29
4.3.1	Overall Comparison	29
4.3.2	NRL	31
4.3.3	Scripps	31
4.3.4	Biospherical	35
4.3.5	UCSB	35
4.3.6	HOBI Labs	35
4.3.7	NASA Code 920.1	38
4.3.8	Satlantic	40
4.3.9	SIMBIOS FEL	41
4.4	Transfer from Primary to Secondary Standard	43
4.5	Irradiance Interpolation	43
4.6	BRF of Spectralon	44
4.7	Effective Distance Correction	47
5	Conclusions	50
A	SXR-II FOV and SQM-II Footprint	52

Chapter 1

Introduction

Optical remote sensing of the earth has become an important data source for various science fields, from biology, geography, and geology to meteorology, oceanography and climate research. Especially for climate studies, it is important to obtain global data sets that cover large time periods of 10 years or more. The only technique to obtain global data sets is satellite data. Unfortunately, satellite life spans are usually on the order of five years or less. For surfaces covered by land, the longest time series available so far is the NOAA (National Oceanic and Atmospheric Administration) AVHRR (Advanced Very High Resolution Radiometer) time series [DAAC, 2001], which combines the data from four satellites into a continuous dataset covering twenty years from 1981 to 2001. No comparable dataset is available for oceans.

The Sensor Intercomparison and Merger for Biological and Interdisciplinary Oceanic Studies (SIMBIOS) Project has a worldwide, ongoing ocean color data collection program, plus an operational data processing and analysis capability. The SIMBIOS Program goal is to assist the international ocean color community in developing a multi-year time-series of calibrated radiances which transcends the spatial and temporal boundaries of individual missions [Barnes et al., 2001].

The specific objectives of the SIMBIOS Program are: (1) to quantify the relative accuracies of the ocean color products from each mission, (2) to work with each project to improve the level of confidence and compatibility among the products, and (3) to develop methodologies for generating merged level-3 products. SIMBIOS has identified the primary instruments to be used for developing global data sets. These instruments are Sea-viewing Wide Field-of-view Sensor (SeaWiFS), Ocean Color and Temperature Scanner (OCTS), Polarization and Directionality of the Earth's Reflectances (POLDER) on ADEOS-I and on ADEOS-II, Moderate Resolution Imaging Spectrometer (MODIS) on Aqua and Terra, MISR (on Terra), Medium Resolution Imaging Spectrometer (MERIS), and Global Imager (GLI). The products from other missions (e.g., Ocean Color Imager (OCI) and the two Modular Optoelectronic Scanner (MOS) instruments) will be tracked and evaluated, but are not considered as key data sources for a combined global data set.

The SIMBIOS Program consists of the SIMBIOS Science Team and the SIMBIOS Project Office [McClain and Fargion, 1999a], [McClain and Fargion, 1999b], [Fargion and McClain, 2001], [Fargion and McClain, 2002]. SIMBIOS Science Team Principal Investigators are primarily composed of persons selected under the SIMBIOS NASA Research Announcement (NRA) 1996 (i.e., SIMBIOS Team 1997-1999) and NRA 1999 (i.e., SIMBIOS Team 2000-2003). The present Science Team is grouped under three working areas: 1) Ocean Bio-optical and Sensor Characterization Studies, 2) Data Merger Studies, and 3) Atmospheric Correction Studies. In addition, there are many more US and international co-investigators and collaborators actively participating in the SIMBIOS Program. The SIMBIOS Project incorporates aspects of instrument calibration, algorithm development and evaluation, product merging, data processing, and interagency and international coordination, see <http://simbios.gsfc.nasa.gov> for more information.

To measure ocean color from space is a very difficult task. Only about 10 % of the signal arriving at a space-based sensor originates from the ocean, about 90 % of the signal comes from the atmosphere. An error in the determination of the atmospheric contribution of only 1 % (relative to the atmospheric signal) will lead to an error in the signal from the ocean of 9 % (relative to the ocean signal). Thus in many cases (e.g. SeaWiFS and MODIS [Barnes et al., 1998]) the satellite sensor is calibrated vicariously with *in-situ* data. In the case of SeaWiFS and MODIS, a buoy called MOBY (Marine Optical Buoy,[Clark et al., 2002]) located in the vicinity of Hawaii is used.

The quality of the calibrated satellite data can be checked with match-up analyses from *in-situ* ocean color measurements taken during ship cruises. The SeaWiFS and the SIMBIOS Project jointly maintain a database called SeaBASS (SeaWiFS Bio-optical Archive and Storage System, [Werdell et al., 2000], <http://seabass.gsfc.nasa.gov>) that contains *in-situ* data from more than 600 cruises from all over the world. The quality of this database is obviously directly related to the quality and comparability of the stored *in-situ* data. Two kinds of activities are performed by the SIMBIOS program to ensure an adequate quality of the SeaBASS database: First, measurement protocols are developed [Mueller and Fargion, 2002a], [Mueller and Fargion, 2002b] and their usage by the science community is encouraged. Second, calibration round-robin intercomparison experiments are conducted by the SIMBIOS Project. The participating laboratories include academic institutions, government agencies and instrument manufacturers that either directly or indirectly contribute to SeaBASS. The purpose of these round-robins is to

1. verify that all laboratories are on the same radiometric scale
2. detect and correct problems at any individual laboratory in a timely fashion
3. encourage the common use of calibration protocols
4. identify areas where the calibration protocols need to be improved
5. document the calibration procedures specific to each laboratory.

This report documents the results from the first SIMBIOS round-robin, the SIMRIC-1. The SIMRIC series was started by the SIMBIOS Project as a successor to the SIRREX (SeaWiFS Intercalibration Round-Robin Experiment) series. The SeaWiFS project initiated the SIRREX series in 1992. So far seven documents have been published as a result of this series ([Mueller, 1992], [Mueller et al., 1993], [Mueller et al., 1996], [Johnson et al., 1996], [Johnson et al., 1999], [Riley and Bailey, 1998]), [Hooker et al., 2002], in which calibration protocols were defined, enhanced and demonstrated to the community. They also include intercalibration experiments. The National Institute of Standards and Technology (NIST) took a leading role in SIRREX-4 and SIRREX-5. For the SIRREX-1 to SIRREX-5, the participants gathered at a single location to conduct the experiments. The objective of SIRREX-7 was to determine the uncertainties of radiometric calibrations at Satlantic, Inc.

SIRREX-6 was a joint venture of the SeaWiFS and the SIMBIOS projects, during which 10 laboratories were visited by NASA personnel, who carried 2 radiance and 2 irradiance radiometers and had them calibrated at each laboratory. The calibration coefficients were compared, and it was found that the average agreement was about $\pm 2\%$, but there were some outliers up to 8 %.

For the SIMRIC-1, SIMBIOS staff visited 7 laboratories (Naval Research Laboratories, Washington, DC; Scripps Institute of Oceanography, University of California, San Diego; Biospherical Instruments Inc., CA; ICESS at the University of California, Santa Barbara; HOBI Labs, CA; NASA Code 920.1, GSFC, MD; Satlantic Inc., Canada), see appendix, section B, for contact persons and affiliations) with a radiometer designed and calibrated by NIST, the SeaWiFS Transfer Radiometer II (SXR-II). The radiometric stability of the SXR-II was monitored by a portable light source, the SeaWiFS Quality Monitor II (SQM-II). The radiances produced by the laboratories for calibration were measured in the six SXR-II channels from 411 nm to 777 nm and compared to the radiances expected by the laboratories. This report documents the various calibration procedures in the laboratories, evaluates the comparison results, and discusses areas where the calibration protocols should be improved. Furthermore, several characteristics of the SXR-II and the SQM-II are described, in particular the radiometric stability and the field of view of the SXR-II, and the stability of the light output and the stability of the internal detector of the SQM-II.

The structure of this document is as follows: chapter 2 introduces the SIMBIOS equipment used for this study. The focus of this chapter is the radiometric stability of the SXR-II and the SQM-II. Some of their characteristics such as the field of view and the lamp footprint are described in the appendix, section A. The calibration facilities and procedures are described in chapter 3, as well as the SXR-II specific measurement procedures. The comparison results are described in chapter 4. Chapter 4 also contains sections on the reproducibility of measurements, the quality of the calibration transfers from primary to secondary standards, the wavelength interpolation for the FEL irradiance, the reflectance factors of the reference plaques, and the problems encountered when using an FEL at distances greater than the standard calibration distance of 50 cm. A discussion of the results of the SIMRIC-1 can be found in chapter 5. A list of the participants and their addresses is given in the appendix, section B.

Chapter 2

SIMBIOS Devices used During SIMRIC-1

2.1 SXR-II

The SXR-II is a portable transfer radiometer with 6 wavelength channels. It has been designed by the Optical Technology Division at the NIST. It was built by Reyer Corp., New Market, MD. Its primary purpose is to measure radiances produced by calibration light sources in laboratories in order to assess the calibration accuracy of the respective laboratory.

The SXR-II (S/N 104) is a clone of the SXR (SeaWiFS Transfer Radiometer), which is described in great detail in [Johnson et al., 1998a], thus here we present only a short overview. Two further clones have been built, the VXR [Johnson et al., 2000] and the LXR [Markham et al., 1998]. All 4 instruments share a common design but measure at different wavelengths. A key feature of the design is the temperature stabilization at 26° C of the Hamamatsu silicon detectors, the wavelength filters from Barr Associates and the precision field stop aperture. Filters produced with ion-assisted beam deposition determine the wavelengths of the individual channels. Each channel has a separate silicon photodiode. The output of the photodiodes is converted to a voltage by a transimpedance amplifier and then read from an external voltmeter, a Fluke 8842A in the case of the SXR-II. If desired, an amplifier inside the SXR-II can be used to increase the signals by factors of 10, 100 or 1000. The selection of channels and gains is controlled via a GPIB interface from a PC. The voltmeter is read through the same interface. The SXR-II can also be operated in manual mode by two switches on the back of the instrument for the channel and the gain setting. An eyepiece allows the operator to look at the FOV of the SXR-II, which is convenient for exact positioning. The SXR-II is shown in several photographs in chapter 3, see e.g. Fig. 3.2 on page 18.

The SXR-II was calibrated in December 2000 at the Optical Technology Division at the NIST, Gaithersburg, MD at the SIRCUS (Spectral Irradiance and Radiance Calibration with Uniform Sources) facility [Brown et al., 2000]. A second calibration at SIRCUS was done in December 2001. The calibration factors are given in Table 2.1. No calibration report was delivered by NIST until early February 2002 for either calibration. A preliminary estimation of the uncertainties is given in Table 2.2. Some estimates were copied from the uncertainties for the original SXR [Johnson et al., 1998a]. We expect to be able to give a better estimate of the uncertainties once the calibration reports are available. For the moment, the combined uncertainty for the SXR-II is estimated to be 0.8 % ($k=1$) by taking the root of the sum of the squares of the contributions listed in Table 2.2 (law of error propagation). It is possible that for channels 1 and 6 this estimate will increase when more data characterizing the SXR-II has been analyzed.

The changes in calibration coefficients for the two SXR-II calibrations on SIRCUS are quite significant, up to 1.6 %, see Table 2.1. To calculate the calibration coefficients at a certain date between these two calibrations, the calibration coefficients are linearly interpolated in time between the December 2000 and the December 2001 calibrations. The error associated with this procedure (u_d) is about 0.5 % (see section 2.3 below).

Although we use the same terminology for the uncertainty contributions as in [Johnson et al., 1998a], the nature of these contributions is different for the size-of-source effect (u_a) and the long-term drift (u_d): u_a is the uncertainty associated with the on-axis cavity measurement (see section 3.3), and u_d is the uncertainty after the linear

	Channel 1	Channel 2	Channel 3	Channel 4	Channel 5	Channel 6
λ_m [nm]	410.69	441.51	487.58	546.89	661.91	776.71
$\langle D_{cs}^{2000} \rangle$	0.65567	0.92652	0.11758	0.20222	0.17658	0.017717
$\langle D_{cs}^{2001} \rangle$	0.65847	0.94104	0.11864	0.20502	0.17827	0.017769
$\Delta \langle D \rangle (2001 - 2000)$ [%]	0.4	1.6	0.9	1.4	1.0	0.3
L_s	16.6	11.8	92.7	53.9	61.7	615.2

Table 2.1: SXR-II calibration coefficients $\langle D_{cs} \rangle$ [$V \text{ cm}^2 \text{sr nm}/\mu\text{W}$] for gain 1 on the SXR-II amplifier (multiplied by -1, the radiometer provides negative voltages) and moment wavelengths λ_m for the 6 SXR-II channels. The coefficients from December 2000 $\langle D_{cs}^{2000} \rangle$ were provided in an email by B.C. Johnson on 9/6/01 (rounded off) and are final. The coefficients from December 2001 $\langle D_{cs}^{2001} \rangle$ were provided in an email by B.C. Johnson on 1/9/02 and are preliminary (expected change is less than 0.1 %). The difference Δ in the coefficients between the two dates is calculated as $\langle D_{cs}^{2001} \rangle$ minus $\langle D_{cs}^{2000} \rangle$ and given in %. The saturation radiances $L_s[\mu\text{W}/(\text{cm}^2 \text{sr nm})]$ in the bottom line are conservative estimates.

u_D [%]	u_d [%]	u_{flux} [%]	u_{rep} [%]	u_a [%]	u_{setup} [%]	u_c [%]
0.5	0.5	0.1	0.1	0.2	0.3	0.8

Table 2.2: Preliminary uncertainty estimates for the SXR-II. The uncertainties u_D , u_d , u_{flux} , u_{rep} , u_a , relate to the calibration coefficient D , the drift of the calibration coefficient, the nonlinearity, the repeatability, the size-of-source effect, respectively (see [Johnson et al., 1998a] for a description of these errors in the original SXR). The statistical error from averaging over several scans/samples and the error produced by the amplifier for different gains are negligible (< 0.1%). u_{setup} is the uncertainty from aligning the SXR-II. u_c is the combined uncertainty.

interpolation in time of the calibration coefficients.

Fig. 2.1 shows the responsivity of the SXR-II channels as a function of wavelength. Note that for most channels the ‘tails’ drop below 10^{-6} , thus they meet the recommendations by [Mueller, 2000].

The SXR-II was designed for typical light levels in oceanography, which are relatively low compared to most calibration standards. Therefore, the responsivity of the SXR-II is quite high, which results in relatively low saturation values. Estimates of the saturation values for the 6 channels are also given in Table 2.1. Comparing calibration coefficients of the original SXR from [Johnson et al., 1998a] and the calibration coefficients of Table 2.1, the SXR-II is between 15 % (channel 4) and 55 % (channel 3) more responsive than the original SXR.

2.2 SQM-II

The SQM-II (SeaWiFS Quality Monitor, S/N 006) is a portable stable light source for monitoring the radiometric stability of oceanographic radiometers. The original SQM has been designed by NASA and NIST, see [Johnson et al., 1998b] for a detailed description.

The SQM-II has two sets of 8 bulbs each. There is no individual bulb control, a set is either completely turned on or off. The light output of the second set is about 3 times brighter than the light output of the first set, see Fig. 2.2 for a spectral plot. In the following, we will refer to these sets as LoBank and HiBank. Both sets can also be used simultaneously. The radiometer to be tested for stability is either mounted into the exit aperture or put in front of the exit aperture, see Fig. 2.3.

The SQM-II has been redesigned from the original SQM and built by Satlantic Inc., Halifax, Canada. It consists of a lamp housing and a power box, which are connected by a cable of about 5 m length. A serial port provides the capability of monitoring and controlling the system with a PC. An internal memory, an LCD display and several buttons on the back also allow manual control and monitoring. The major differences between the original SQM and the SQM-II are

- SQM-II has only 1 detector at 490 nm, there are 3 detectors in the original SQM (for panchromatic, blue and red wavelengths).
- SQM-II detector faces Spectralon, which covers the internal of the light chamber. In the original SQM,

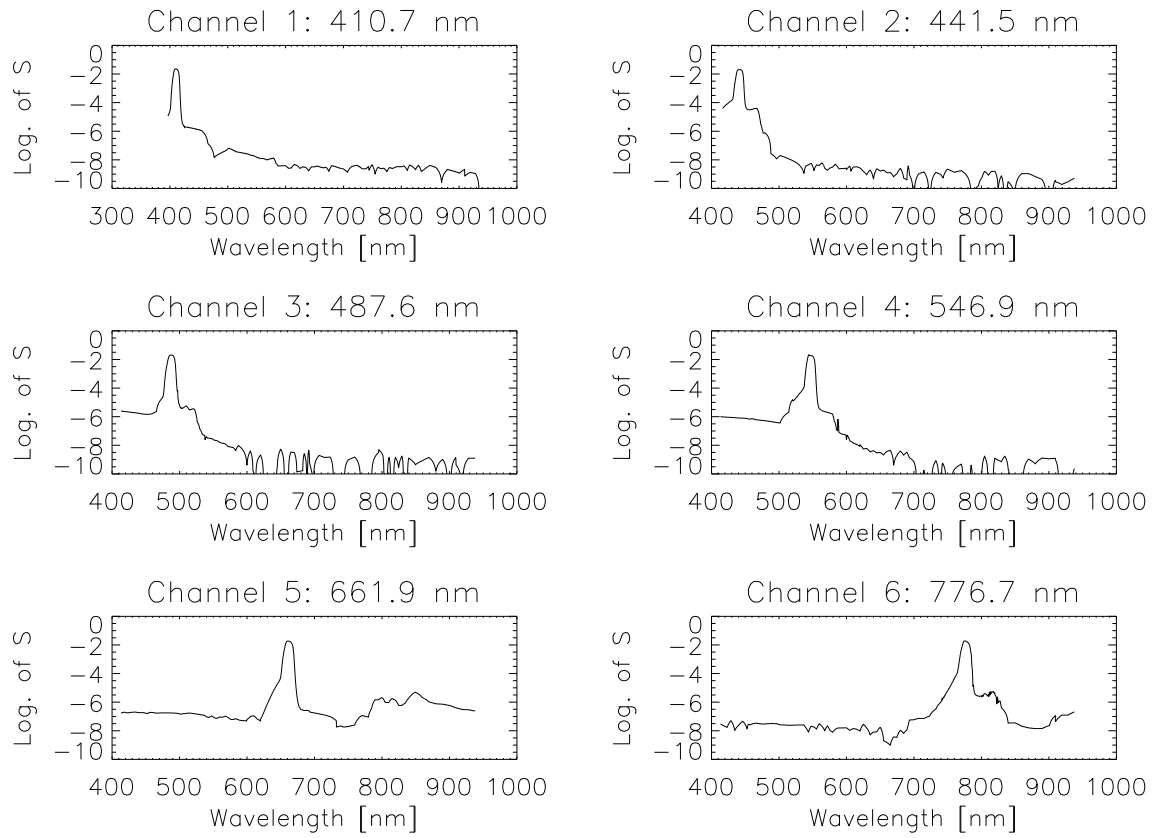


Figure 2.1: Logarithm to the base 10 of the responsivity $S(\lambda)$ (see eq. 4.2, page 29) of the SXR-II channels as a function of wavelength (interpolated values from the SIRCUS 2000 calibration).

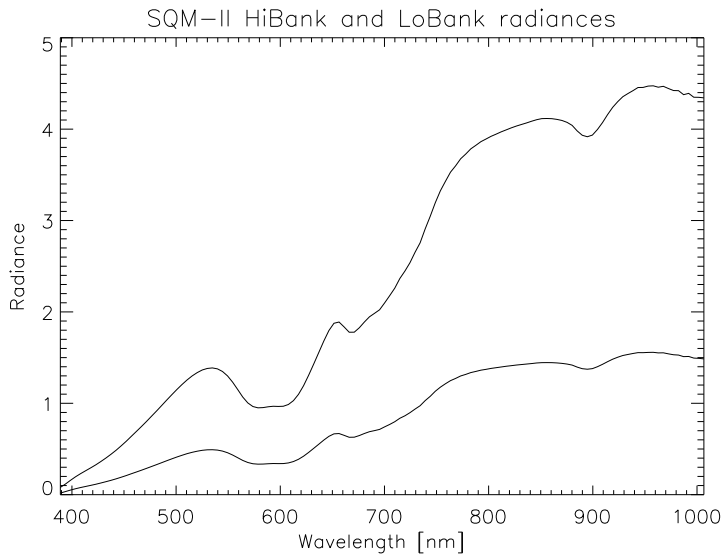


Figure 2.2: Radiances of the SQM-II HiBank (top) and LoBank (bottom) measured during SIMRIC-1 at NRL with the PHILLS radiometer placed right in front of the SQM-II exit aperture. Radiance unit is $\mu\text{W}/(\text{cm}^2 \text{ sr nm})$. The wavelength resolution of the PHILLS is about 5 nm. The data is averaged over 150 pixels in the center, corresponding to a FOV of about 8.25° .

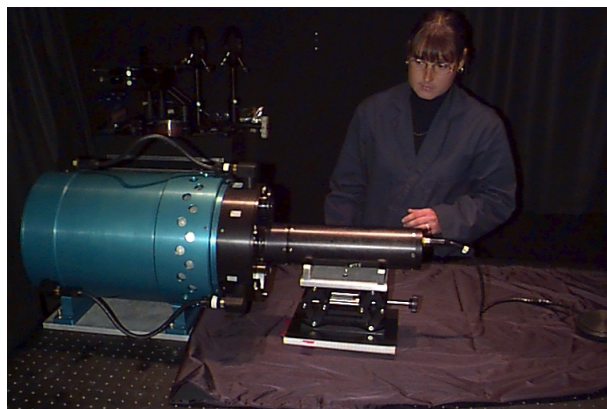


Figure 2.3: On the left, a Satlantic radiometer is mounted into the exit aperture of the SQM-II by Jennifer Sherman. On the right a Biospherical radiometer is mounted flush to the SQM-II.

detectors face the exit aperture and no Spectralon is used).

- SQM-II does not have a preheater.
- Design of SQM-II is more compact and integrated.
- SQM-II has a 1 hour warmup period where current is coarsely adjusted.
- Light output of SQM-II LoBank is about 4 times (at 780 nm) to 10 times (at 410 nm) greater than for the original SQM.

The usage of the SQM is described in [Hooker, 2000], detailed results are presented in [Hooker and Aiken, 1998]. The internal monitors are supposed to be used to correct the light output by dividing the readings from the external radiometer (in this case the SXR-II signal) through the simultaneously measured internal monitor signal. But the SQM-II internal detector shows an increase of about 9 % over one year for the HiBank and about 9.5 % for the LoBank. This increase is not supported by the SXR-II measurements, which indicate changes of less than 0.5 % at 490 nm, see Table 2.3 below. Thus it is likely that the responsivity of the internal detector has increased for an unknown reason (e.g. filter transmittance change). The increase can be seen for all kinds of SQM-II measurements: with the white fiducial inserted and with the cap closing the aperture before the SXR-II measurements (see measurement protocol, section 2.3) shown in Fig. 2.4, and for the SQM exit aperture open during the SXR-II measurements (see Figs. 2.7 and 2.8 below). As a consequence, we did not follow the protocol suggested by [Hooker, 2000] and did not correct the light output. It is interesting to note that the detector readings are relatively stable since September 2001. Up to August 2001, the HiBank and the LoBank had been used simultaneously once a month. This protocol was discontinued in September 2001. Since the temperatures inside the SQM-II are higher when using both banks together than when using only one bank alone, perhaps the internal detector was adversely affected by the high temperatures.

2.3 Stability monitoring

2.3.1 Method

A time series of measurements of the SQM-II with the SXR-II was taken in the SIMBIOS Optical Laboratory at NASA Goddard Space Flight Center, Greenbelt, MD. The facilities can be seen in Fig. 2.5. The room is climate controlled, but not at a stable temperature. Temperatures varied from 63° F in winter to 77° F in summer, usually temperatures rise by about 5° F from morning to midday. The humidity varied between 18 % and 55 %, a low humidity is usually correlated with a high temperature. The baffling material is felt, which has a bidirectional reflectance factor $R(0^\circ/45^\circ)$ (see section 4.6) of about 0.02 in the wavelength range of the SXR-II. An optical table has been installed in the beginning of 2002 for future monitoring activities.

For a measurement of the SQM-II with the SXR-II, the following measurement protocol is used:

- Turn on SXR-II, ILX temperature controller and Fluke voltmeter, at least 4 hours before taking measurements, preferably on the day preceding the measurements. Make sure SXR-II optics are set to 1 m and $f/1.4$.
- Assemble aluminum plates that hold SQM and SXR at a 1 m distance (see Fig. 2.6). Fine tune SXR-II orientation using SXR-II eyepiece and center of the SQM-II exit aperture marked on the SQM cap.
- Turn on SQM-II power (power box and switch on lamp housing). If there is no time pressure, wait for at least half an hour to let temperature of the internal detector reach its target temperature.
- Start computer logging of SQM-II data
- Note previous total burn time of HiBank and LoBank (stored in SQM-II memory).
- Ramp up LoBank.
- Insert white fiducial 65 minutes after LoBank ramp-up for 3 minutes (only in SIMBIOS optical laboratory, not during SIMRJC-1 field trips).

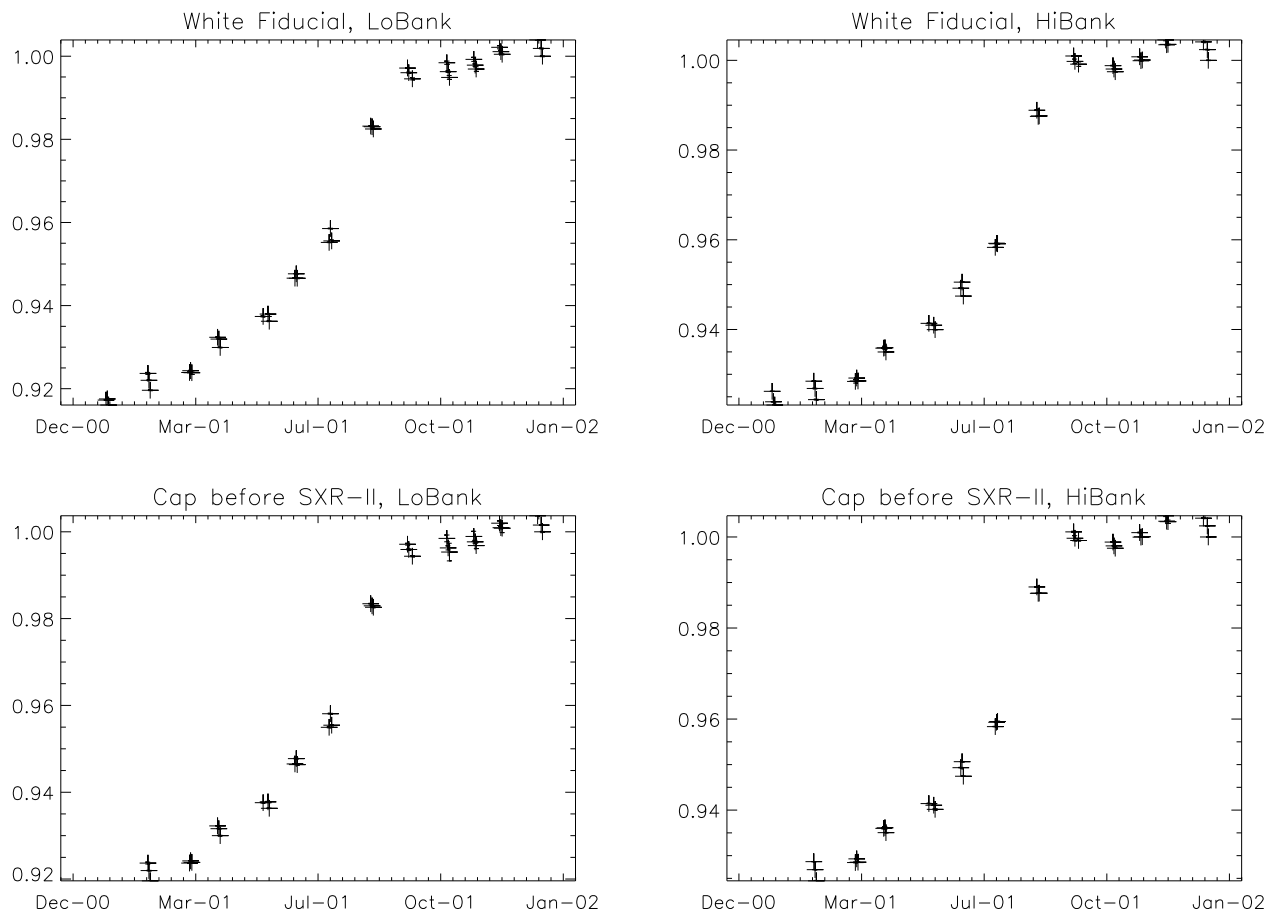


Figure 2.4: Time series of the internal detector measurements for SQM-II LoBank (left column) and HiBank (right column) for white fiducial inserted in the aperture (top row) and cap closing the aperture (bottom row). Type of lamp bank and SQM-II mode are given in the plot title. All values are normalized to the most recent measurement.



Figure 2.5: Pictures of the SIMBIOS optical laboratory. The left picture shows the curtains blocking the measurement area from ambient light, the right picture shows the measurement area.

- SQM internal detector measures with SQM closed with cap after 70 minutes after LoBank ramp-up for 3 minutes.
- Take SXR-II signal measurements 75 minutes after LoBank ramp-up. Turn room lights off during SXR-II measurements. Take SXR-II dark current readings before and after the signal measurements. The internal SQM detector measures during the SXR-II measurement with open SQM. For each wavelength, 11 samples taken with a delay of 0.5 seconds are averaged. One scan over all wavelengths takes about 70 seconds. 3 scans are taken for gains 1 and 10 each, thus the total measurement time is about 7 minutes. In October 2001, this protocol item was changed: 6 scans were taken at constant gains. For LoBank, channels 1, 3, and 6 are measured at gain 10, the other channels at gain 1. For HiBank, gain 1 is chosen for all channels except for channel 6, which is set to gain 10.
- Internal SQM detector measures with closed cap for 1 minute right after SXR-II signal measurements.
- During SIMRIC-1 field trips, radiometers from the participating laboratories measured the SQM-II after the above steps.
- Ramp down LoBank.
- Use the internal SQM detector to measure the SQM dark current with closed cap for 3 minutes.
- Ramp up HiBank and repeat all the above steps (after 'Ramp up LoBank').
- Note total burn time for HiBank and LoBank.
- Stop computer logging of SQM-II data. Backup SXR-II and SQM-II data.

The times when turning on or off any equipment are logged manually, as well as the total bulb burning times and the times of taking measurements. SXR-II signals for each of the 6 channels (without subtracting background) are also written down manually for immediate comparisons.

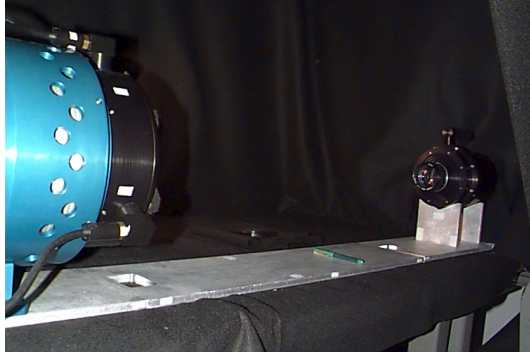


Figure 2.6: Setup for the long term stability monitoring experiment in the SIMBIOS optical laboratory. The SXR-II (on the right) measures the light exiting the SQM-II (on the left), their relative positions are fixed with aluminum plates-mounts. The aluminum plates are covered with black felt during the measurements, see Fig. 2.5.

SXR-II λ [nm]	410.69	441.51	487.58	546.89	661.91	776.71
SQM-II HiBank [%]	-1.3	-0.7	-0.2	-0.4	0.4	0.2
SQM-II LoBank [%]	-0.3	-0.2	0.3	0.1	0.7	0.6

Table 2.3: Change of the SXR-II measured radiance of the SQM-II HiBank and LoBank from January 2001 to November 2001.

2.3.2 Results

A long term time series of SXR-II measurements of the SQM-II is shown in Figs. 2.7 and 2.8. The SXR-II measured radiances are calculated using the linear interpolation described above (section 2.1). The values in the plots have been normalized to the most recent measurement. It can be seen that the changes of the SQM-II light output are very small, Table 2.3 compares the values from January 2001 and November 2001. These dates are very close to the dates of the calibration of the SXR-II on SIRCUS, thus the SXR-II radiances at these dates have the highest degree of confidence. The changes of the SQM-II LoBank are possibly within the measurement uncertainties, the only significant change is the decrease of 1.3 % of the SQM-II HiBank in SXR-II channel 1. The SQM-II HiBank decreased relative to the SQM-II LoBank by about 0.5 % for SXR-II channels 2 to 6 (1.0 % for channel 1). Over the more than one year period shown in the plots, the SQM-II HiBank was used for 128 hours, the SQM-II LoBank was used for 156 hours.

A similar time series has recently been published [Hooker et al., 2002], where the SXR (the SXR-II's predecessor) measured another SQM-II (S/N 004). It shows a much larger variation of the SXR-II measured signal, a decrease of about 2.2 % for every 100 days. The SQM-II S/N 004 participated in three ship cruises during the period of the time series, whereas the SIMBIOS SQM-II (S/N 006) never went onboard a ship.

The SQM-II has an internal detector at 490 nm. Unfortunately, the readings from the SQM-II internal detector increased by about 9 %, see Figs. 2.7 and 2.8, in strong disagreement with the SXR-II measurements. We have no explanation for this strong increase, a malfunctioning of the detector is suspected.

The main purpose of the monitoring with the SQM-II is to detect short term changes in radiometer stability. Over periods of several months, a change in the SQM-II light output has to be considered. Thus in Figs. 2.7 and 2.8, borders are drawn (dashed lines), that connect the measured radiances from January 2001 and November 2001, adding 0.5 % and subtracting 0.5 %. If the measured data between these dates is not contained within these lines, a short term change has occurred that cannot be explained by either the linear change of the SXR-II calibration or a linear change in the SQM-II light output. It can be seen that for channels 2 to 6, the data is contained within the dashed borders, thus we can assume that both the SQM-II intensity and the SXR-II responsivities for these channels evolved linearly ($\pm 0.5\%$). For channel 1, the data from July to September/October are below the dashed borders, thus either the SXR-II channel 1 or the SQM-II light output at that wavelength changed. This behaviour can be seen for both SQM-II HiBank and LoBank, but there is no sign of this behaviour in the neighboring channel 2 of the SXR-II. Thus it is very likely that the SXR-II channel 1 responsivity decreased in this period, up to about

1.5 %. This change is a likely cause of the differences between channels 1 and 2 seen for the comparisons at Satlantic in September, see section 4.3.8 below. Thus the SXR-II channel 1 data will be considered as unreliable for comparisons after July 2001 (the comparisons at Satlantic are the only ones affected).

The time series of SQM-II/SXR-II measurements during SIMRIC-1 is shown in Figs. 2.9 and 2.10. No measurements were taken in the NASA Code 920.1 facility, because measurements were made on the following days in the SIMBIOS Optical Laboratory (long term stability monitoring sessions, June 20th to June 22nd), and the shipping stress on the SXR-II was very limited because the radiometer had simply to be moved from one building to another at Goddard Space Flight Center.

It is interesting to take a closer look at the measurements taken in the non-SIMBIOS laboratories from April to June. Note that at Biospherical (third data point in Figs. 2.9 and 2.10), the protocol was not exactly followed, the HiBank was run without prior use of the LoBank. This resulted in a drop of about 0.2 % for SXR-II channels 2 to 6 and the internal SQM detector, but not for SXR-II channel 1. Furthermore, the LoBank was not measured 75 minutes after ramp up, but 135 minutes after rampup. This resulted in an increase of about 0.3 % for the SXR-II channels and the SQM-II internal detector. The internal detector measured the SQM-II light field with the aperture closed by the cap at 75 minutes and 130 minutes. The results show an increase of 0.25 % from 75 minutes to 130 minutes. This indicates that indeed the intensity of the light field of the SQM-II increased. Thus the small spikes of the SQM-II data at Biospherical is explained. Overall, neither the SQM-II nor the SXR-II were affected by the frequent transports in that period.

We suspect that the SQM-II light output is slightly sensitive to environmental conditions, but the variations seen in Figs. 2.9 and 2.10 are small (less than 0.5 %). Shipping did not adversely affect the stability of the SQM-II light output. The variations of the SQM-II internal detector are much greater than the SXR-II measured variations, increasing by about 9 % over one year, thus this internal monitor is not useful for long term monitoring. The internal monitor of another SQM-II did not show such a strong variation for a similar time series (Stan Hooker, personal communication). The SQM-II was designed to monitor the stability of radiometers during cruises, which typically last about one month. To use the SQM-II over a period of a whole year was not part of the original design purpose.

2.4 FEL Lamp F-474

FEL type lamps of 1000 W, modified to a medium bipost stage [Walker et al., 1987] are the most common type of source used as spectral irradiance standards [Harrison et al., 2000]. The SIMBIOS Project owns an FEL lamp calibrated by Optronics Laboratories (OL) in September 1997, labelled as F-474. This lamp was used at all those participating laboratories who also used FEL lamps as calibration source. It illuminated a Spectralon plaque and the radiance reflected from the Spectralon plaque was measured by the SXR-II and a local radiance radiometer, except at the NASA Code 920.1 laboratory, where no plaque is used, thus the lamp was only measured by an irradiance radiometer.

The calibration by OL is invalid since September 1998. Although it would have been easy to simply use the calibration from one of the participating laboratories, this was not done because it would have favored that particular laboratory over the other laboratories. Instead, the OL calibration is used and the results from all other laboratories are compared against it, keeping in mind that our goal is not to verify the OL calibration, but to compare how the laboratories are doing relative to each other. The OL calibration data of those wavelengths comparable to the SXR-II channels is given in Table 4.8, page 41.

The data of the F-474 should be treated with caution, because unforeseeable jumps of 0.5 % to 1 % have been reported due to the sensitivity to shock and vibration during transport of modified type FEL lamps, see [Stock et al., 2000], [Harrison et al., 2000].

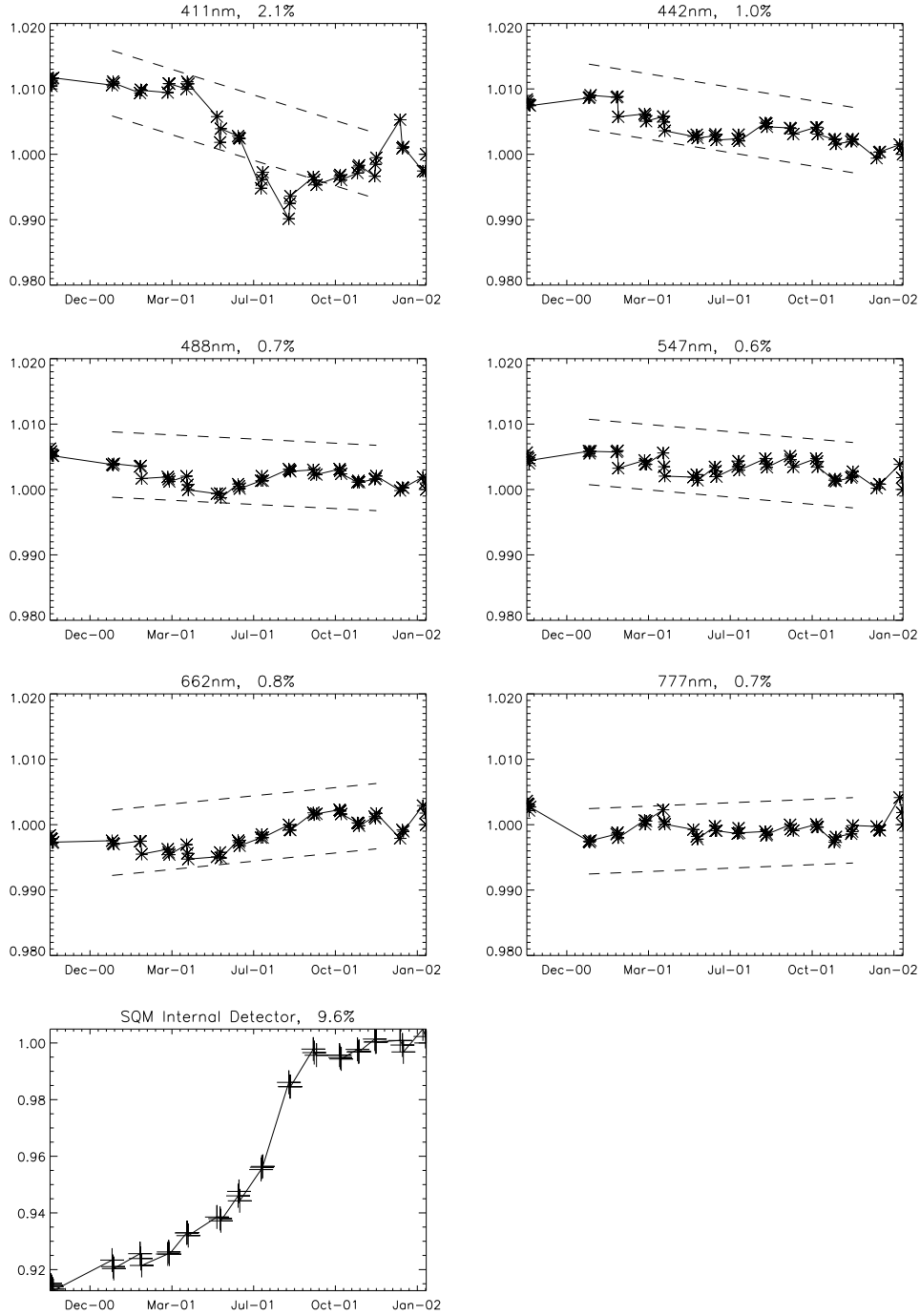


Figure 2.7: Long term time series of SXR-II measurements of the SQM-II HiBank from November 2000 to February 2002. All values are normalized to the most recent measurement. The title of the plot gives the wavelength of the respective SXR-II channel. The dashed line shows a deviation of the linear trend of $\pm 0.5\%$. The last plot shows the SQM-II internal detector measurements during the SXR-II measurements. The percentage number in the title gives the difference between maximum and minimum in %.

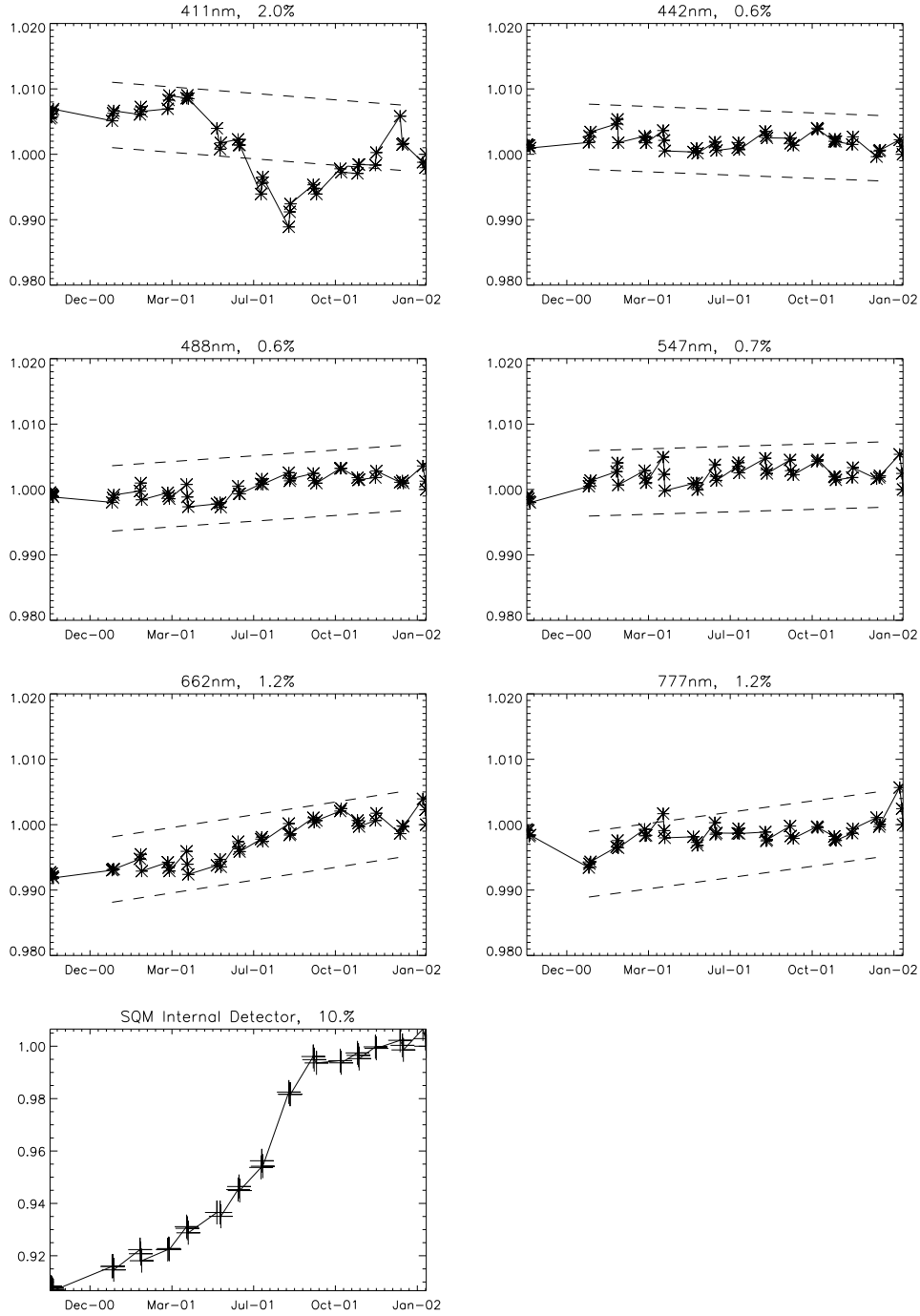


Figure 2.8: Long term time series of SXR-II measurements of the SQM-II LoBank from November 2000 to February 2002. All values are normalized to the most recent measurement. The title of the plot gives the wavelength of the respective SXR-II channel. The dashed line shows a deviation of the linear trend of $\pm 0.5\%$. The last plot shows the SQM-II internal detector measurements during the SXR-II measurements. The percentage number in the title gives the difference between maximum and minimum in %.

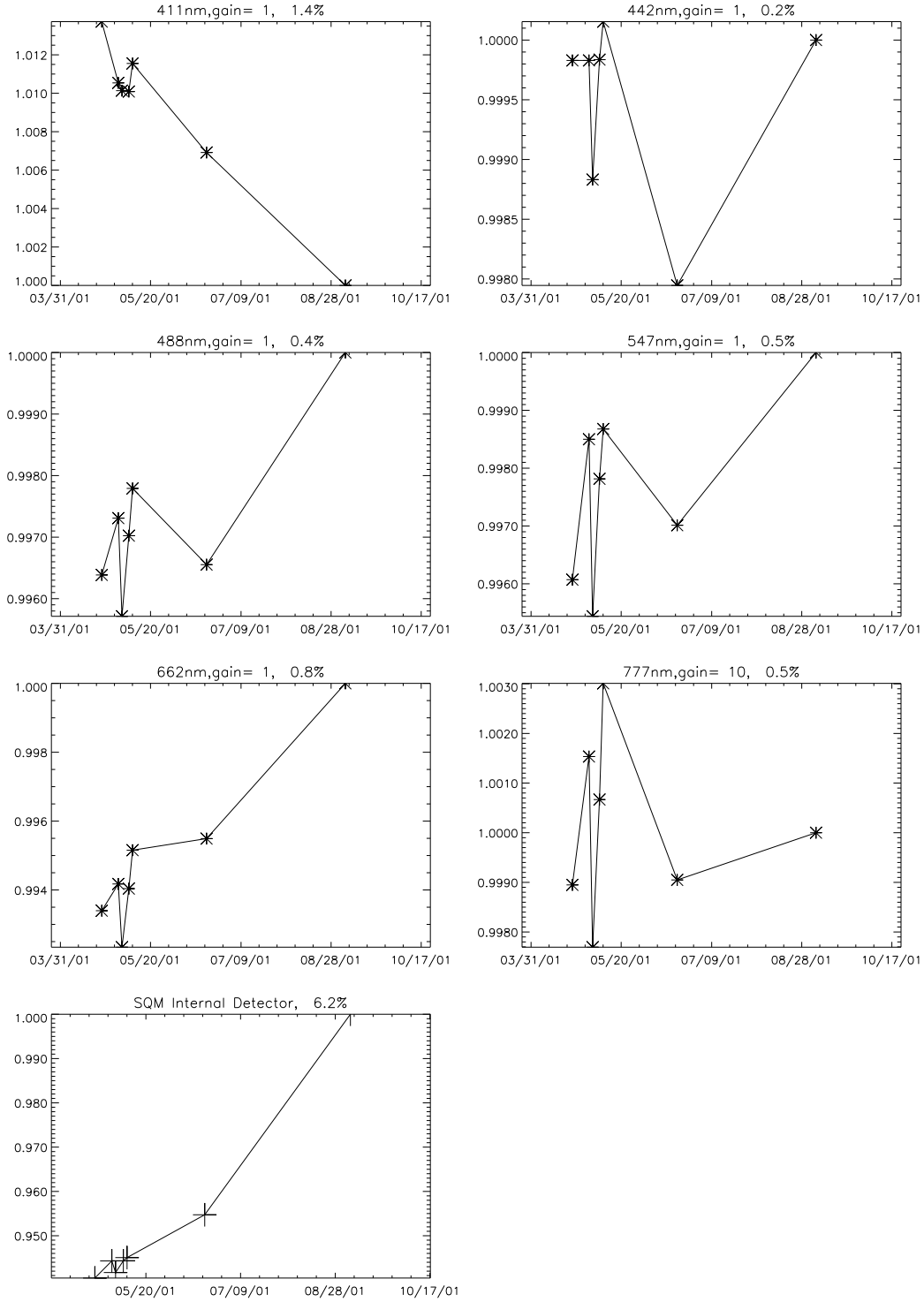


Figure 2.9: Time series of SXR-II measurements of the SQM-II HiBank at the SIMRIC-1 participants (in the order NRL, Scripps, Biospherical, HOBI Labs, NASA, Satlantic). All values are normalized to the measurement at Satlantic. The title of the plot gives the wavelength of the respective SXR-II channel and the maximum variation in measurements during the SXR-II measurements. The percentage number in the title gives the difference between maximum and minimum in %.

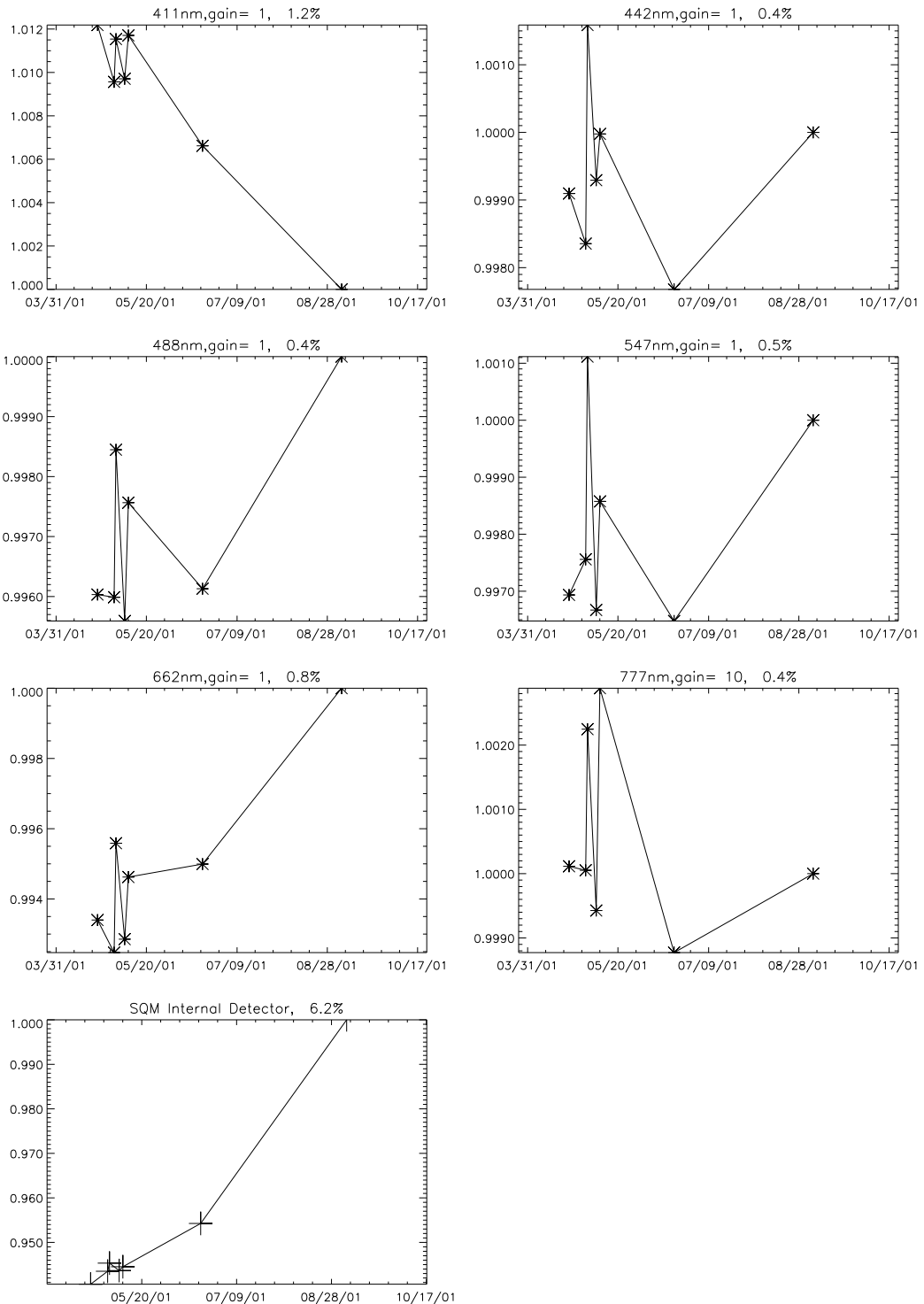


Figure 2.10: Time series of SXR-II measurements of the SQM-II LoBank at the SIMRIC-1 participants, see Fig. 2.9 for explanations.

Chapter 3

Documentation of Calibration Techniques

3.1 Introduction

This section documents the calibration procedures performed in each of the participating laboratories. Specifically, the items described include light sources, plaques, transfer radiometers, baffling techniques, installation details and algorithms used. Unless otherwise noted, all laboratories record the burn times for their calibration lamps. All lamps are always warmed up for at least 10 minutes. Table 3.1 gives an overview of the laboratories visited, the dates the measurements took place and the primary calibration standards.

3.2 Laboratories

3.2.1 NRL

Baffling

The room used for calibration at NRL has a size of about 6 m x 4 m x 3 m (W x L x H) and does not contain any windows. Light entering through the two closed doors is negligible. There is an optical table with a size of 4' x 8', see Fig. 3.1. Portable baffling walls (anodized bead blasted AL) with a height of about 50 cm can be positioned in various positions on the optical table (see Fig. 3.1, left). No baffles are placed between the FEL and the plaque. Different bafflings are used when using the monochromator (Fig. 3.1, right). Basically the FEL lamp is surrounded by baffles, light exits only into the direction of the plaque/monochromator and towards the ceiling.

Lamps

The primary irradiance standard at NRL is an FEL lamp calibrated by Optronics Laboratories with the identification number F-400. The calibration from this lamp is transferred to another FEL lamp (FEL-399). Furthermore, there is an integrating sphere with a diameter of 1m and an exit port with a diameter of 35.5cm (Fig. 3.2). It is illuminated by up to 10 internal halogen lamps, which can be turned on individually. For the SIMRIC-1, only 2 of the internal lamps were turned on because of the low saturation levels of the SXR-II. The sphere is mounted on a rack with wheels, which makes it easy to move the sphere around. However, repositioning of the sphere to exactly the same spot is tedious. The sphere is measured after a 1 hour warmup time.

Plaque and Geometrical Setup

A square Spectralon plaque (SRT-99-100) with a size of 10" by 10" (see Fig. 3.2) is used in conjunction with the FEL lamps to perform radiance calibrations. The distance from the plaque to the light source is 0.5 m. The illumination zenith angle is 0°, the viewing angle is 45°. The positioning of the sensor relative to the plaque is repeated each time by pointing the FOV of the radiometer to the center of the plaque. A laser is used to align the lamp and the

Laboratory	Acronym	Date	Calibration Standard
Naval Research Laboratory, Optical Sensing Section, Code 7212	NRL	4/23/01	FEL calibrated by Optronics Laboratories
Scripps Institution of Oceanography	Scripps	5/1/01	Sphere calibrated by Labsphere
Biospherical Instruments Inc.	Biospherical	5/3/01	FEL calibrated by NIST
Institute for Computational Earth System Science, University of California at Santa Barbara	UCSB	5/7/01	FEL calibrated by NIST
HOBI Labs	HOBI Labs	5/10/01	Irradiance standards calibrated by Oriel
NASA Code 920.1 Calibration Facility	NASA Code 920.1	6/18/01	FEL calibrated by NIST
Satlantic Inc.	Satlantic	9/5/01	FEL calibrated by Optronics Laboratories

Table 3.1: Overview of the laboratories participating in the SIMRIC-1. The column 'Date' gives the first day of measurements (month/day/year). The last column shows the primary calibration standard.

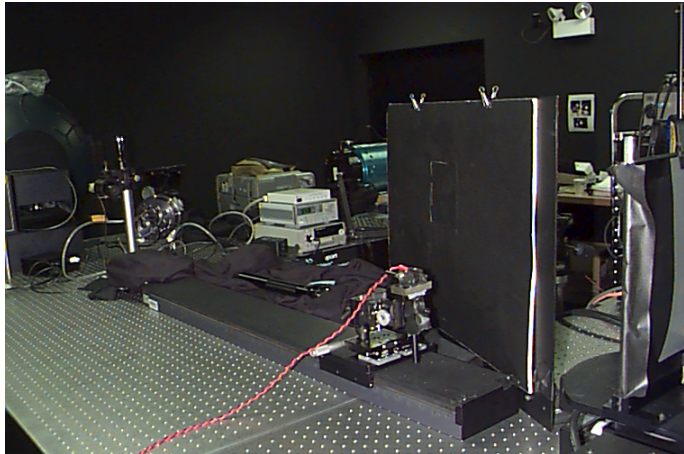


Figure 3.1: The picture on the left shows the setup for radiance calibrations with the FEL lamp at NRL, with a laser (at the left of the picture) for alignment purposes. The picture on the right shows the baffling for monochromator measurements of an FEL lamp at NRL.

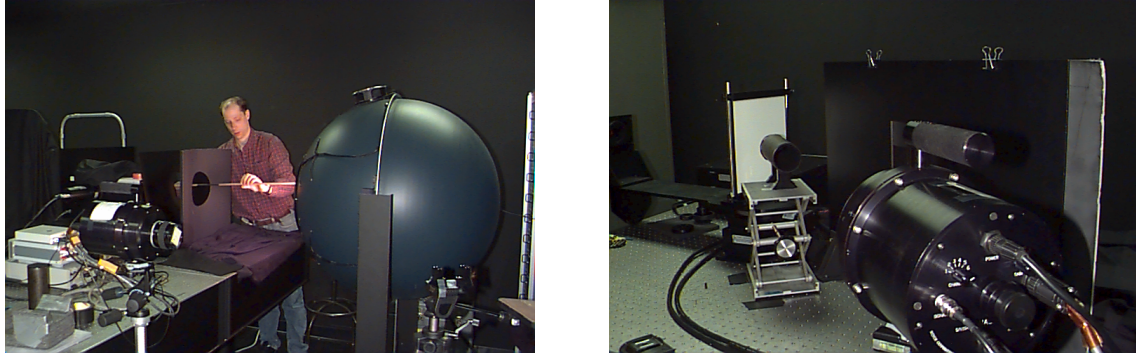


Figure 3.2: Left picture: Dan Korwan from NRL measuring the distance between the integrating sphere and the monochromator. Right picture: SXR-II, on-axis-cavity and Spectralon measurement configuration at NRL.

plaque by directing the laser (Fig. 3.1) through a fiducial lamp to the center of the plaque. A reflecting surface is placed on the plaque, and the setup is aligned until the reflection of the laser hits the laser origin to obtain an incidence angle of 0° .

Transfer Radiometers

A monochromator is used to transfer the calibration from the OL calibrated FEL lamp to another FEL lamp and to the sphere. The FEL-400 lamp is sent out aperiodically to get calibrated by OL. The calibration of this lamp is transferred to the other FEL lamp which is then used to perform instrument calibrations. This reduces the use of the calibrated lamp. The monochromator is made by Optronics Laboratories (750/M/S) using a OL 750/C controller. Light is collected by an integrating sphere of about 8 inches diameter with an entrance aperture of 1.25 inches. The light then enters the monochromator through a circular aperture of 1.5 mm, hits the a grating with 600 grooves/mm and passes through a 1.25 mm slit before hitting a silicon detector (DSM/1A). The bandwidth is 8 nm, measurements are taken at 10 nm steps.

A radiance radiometer called PHILLS was also used during the SIMRIC-1, for measurements of the plaque and of the sphere. PHILLS is a hyperspectral radiometer with a 60° FOV. Unfortunately, these measurements were found to be unreliable by the NRL scientists and were thus not provided to the main author of this study.

Calibration Algorithms

The NRL Spectralon plaque was calibrated by Labsphere in term of the 8° /hemispherical reflectance factor $R(8^\circ/h)$. Starting with the SIMRIC-1, the radiances reflected (L_r) from this plaque are calculated with the conversion factor described in section 4.6:

$$L_r = \frac{E_i}{\pi} \cdot R(8^\circ/h) \cdot 1.028 \quad (3.1)$$

where E_i is the incident irradiance from the FEL. For the interpolation between the wavelengths at which OL provides the irradiances of the FELs, the 4 point Lagrange method is used.

The radiance of the sphere is calculated using the irradiance of the OL-calibrated FEL lamp. The FEL and the sphere are measured by the monochromator successively. The radiance of the sphere L_s is calculated with

$$L_s = E_i \cdot (I_s/I_l) \frac{r_1^2 + r_2^2 + r_3^2}{\pi r_1^2} \quad (3.2)$$

where E_i is the incident irradiance from the FEL, r_1 is the radius of the entrance port to the monochromator, r_2 is the radius of the exit port of the sphere, r_3 is the distance between sphere and monochromator, and $I_{s/l}$ are the monochromator signals for sphere and FEL lamp, resp.



Figure 3.3: Left: Calibration room at Scripps. Right: Robert Frouin behind the optical table at Scripps with the SXR-II on the right and the sphere on the left.

3.2.2 Scripps

Baffling

The calibration room is situated in the corner of a large room, separated by thick, black, pleated curtains, see Fig. 3.3. The large room has no windows, but light can enter through the door from the outside aisle. However, no light seems to leak through the curtains. The separated area is about 3.5 m x 4.5 m x 3.5 m (W x L x H). In the center is an optical table (size 0.9 m x 2.0 m), on which an integrating sphere and its racks are mounted (Fig. 3.3). The baffling of the external lamp was clearly insufficient, a provisional dark foam slab was placed in front of the external lamp.

Lamps

Scripps owns an integrating sphere from Labsphere, model number XTH-2000V. The sphere has 3 different lamps: a Xenon lamp (which was not used during the SIMRIC-1), an EHLS (External Halogen Light Sources) Tungsten Lamp (EHLS-100-150) an Internal Tungsten Lamp (HLS-DM-150). The external lamp can be attenuated by an aperture with discrete settings ranging from 0 to 255, but with only certain settings available (e.g. '200' was not available, thus '199' was chosen). The sphere was calibrated by Labsphere in January 2001.

Geometrical Setup

Labsphere recommends to place the radiometer in front of the sphere at a distance of 0.5 m and a 0° viewing angle (Fig. 3.3). As the SXR-II is designed to measure at distance greater than 85 cm, this recommendation was not followed and the SXR-II measured the sphere at a distance of 1.0 m. We do not expect the distance to have a measureable effect on the radiance.

Calibration Algorithms

The calibration report available for the sphere is from Labsphere for both the internal and external lamp turned on simultaneously, together with the monitor readings during the Labsphere calibration. There are two monitors, a silicon detector (SDA) for the short wavelengths (below 1000 nm) and a germanium detector for longer wavelengths. The silicon detector was used for the SXR-II wavelengths. For each measurement of the sphere radiance, the



Figure 3.4: *Left:* Curtains separate measurement area at Biospherical, mechanical mount holds PRR800 radiometer at a viewing angle of 45° to the Spectralon plaque. *Right:* Three baffles perpendicular along the optical axis at Biospherical.

calibration radiances provided by Labsphere are supposed to be multiplied by the ratios of the actual monitor reading during the measurement and the monitor reading provided by Labsphere. Unfortunately, this is not reasonable if only one of the two lamps is turned on due to the different spectra of the lamps, see section 4.3.3 below. Thus the only possible comparison is for both internal and external lamp on.

3.2.3 Biospherical

Baffling

There are two adjacent dark rooms at Biospherical. The FEL lamp setup and a sphere are in a room with dimensions $6 \text{ m} \times 7 \text{ m} \times 2.5 \text{ m}$ (W x L x H). This was the only room used for SIMRIC-1. One part of this room (about $5 \text{ m} \times 1.5 \text{ m}$) is separated by curtains (Fig. 3.4), containing an optical rail of length 3 m. There are three baffles perpendicular to the line connecting plaque and lamp, see Fig. 3.4. Walls are painted black.

Equipment

There are two NIST FEL lamps available as primary standards. During SIMRIC-1, only one of them, calibrated in 1997, was used. OL FELs are used as secondary standards, the calibration from the NIST FEL is transferred to the secondary standards. A warmup time of 15 minutes is used for the FELs. Four Labsphere Spectralon plaques of size 1 foot by 1 foot are merged to form a square with edges of 2 feet length.

As transfer radiometer, Biospherical uses their PRR-800 High-Resolution Profiling Reflectance Radiometer. It is a 19 channel radiometer including seven out of the eight SeaWiFS channels. The FOV is 10° half angle in water.

Geometrical Setup

The illumination angle of the plaque is 0° , the viewing angle is 45° . There is a mechanical mounting to hold Biospherical radiometers (Fig. 3.4), thus the angle can be reproduced quickly and exactly, however there is the danger of a systematic error if the mounting is not exactly at 45° . The plaque was supposed to be at a distance of 3 m from the FEL lamp. However, analyzing the results several weeks later, it became clear that the expected values were considerably lower than the SXR-II measured values. The distance lamp/plaque was remeasured, and

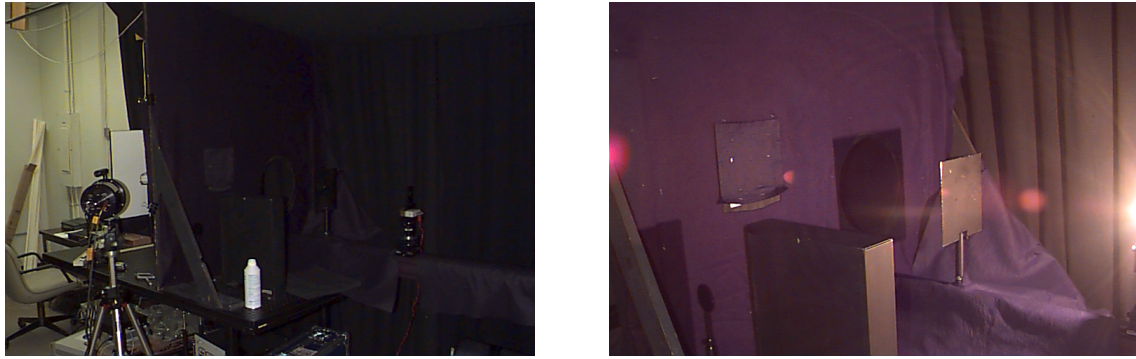


Figure 3.5: *Left:* SXR-II, fiducial FEL lamp and Spectralon plaque at UCSB. Top left are some of the strings for the curtains that are used to separate this setup from the remaining room. *Right:* Illuminated FEL lamp at UCSB with two light blocks installed along the optical axis: one on a post, the second block seals a whole in the baffling wall.

it turned out to be 2.952 m. The FEL lamp is positioned with a laser and a fiducial FEL lamp in the same way as at NRL, see above.

Calibration Algorithms

Starting with the SIMRIC-1, Biospherical uses the reflectance conversion factor (see section 4.6). The effective distance correction (see section 4.7) is not used. Its use would increase the predicted radiances by 1.1 %.

3.2.4 UCSB

The calibration facility of UCSB has been described in great detail in [O'Brien et al., 2000]. Several features described below are quoted from this publication.

Baffling

The climate-controlled calibration room has a size of about 8 m x 3.5 m x 3 m (L x W x H). A section of size 4 m x 1.2 m x 2.3 m can be separated from the room by black, pleated curtains (Fig. 3.5). Light can enter the room through two small windows to the outside. Except for a slit between the curtains and the floor, light is effectively blocked by the curtains. The light entering through the slit above the floor should be negligible, because the measurements take place on an optical table of about 1 m height. A black wooden baffle positioned 1.2 m from the plaque extends to the curtains on all sides thus dividing the area into two sections: one for the light source and one for the plaque/radiometer. A 28 cm hole centered on the optical axis allows illumination of the plaque. A shadow form can be placed over the hole to block direct light for stray light measurements.

Lamps

An FEL lamp calibrated by NIST (F-514) in Dec. 2000 is the primary standard. Several other FELs with calibrations from OL are available, but their irradiances have shown consistent differences among each other and to the NIST FEL in the past, thus it was chosen to transfer the calibration of the NIST standard to all other UCSB lamps.

All lamps are allowed at least a 10 minute warmup period. The voltage of the FEL lamps is monitored during measurements and recorded manually.

Geometrical Setup

Four square Labsphere Spectralon plaques are merged to form a square of 60.1 x 60.1 cm. For SXR-II measurements, a point about 1 inch off the center was chosen as FOV center to avoid the merging point of the 4 plaques. A distance from plaque to FEL of 2.0 m was used, an optical rail of length 2.4 m allows lamp distances from 1.5 to 2.4 m. A laser is used, as at NRL, to align the plaque and the lamp. For measurements with UCSB radiometers, a support mount is placed on the optical table about 33 cm from the center of the plaque and at an angle of 45°.

Transfer Radiometers

UCSB uses a MER-2040 from Biospherical as transfer radiometer. It has 13 channels (nominal 10 nm FWHM) from 340 nm to 683 nm with 6 channels matching the SeaWiFS wavelengths and 5 of these channels matching the SXR-II wavelengths. The highest wavelength processed at UCSB is only 683 nm. The SXR-II channel 6 (777 nm) is only included in the analysis for the FEL F-514 calibrated by NIST. The results for this channel for the remaining FELs, which need a calibration transfer with the UCSB radiometer, are not presented here.

The MER-2040 was designed as an underwater radiometer for depths up to 200 m. The noise level (standard deviation) is usually below 0.1 %.

Calibration Algorithms

The Spectralon plaque was calibrated by Labsphere in 1994 and 1999. The 1994 calibration gives a '0°/45° Reflectance Factor' in two quantities, corrected and uncorrected. The corrected quantity is higher than the uncorrected, between 0.2 % (at 380 nm) and 1.6 % (at 770 nm). The 1999 calibration gives two quantities as well, called 'Relative 0°/45° Reflectance Factor' and '0°/45° Spectral Reflectance Factor'. The later is higher than the former, between 0.2 % (at 380 nm) and 1.6 % (at 770 nm). The '0°/45° Spectral Reflectance Factor' from 1994 is about 1 to 2 % higher than the one from 1999. Calibrations at UCSB were done using the 'Relative Reflectance Factor' from 1994 until the SIMRIC-1 (including the SIMRIC-1 measurements). Since the SIMRIC-1, calibrations are done using the 1999 'Spectral Reflectance Factor'. The later are up to 1 % lower than the former (depending on wavelength), thus radiance calibrations made after the SIMRIC-1 use calibrations that are up to 1 % lower.

For the scaling of the lamp irradiance from 50 cm to 200 cm, the effective distance correction suggested by [Biggar, 1998] is not used, because it contradicts unpublished measurements made at UCSB.



Figure 3.6: *Left picture:* Spectralon plaque on an optical rail at Hobilabs. The ORIEL lamp is situated on the right of the picture. A sphere can be seen in the background. The picture on the right shows an ORIEL lamp in its mount after removing the baffles between the lamp and the Spectralon plaque.

3.2.5 HOBI Labs

HOBI Labs moved to a new facility in Moss Landing, CA, in summer 2001. SIMRIC-1 took place in the old facilities in Watsonville, CA, that are described below.

Baffling

The dimensions of the calibration room are relatively small, about 4 m x 3 m x 2.5 m (L x W x H), Fig. 3.6. Light entering through the closed door is noticeable (a slit between floor and door), but the door area is separated from the remaining room by a curtain, thus eliminating the problem. There are two optical tables in the room, one for the FEL setup, one for the sphere setup (Fig. 3.6). Climate control was turned off to prevent dust contamination, the temperatures varied from 72° F to 82° F. After SIMRIC-1, HOBI Labs moved into new facilities, with a larger calibration room with better climate control and improved stray light shielding.

Lamps

Light bulbs of 200 W (Fig. 3.6) from Oriel Instruments, Stratford, CT, are used instead of the modified type FEL lamps used in the other laboratories. Their mounts differ significantly from the modified type bipost FEL lamps (compare Fig. 3.6 and Fig. 4.17 on page 48), thus the SIMBIOS FEL F-474 could not be used at HOBI Labs. The ORIEL lamps are operated at 6.5 A and about 33 V. They are described as quartz tungsten halogen lamps, their Oriel part number is 63355 or 63356. The lamps are calibrated by ORIEL. ORIEL transfers the calibrations from a NIST FEL with the number F-420 whose calibration date is August 1994.

Plaque and Geometrical Setup

HOBI Labs uses a relatively small Spectralon plaque, a square of only 12.5 cm x 12.5 cm (part no. SRT-99-050). The plaque is illuminated from an incidence angle of 0°. The radiometers view the plaque at an angle 45° starting from the SIMRIC-1. No laser is used to align the FEL/plaque configuration. The distance from lamp to plaque is 0.5 m. As the bulbs are much dimmer than the typical modified type FELs, the radiances reflected from the plaque are still relatively low and there is no need to increase lamp-plaque distance to reduce light intensity.

Transfer Radiometers

The transfer radiometer used is called HydroRad, and it is produced by HOBI Labs. It is a hyperspectral radiance radiometer. The temperature correction was not available at the time of the SIMRIC-1 measurements. The radiometer uncertainty is about 1.5 % due to noise (without calibration uncertainty).

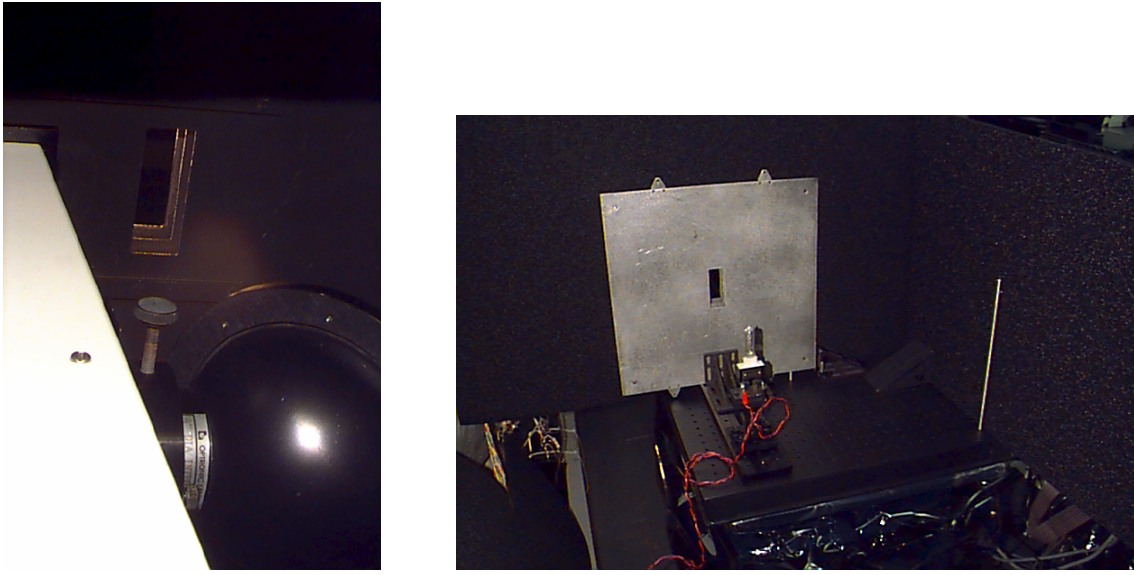


Figure 3.7: Setup at NASA Code 920.1 for FEL measurements with the OL 746. The left picture shows the collecting sphere attached to the OL 746, FEL light enters through a 3-layer baffle. The right picture shows the 3-layer baffle from the other side with the FEL in front of the slit.

Calibration Algorithms

The reflectance conversion factor (see section 4.6) is used at HOBI Labs since the SIMRIC-1 measurements.

3.2.6 NASA GSFC Code 920.1

Two adjacent clean rooms class 10000 (M 5.5) are available for optical calibrations at NASA Code 920.1. All SIMRIC-1 related measurements took place in the room with the Hardy sphere (Fig. 3.8). A description of the calibration procedures is also available online [NASA-Code-920.1, 2001].

Baffling

The calibration room is relatively dark, but there are several bright objects around. No baffling is used for measurements of the Hardy sphere. A 3-layer baffle with a small slit aperture (Fig. 3.7) is used for the measurements with the OL 746 radiometer of FEL lamps.

Lamps

NASA Code 920.1 owns an FEL calibrated by NIST with the 2000 irradiance scale. This FEL is used only once a year. The calibration is transferred to several FEL working standards, one of which (Hoffmann 96586) was used for SIMRIC-1 (Fig. 3.7). The Hardy sphere (Fig. 3.8) is calibrated by transferring the calibration of a working standard with a transfer radiometer OL 746 (described below) once a month. A 2 hour warmup time is recommended for the Hardy sphere to achieve a stable light output, with shorter wavelengths requiring a longer warmup time. There is an internal monitor for the Hardy, with 6 wavelengths, four of which overlap relatively well with SXR-II channels (410 nm, 440 nm, 640 nm and 840 nm). During SIMRIC 1, the data was taken continuously throughout the operating time of the Hardy sphere, in about 2 minute intervals. The Hardy sphere has sixteen internal halogen bulbs that can be turned on separately in any configuration. Only six lamps were used for the SIMRIC-1 because of the low saturation levels of the SXR-II.

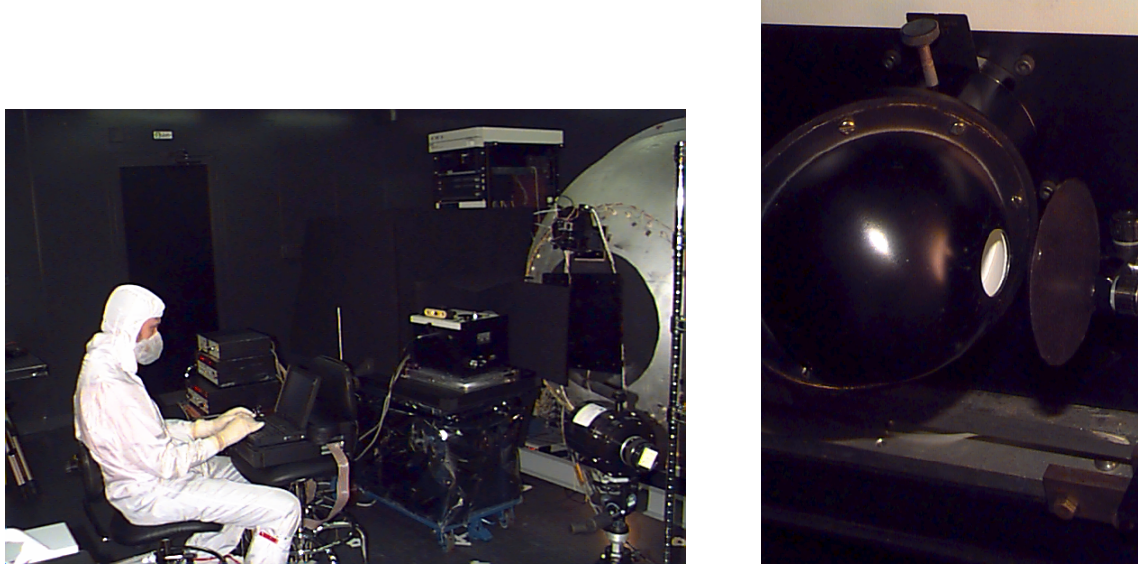


Figure 3.8: Left picture: GSFC Hardy sphere (made of fiberglass, painted a silvery color on the right), aperture covered for FEL measurements. Above the covered aperture the internal monitor can be seen. For Hardy measurements, the OL 746 (in front of the Hardy sphere) is rotated 90° so that the collecting sphere faces the Hardy exit aperture. John Cooper in the white cleanroom suit is using a PC to control the OL 746. Right picture: Collecting sphere of the GSFC 746 with circular disk acting as a block to take ambient measurements.

Transfer Radiometer and Calibration Algorithms

The OL 746 is a monochromator produced by Optronics Laboratories, see Fig. 3.8. The OL 746 cannot hold its calibration over long periods of time, thus for each calibration of the Hardy sphere, an FEL working standard is measured immediately before the Hardy measurement. First the working standard is measured, then the OL 746 collecting sphere is turned 90° to measure the Hardy sphere. All distances have been measured before the measurements to reduce the time between FEL measurement and Hardy measurement. Ambient measurements are only done for the Hardy measurements, for the FEL measurements the ambient signal was found to be negligible. The OL 746 measures the FEL irradiance at a distance of 50 cm and the sphere irradiance at a distance of 30 to 40 cm using a collecting sphere. The sphere irradiance E_s is converted to radiance L_s using the following equations:

$$\begin{aligned} L_s &= E_s \cdot K \\ E_s &= E_l / I_l \cdot (I_s - I_b) \\ K &= (r_a / r_b)^2 / F \cdot \pi, \quad F = (Z - \sqrt{Z^2 - 4 \cdot X^2 \cdot Y^2}) / 2 \\ X &= r_a / d, \quad Y = d / r_b, \quad Z = 1 + (1 + X^2) \cdot Y^2 \end{aligned}$$

where subscript l denotes the FEL lamp, I is the monochromator signal, I_b is the monochromator signal with direct light from the sphere being blocked (ambient measurement), r_a is the radius of the OL 746 input aperture, r_b is the radius of the sphere aperture, and d is the distance between sphere aperture and OL 746 input aperture. See [NASA-Code-920.1, 2001] for further explanations.

For SIMRIC 1, the wavelength sampling was set to 10 nm intervals for wavelengths from 380 nm to 1090 nm. For each wavelength, the bandwidth is also 10 nm. Shorter wavelength bins are possible, but come at the expense of a worse signal-to-noise ratio. NASA Code 920.1 has put considerable effort into deriving an uncertainty estimate for the OL 746 of the Hardy sphere. The estimated combined standard uncertainties for 6 lamps range from 4.7 % at 400 nm to 1.0 % at 800 nm.

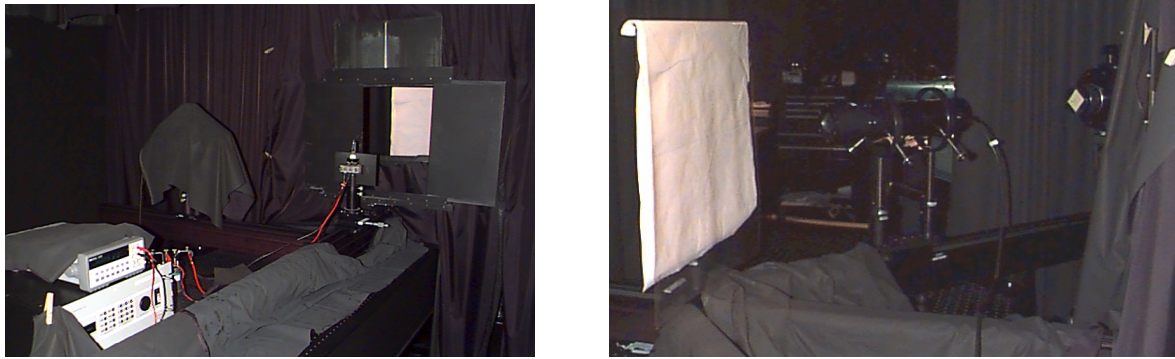


Figure 3.9: Left picture: Lamp holder on optical rail at Satlantic. The lamp power source can be seen on the left, the plaque can be seen through the square opening in the baffling wall on the right. Right picture: on the other side of the baffling wall, the Satlantic radiometer MVD046 (in the center) and SXR-II (on the right of the MVD046) measure the plaque (covered with a plastic sheet for dust protection in this picture).

3.2.7 Satlantic

Baffling

The calibration room at Satlantic is quite large with dimensions 6.17 m x 11.35 m x 3 m (W x L x H), with several large black optical tables inside. There are several black curtains that can separate different areas from each other, which allows convenient monitoring of instrument output without light contamination while measuring. The calibration room is a clean room class 10000 (M5.5). An optical rail connects the lamp holder and the plaque holder, there is a baffling wall with a square opening between lamp and plaque, see Fig. 3.9.

Lamps

Satlantic's modified type FEL F-409 was calibrated by NIST in 1996, thus the 1 year validity period for its calibration expired 4 years ago. It is not used for routine calibration purposes, only for special experiments. Satlantic acquires calibrated FELs from Optronics Laboratories on a regular basis, typically the 50 hours burn time is used after only a few months. OL provides lamps to Satlantic that are screened to provide similar light intensity. During SIMRIC 1, F-646 and F-662 were used.

Plaque and Geometrical Setup

A square Spectralon plaque (SRT-99-180) with edges of 45 cm length is used to produce radiances. A laser and a mirror are used to align the plaque with respect to the lamp. Satlantic has a special procedure for aligning the radiometer: the radiometer is aligned to view the center of the Spectralon plaque at an angle of 45°, with the distance between lamp and plaque set to 141.3 cm. Due to the wide FOV of oceanographic radiometers, the area viewed by the radiometer on the plaque is not centered on the plaque, but shifted towards a larger viewing angle. In order to center the FOV on the plaque, the plaque is moved closer to the lamp, to a distance of 130 cm. The measurements are made at this distance. This procedure was only employed for the measurements with the Satlantic radiometer, the SXR-II was aligned to view the plaque at 45° with a distance between plaque and lamp of 130 cm (see appendix A for a discussion of the small FOV of the SXR-II).

Transfer Radiometers

Satlantic does not transfer calibrations, thus they do not need a transfer radiometer. A 13 channel radiometer called MVD046 routinely monitors the radiances produced in the laboratory. The setup at Satlantic allows the

simultaneous measurement of the plaque with two radiometers at 45° viewing angle at opposite sides. This feature was not used during SIMRIC 1, because it was deemed more important that SXR-II and MVD046 view the plaque from the same side, as shown in Fig. 3.9.

Calibration Algorithms

Satlantic does not use the effective distance correction (see section 4.7). Assuming a distance between front of the pin and center of the lamp of 0.32 cm, the expected radiances would increase by 0.8 % for a distance between lamp and plaque of 130 cm. Satlantic corrects for the drop-off of irradiance expected for points away from the center of the plaque, see section 4.7.

Bidirectional reflectance factors $R(0^\circ/45^\circ)$ are used at Satlantic since 1995. Initially, a different quantity (called 'Relative Reflectance Factor' by Labsphere) was mistakenly supplied in an electronic file to the main author of this report to calculate the expected radiances. Fortunately, no calibrations were ever done by Satlantic using this quantity, and an electronic file containing the Bidirectional reflectance factors $R(0^\circ/45^\circ)$ was supplied to the main author of this report in December 2001.

3.3 SXR-II Specific Procedures

The SXR-II was positioned about 1 m apart from the plaque or sphere (Figs. 3.2 and 3.5). A 45° viewing angle relative to the plaques was obtained by projecting the adjacent leg and the opposite leg (both of length $\sqrt{0.5}$ m for a triangle with a right angle and a hypotenuse of 1 m) onto a common horizontal plane. The SXR-II was mounted on a tripod (Figs. 3.3 and 3.5). An on-axis-cavity (Fig. 3.2) was placed in the center of the FOV to perform a measurement (called 'ambient measurement' from here on) that determines the size-of-source effect, see appendix A. The ambient measurement was subtracted from the measurement with the cavity removed (i.e. the actual measurement of the plaque/sphere, called 'signal measurement' from here on). In Fig. 3.3 the cavity can be seen covered with a lid that has a mark on the cavity center to facilitate aiming the SXR-II. A cap is placed in front of the SXR-II lens to obtain background measurements.

The following setting was chosen in the SXR-II control software:

- 11 samples are taken for a given gain and channel.
- The delay between sample readings was set to 0.5 seconds.
- Do several consecutive wavelength scans (i.e. read channels 1 to 6 in ascending order). Typically 4 scans were chosen for the signal measurements, which resulted in a total measurement time of 5 minutes for the light source. Ambient measurements were usually 2 scans or less, background measurements were 3 scans or more.

The standard order of measurements is

1. Background
2. Ambient
3. Signal
4. Background,

but this sequence was not always used. During the light source warmup, the appropriate gain was chosen for each of the channels. The optimal gain gives a voltage reading between 100 mV and 1 V, because in this range the accuracy of the voltmeter is highest. All types of measurements (signal, ambient, background) used the gain setting optimized for the signal measurement.

The SXR-II noise uncertainty u_{stat} (Type A uncertainty) is calculated as

$$u_{\text{stat}} = \sqrt{\sigma_I^2 + \sigma_A^2} \quad (3.3)$$

where σ_I is the standard deviation of the signal readings of all samples and scans, and σ_A is the standard deviation of the ambient measurements.

Chapter 4

Results

At each laboratory, measurements were made on two consecutive days to evaluate the reproducibility and detect potential measurement errors. Although it is possible to use the average of both measurements as a final value to arrive at a more exact value, this was not done for SIMRIC-1, because the purpose of the SIMRIC-1 was to evaluate the laboratories' performance for an individual calibration measurement. Apart from getting an idea about the reproducibility, the measurements on the second day were meant as a backup in case it turned out that there are problems with the first day's measurements (problems related either to the SXR-II or the equipment in the laboratories). As it will be described below, if there were differences between the measured radiances of the two days, they were traced to problems on the second day. Thus in this report, all radiance comparisons between expected radiances and SXR-II measured radiances are based on the measurements of the first day.

4.1 Reproducibility

In this section, the reproducibility of the SXR-II measurements from the first day compared to the SXR-II measurements of the second day is presented. Reproducibility is calculated as the relative difference between measurements on different days. The repeatability of the SXR-II and the repeatability of the light source, as well as possible alignment variations affect the reproducibility. The repeatability of the SXR is given in [Johnson et al., 1998a] as 0.1 %.

With the exception of the measurements at NASA Code 920.1 and Satlantic, the reproducibility is very good. The average reproducibility is 0.3 % for channels 2 to 6 and 0.5 % for channel 1. At NASA Code 920.1, the internal monitor of the sphere confirms the relatively large differences from day 1 to day 2 for SXR-II channels 1 and 2 of 0.8 % and 0.5 %, resp. At Scripps, the increase of 0.6 % for SXR-II channel 1 from day 1 to day 2 is not well predicted by the internal broadband monitor, which shows an increase of only 0.2 %, which agrees well with the increases of SXR-II channels 4 and 5 (547 nm and 662 nm). At HOBI Labs, the reproducibility is usually better than 0.5 %, but at 777 nm there is a significant outlier for lamp 7-1244 (the radiance measured on the first day is 1 % higher than on the second day). NRL shows excellent reproducibility values with a maximum difference of only 0.15 %. The reproducibility at UCSB is excellent for its own two irradiance standards F-305 and F-473 (better than 0.15 %, except for channel 1 with a reproducibility of 0.2 %). The SIMBIOS FEL had a reproducibility at UCSB of 0.3 %, which is still very good.

At Satlantic, the measured radiances of the second day are significantly higher on the second day for all three Satlantic lamps F-646, F-662 and F-409, see Table 4.9, but not for the SIMBIOS FEL F-474, which was measured before the Satlantic lamps. A difference was confirmed for only one lamp (F-646) by the Satlantic transfer radiometer (see Table 4.10), whereas the other lamps appeared to be stable according to the Satlantic radiometer. The voltage of the lamps is measured routinely at Satlantic. For F-646 (but not for the other lamps), the voltage measured on the second day was 115.2 V, 0.7 V higher than on the first day (the voltage on the first day was similar to previous Satlantic calibration sessions with this lamp). After the differences were discovered, the measurements were repeated for the SIMBIOS F-474 (still on the second day), although the previous measurement of the F-474 on that day did not show a significant change (stars in Fig. 4.1, all the F-474 measurements of the second day are shown in Fig. 4.1 (plot at the bottom, right), as difference to the first day).

The new measurement showed significantly higher values than before (rhombs in Fig. 4.1). A check of the SXR-II alignment showed that the SXR-II was not aligned properly, it was turned around its optical axis by about 20° (but still the FOV was centered on the plaque) because the support plate on the tripod for the SXR-II was not level. This problem was corrected in the following measurements of the F-474 (triangles and rhombs in Fig. 4.1), but they did not result in the expected return to the values of the previous day. In effect, the difference to the previous day increased slightly, to values comparable to the difference found for Satlantic's FELs F-646 and F-662 (Fig. 4.1, plot at the bottom, right). Thus the reason for the bad reproducibility of lamps F-409 and F-662 cannot be determined with certainty, but SXR-II alignment errors are a likely reason.

4.2 Radiance Calculation

The formula for calculating band-averaged radiances L_b is

$$L_b(\text{channel}) = \int_0^{\infty} L_r(\lambda) \cdot S(\lambda, \text{channel}) d\lambda \quad (4.1)$$

where $L_r(\lambda)$ is the radiance reflected from either a plaque or out of a sphere, $S(\lambda, \text{channel})$ is the responsivity of the respective radiometer channel (1-6 in the case of the SXR-II). The responsivity is normalized to one:

$$\int_0^{\infty} S(\lambda, \text{channel}) d\lambda = 1 \quad (4.2)$$

Note that $S(\lambda, \text{channel})$ has the unit nm⁻¹, because it is sensitivity per wavelength interval. In reality, $S(\lambda, \text{channel})$ and $L_r(\lambda)$ are not given as continuous functions, but only at discrete wavelengths. Thus interpolation becomes necessary. For this study, for $L_r(\lambda)$ the interpolated data calculated by the laboratory in which the measurement was taken is used, see section 4.5. $S(\lambda, \text{channel})$ was measured by NIST and is given in 1 nm intervals (or smaller) in the high sensitivity regions, and in 5 to 10 nm intervals in low sensitivity regions. The wavelength range varies with channel, from about 400 nm to 940 nm, see Fig. 2.1. The actual calculation of eqs. 4.1-4.2 was carried out as a sum by the main author of this study, linearly interpolating to 0.1 nm wavelength intervals.

Using only the center wavelength (preliminarily provided by B.C. Johnson from NIST) for each SXR-II channel, the expected radiances were calculated by the main author of this study as well as by the participating laboratories independently, except for Biospherical and those laboratories using an integrating sphere. No significant differences were found. The basic formula to calculate these expected radiances is eq. 3.1 presented in section 3.2.1, for laboratory specific variations see the 'Calibration Algorithm' sections of chapter 3.

To account for the size-of-source effect (see appendix A), measurements with an open cavity (see section 3.3) placed in the FOV of the SXR-II were subtracted from the actual signal measurements. The difference was divided by the calibration factors in Table 2.1. The resulting values are called SXR-II measured radiances in this report.

4.3 Radiance Comparisons

4.3.1 Overall Comparison

Figs. 4.2 and 4.3 show a comparison of the expected and the measured radiances of the principal standard of each laboratory. On average, the SXR-II measures radiances are 1 to 2 % higher than the expected radiances. All differences are within the combined (SXR-II and laboratory) standard uncertainties ($k=2$), except at HOBI Labs, where two of three lamps were off by more than 5 %. The differences are even within the $k=1$ combined standard uncertainties for SXR-II channels 1 to 5 (411 to 662 nm), excluding the two 'bad' HOBI Labs lamps. In many labs, the radiances measured by the SXR-II are higher than the expected radiances, by about 2 % for NRL, HOBI Labs and Satlantic. Note that all the above labs are still on the 1992 irradiance scale (source based) or even on previous scales, whereas the SXR-II is on the 2000 irradiance scale (detector based), see [Yoon et al., 2002] for more information on source and detector based scales at NIST. Comparisons between the 1992 scale and the 2000 scale have shown about 0.5 to 1.0 % higher values for the 2000 scale [Yoon et al., 2002]. Thus we expect the SXR-II to measure about 0.5 to 1 % higher radiances than expected by those laboratories who are not on the 2000 scale.

The expected radiances of Scripps and Biospherical (both with irradiance scales older than the 2000 scale) agree within ± 1.0 % with the SXR-II measured radiances.

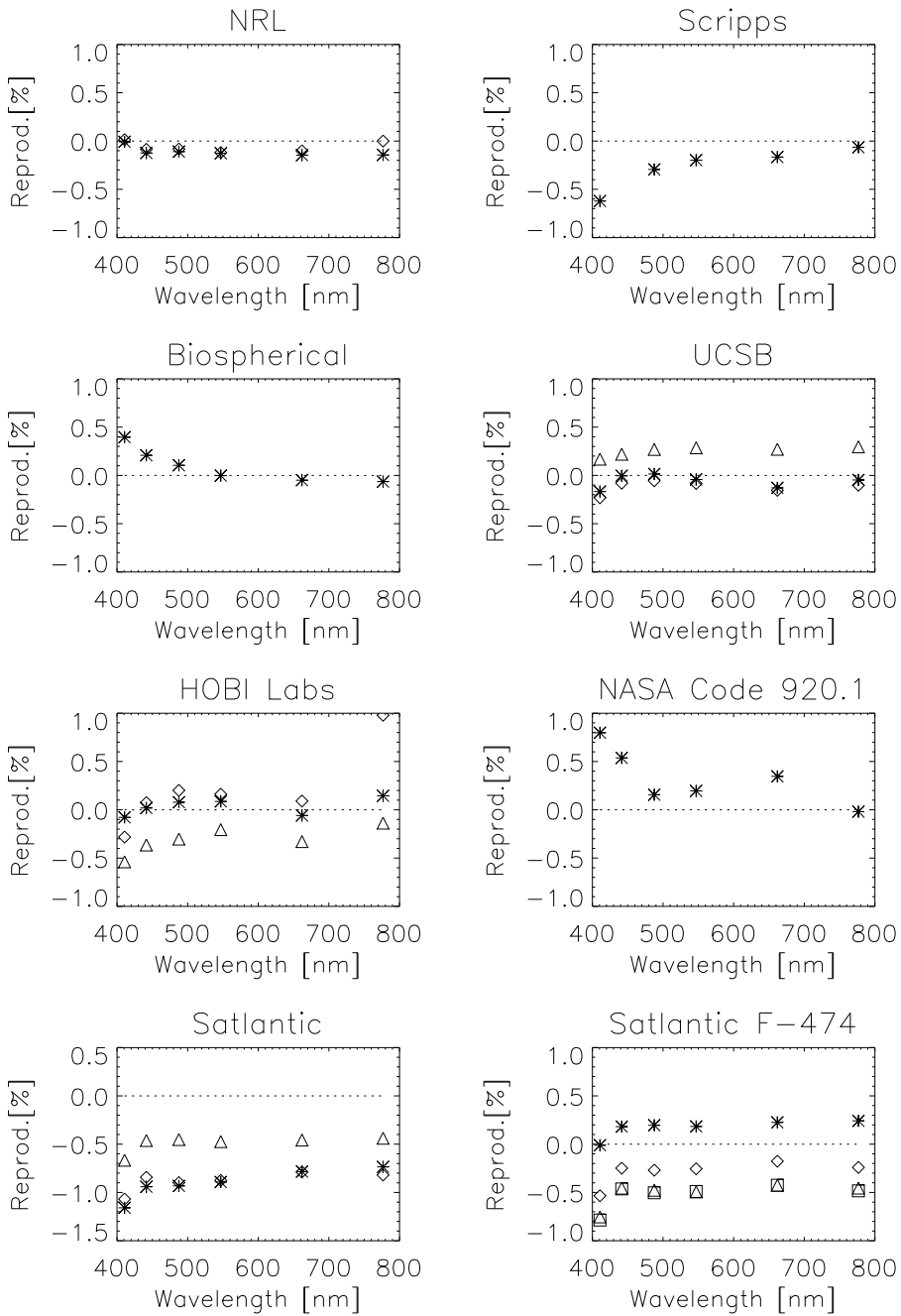


Figure 4.1: Reproducibility of the SXR-II measurements, calculated as radiance of first day minus radiance of the second day (in %). Legend for multiple symbols plots: NRL F-399: stars; NRL F-474: rhombs; UCSB F-473: stars; UCSB F-305: rhombs; UCSB F-474: triangles; HOBI Labs 7-1259: stars; HOBI Labs 7-1244: rhombs; HOBI Labs 7-1339: triangles; Satlantic F-646: stars; Satlantic F-662: rhombs; Satlantic F-409: triangles. The last plot shows the reproducibilities at Satlantic for the F-474 calculated using a measurement on the first day and the following measurements from the second day: first (stars), second (rhombs), third (triangles), and forth measurement (squares).

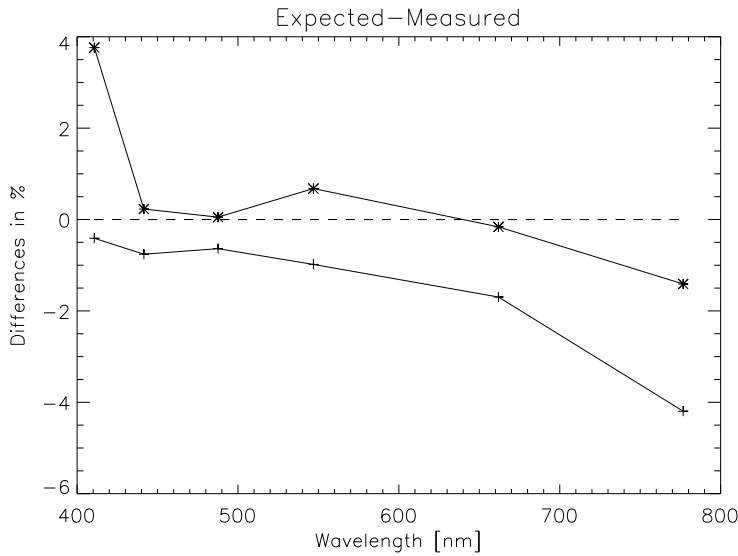


Figure 4.2: The average differences of the expected (laboratory predicted) radiances and the SXR-II measured radiances for UCSB (FEL F-514, '+' symbols) and NASA Code 920.1 (Hardy sphere, '*' symbols). Both laboratories are on the NIST 2000 scale.

For the laboratories which are on the NIST 2000 scale (NASA Code 920.1 and UCSB), the agreement between SXR-II measured radiances and expected radiances is about 1 %, except for certain wavelengths.

In the following sections 4.3.2 to 4.3.8, the results are analyzed for each laboratory separately in more detail.

4.3.2 NRL

The SXR-II measured radiances are compared to the expected radiances calculated with eq. 4.1 in Table 4.1. On average, the expected radiances are about 2 % lower than the SXR-II measured radiances, see Fig. 4.4. The calibrations of the two FELs agree extremely well with each other, differing by less than 0.3 %. The transfer of the calibration of the FEL 400 to the sphere was done in good agreement with the SXR-II measurements: comparing the differences (Expected-Measured) for the FEL 400 and the sphere, they agree better than 0.5 %, except for channel 6, where they differ by 1.5 %. All differences (Expected-Measured) are within the $k=1$ combined standard uncertainties (combined standard uncertainty of SXR-II and NRL is 2.8 %), except for channel 6, where the difference is 3.1 %.

4.3.3 Scripps

The calibration of the sphere at Scripps was done by Labsphere in January 2001. An FEL (F-500) calibrated by OL was used by Labsphere. F-500 was calibrated by OL in September 1998, using an FEL that is on the NIST irradiance scale from 1973. (This information was obtained from a telephone call by the main author of this study to Labsphere). The agreement is still well within the combined $k=1$ uncertainties.

There is a noticeable wavelength dependence in the differences for the Scripps data: SXR-II measured radiances are 0.4 % higher for channel 1 than the expected radiances, and 0.7 % lower for channel 6.

The sphere is only calibrated for both the external and the internal lamp turned on simultaneously. The agreement between expected and measured radiance for the external and internal lamp separately varies between 2 and 40 %. The spectra of internal and external lamp (shown in Fig. 4.6) are so different that it is impossible to use the broadband detector to scale the calibration from the 'both lamps on' mode to a single lamp mode. The next calibration of the sphere by Labsphere will be for external and internal lamp turned on separately.

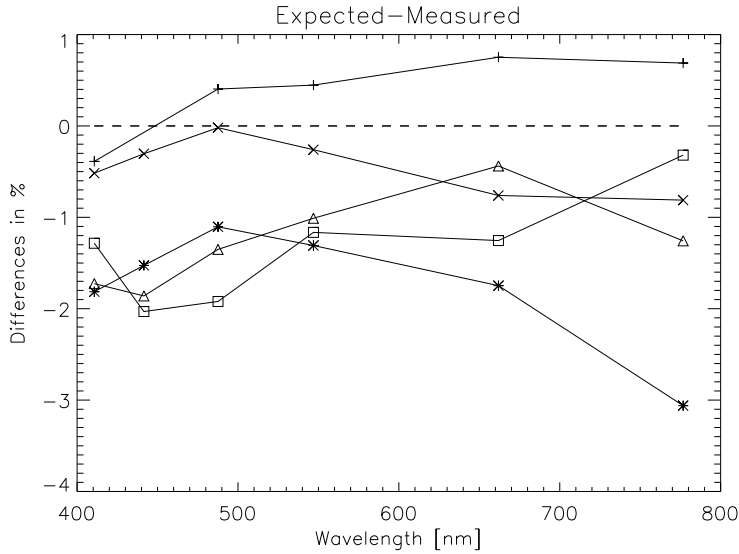


Figure 4.3: The average differences of the expected (laboratory predicted) radiances and the SXR-II measured radiances for NRL (FEL F-400, '*' symbols), Scripps (Labsphere sphere, '+' symbols), Biospherical (FEL F-473, 'x' symbols), HOBI Labs (Oriel 7-1259, '△' symbols), and Satlantic (FEL F-662, '□' symbols). Neither of these laboratories is on the NIST 2000 scale. Some of these laboratories have several primary standards. At HOBI Labs, two further lamps showed differences of about 6 % and were recalibrated after the SIMRIC-1, see section 4.3.6. At Satlantic, another primary standard measured during SIMRIC-1 was F-646. It agrees better with the SXR-II measurements, but was unstable on the second day. Satlantic's FEL calibrated by NIST in 1996 gives similar differences as the shown F-662, see section 4.3.8.

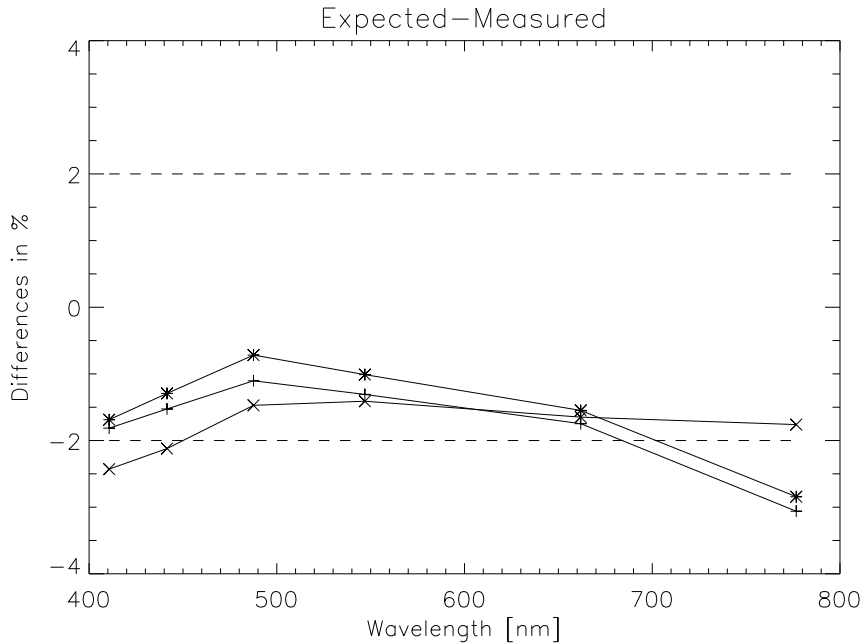


Figure 4.4: Difference of the expected radiance and the SXR-II measured radiance at NRL. *: FEL 400, +: FEL 399, x: sphere, dashed line: NRL estimated $k=1$ uncertainty for FEL/plaque radiance.

FEL F-400, calibrated by OL

λ [nm]	L_m	L_e	$\Delta(4/24/01)[\%]$
410.69	0.72405	0.710913	-1.8
441.51	1.12626	1.10721	-1.5
487.58	1.87932	1.85832	-1.1
546.89	3.02200	2.98227	-1.3
661.91	5.17386	5.08337	-1.7
776.71	6.66606	6.46199	-3.1

FEL F-399, calibration transferred from FEL F-400

λ [nm]	$L_m(4/23/01)$	L_e	$\Delta(4/23/01)[\%]$	$L_m(4/24/01)$	$\Delta(4/24/01)[\%]$	Stabil. [%]
410.69	0.74777	0.73515	-1.7	0.74782	-1.7	-0.0
441.51	1.15803	1.14115	-1.3	1.15943	-1.4	-0.1
487.58	1.92442	1.91034	-0.7	1.92648	-0.8	-0.1
546.89	3.08018	3.04884	-1.0	3.08395	-1.1	-0.1
661.91	5.24231	5.16109	-1.5	5.24986	-1.7	-0.1
776.71	6.73094	6.53959	-2.8	6.74062	-3.0	-0.1

Sphere US 4000, 2 bulbs on, calibration transferred from FEL F-400

λ [nm]	$L_m(1st\ mmt.)$	L_e	$\Delta(1st\ mmt.)[\%]$	$L_m(2nd\ mmt.)$	$\Delta(2nd\ mmt.)[\%]$	Stabil. [%]
410.69	1.04338	1.01804	-2.4	1.04173	-2.3	0.2
441.51	1.84569	1.80292	-2.1	1.84239	-1.9	0.2
487.58	3.47998	3.42822	-1.5	3.47284	-1.3	0.2
546.89	6.22151	6.13333	-1.4	6.21134	-1.2	0.2
661.91	11.9654	11.7680	-1.6	11.9513	-1.5	0.1
776.71	16.0872	15.8039	-1.8	16.0607	-1.6	0.2

SIMBIOS FEL F-474, calibrated by OL

λ [nm]	$L_m(4/23/01)$	L_e	$\Delta(4/23/01)[\%]$	$L_m(4/24/01)$	$\Delta(4/24/01)[\%]$	Stabil. [%]
410.69	0.73335	0.74062	1.0	0.73323	1.0	0.0
441.51	1.13656	1.15060	1.4	1.13748	1.3	-0.1
487.58	1.89120	1.92601	1.9	1.89272	1.8	-0.1
546.89	3.03431	3.08197	1.6	3.03781	1.5	-0.1
661.91	5.18420	5.20768	0.5	5.18936	0.4	-0.1
776.71	6.68391	6.57111	-1.7	6.68386	-1.7	0.0

Table 4.1: Radiances at NRL. Radiance unit is $\mu\text{W}/(\text{cm}^2 \text{ sr nm})$. L_m is the SXR-II measured radiance of the respective date, L_e is the expected radiance. Δ is the difference $L_e - L_m$ of the respective date. Stabil. is the stability from one day to another, calculated as $L_m(\text{day1}) - L_m(\text{day2})$.

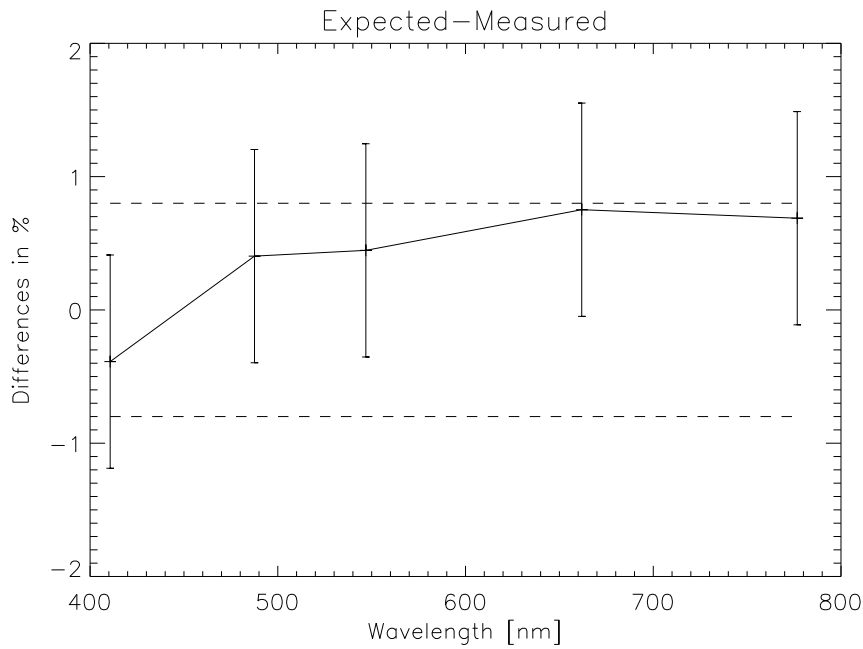


Figure 4.5: *Difference of the expected radiance and the SXR-II measured radiance at Scripps for the Labsphere sphere with both internal and external lamp turned on. The vertical bars show the estimated SXR-II $k=1$ uncertainties. The dashed line shows the estimated $k=1$ uncertainty for sphere radiance given by Labsphere.*

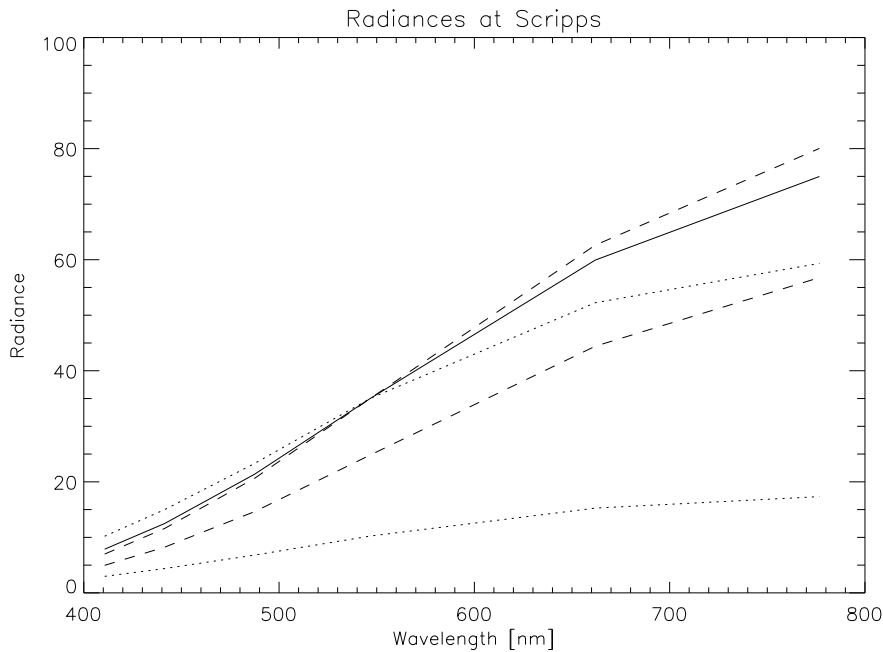


Figure 4.6: *SXR-II measured radiances of the Labsphere sphere at Scripps. Solid line: both lamps on. Lower dashed line: internal lamp on. Lower dotted line: external lamp on. The upper dashed (dotted) line shows the internal (external) lamp radiance normalized to the radiance at 547 nm of both lamps on. The normalized radiances show clearly the different spectral shape of external and internal lamp.*

Labsphere sphere on 5/1/01, external and internal lamp on

λ [nm]	L_m	L_e	Δ [%]
410.69	7.89844	7.8678	-0.4
441.51	(saturated)	12.5092	
487.58	21.3134	21.3994	0.4
546.89	34.8963	35.0522	0.4
661.91	59.4880	59.9351	0.8
776.71	74.4775	74.9899	0.7

Labsphere sphere on 5/2/01, external and internal lamp on

λ [nm]	L_m	L_e	Δ [%]	Stabil. [%]
410.69	7.94739	7.88117	-0.8	-0.6
441.51	(saturated)	12.5306		
487.58	21.3755	21.4362	0.3	-0.3
546.89	34.9642	35.1121	0.4	-0.2
661.91	59.5853	60.0374	0.8	-0.2
776.71	74.5247	75.1181	0.8	-0.1

Table 4.2: Radiances at Scripps. See Table 4.1 for explanation of symbols and abbreviations.

4.3.4 Biospherical

The expected radiances for the primary standard at Biospherical are less than 1% lower than the SXR-II measured radiances. The secondary standard is very close to the primary standard. Biospherical did not provide uncertainty estimates for its expected radiances.

4.3.5 UCSB

The staff of UCSB was very reluctant to provide an uncertainty estimate. They view their estimate of a 2 % uncertainty as an estimate with a very high level of uncertainty and question its usefulness. The primary standard at UCSB from NIST agrees very well with the SXR-II measurements. The expected radiances are 0.9 % (averaged over SXR-II channels 1 to 5) lower than the SXR-II radiances, see Fig. 4.8. The agreement deteriorates with increasing wavelengths.

Two secondary irradiance standards were measured at UCSB, F-305 and F-473. Their calibrations were transferred from the F-514 measurements with the UCSB MER-2078 during the SIMRIC-1. The differences between SXR-II measured radiances and expected radiances are spectrally very similar to the F-514 differences, see Fig. 4.8, the differences increase with wavelength. The differences for F-473 are about 0.5 % lower than for F-514, for F-305 they are about 0.2 % higher.

Although only wavelengths up to 683 nm are calibrated at UCSB (see section 3.2.4), we also calculated the expected radiances at 777 nm as well, extrapolating the plaque reflectance from 770 nm to higher wavelengths using the reflectance at 770 nm. For all three FELs, the expected radiances are about 4 % lower than the SXR-II radiances for channel 6 (777 nm), continuing the downward trend of Fig. 4.8. UCSB staff suspected stray light as a possible error source. As no calibrations for wavelengths above 700 nm are performed at UCSB, this discrepancy does not compromise the quality of the calibrations at UCSB.

4.3.6 HOBI Labs

The primary standards at HOBI Labs gave very different results. From Table 4.5 and Fig. 4.9, it can be seen that only lamp 7-1259 agrees well with the SXR-II measurements, lamps 7-1244 and 7-1339 are between 5 and 9 % too low. Because of these large differences, it was decided to have lamps 7-1244 and 7-1339 recalibrated by the manufacturer Oriel. Applying the new lamp calibrations and correcting for lamp drift, the differences for these two lamps reduce to between -0.5 % and -4.7 %, with a difference averaged over wavelength of -3.4 % for 7-1244 and -1.8 % for 7-1339. This shows that the previous calibration for these two lamps was at least 5 % too low. The differences calculated using the new calibrations are within the combined uncertainties. Note that the recalculation of the

FEL F-473, calibrated by NIST

λ [nm]	$L_m(5/3/01)$	L_e	$\Delta(5/3/01)[\%]$
410.7	0.024951	0.024822	-0.5
441.5	0.038349	0.038232	-0.3
487.6	0.062949	0.062936	-0.0
546.9	0.099351	0.099093	-0.3
661.9	0.165759	0.164498	-0.8
776.7	0.209427	0.207727	-0.8

FEL 91773, calibration transferred from F-473

λ [nm]	$L_m(5/4/01)$	L_e	$\Delta(5/4/01)[\%]$
410.7	0.021642	0.021590	-0.2
441.5	0.033389	0.033294	-0.3
487.6	0.055078	0.054990	-0.2
546.9	0.087437	0.087190	-0.3
661.9	0.147289	0.146209	-0.8
776.7	0.187334	0.184909	-1.3

SIMBIOS FEL F-474, calibrated by OL

λ [nm]	$L_m(5/3/01)$	L_e	$\Delta(5/3/01)[\%]$	$L_m(5/4/01)$	$\Delta(5/4/01)[\%]$	Stabil. [%]
410.69	0.020764	0.021128	1.8	0.020681	2.2	0.4
441.51	0.032272	0.032903	2.0	0.032203	2.2	0.2
487.58	0.053754	0.054999	2.3	0.053696	2.4	0.1
546.89	0.086264	0.088141	2.2	0.086262	2.2	0.0
661.91	0.147325	0.148808	1.0	0.147394	1.0	-0.0
776.71	0.188874	0.188324	-0.3	0.188994	-0.4	-0.1

Table 4.3: Radiances at Biospherical. See Table 4.1 for explanation of symbols and abbreviations.

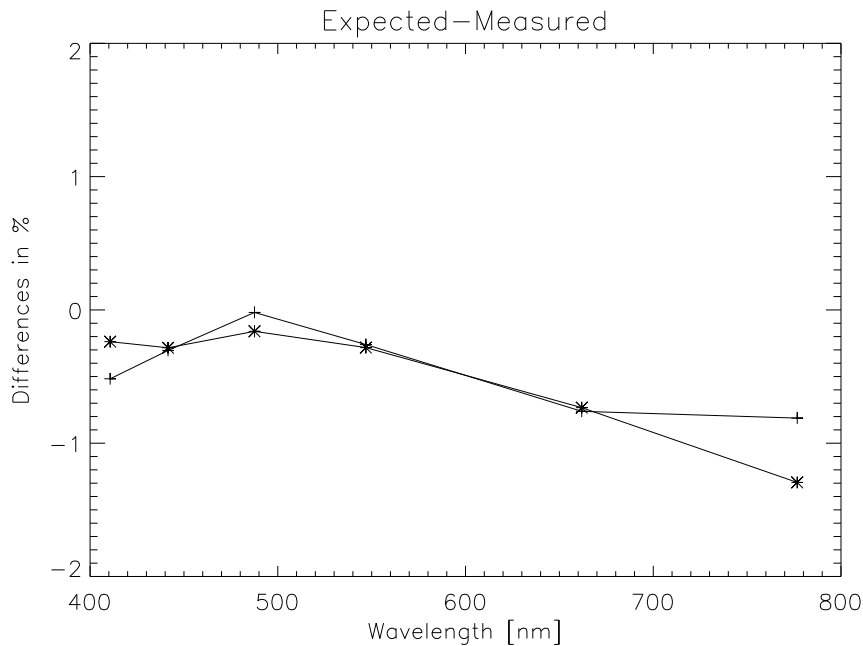


Figure 4.7: Difference of the expected radiance and the SXR-II measured radiance at Biospherical. +: FEL 473 (calibrated by OL), *: FEL 91773 (calibration transferred from FEL 473 using Biospherical radiometer).

FEL F-514, calibrated by NIST

λ [nm]	L_m	L_e	$\Delta(5/8/01)[\%]$
410.69	0.048875	0.0486742	-0.4
441.51	0.075850	0.075274	-0.8
487.58	0.125863	0.125061	-0.6
546.89	0.201227	0.199249	-1.0
661.91	0.342211	0.336407	-1.7
776.71	0.443566	0.424960	-4.2

FEL F-473, calibration transferred from FEL F-514

λ [nm]	$L_m(5/7/01)$	L_e	$\Delta(5/7/01)[\%]$	$L_m(5/8/01)$	$\Delta(5/8/01)[\%]$	Stabil. [%]
410.69	0.045710	0.0454243	-0.6	0.045786	-0.8	-0.2
441.51	0.071303	0.0705495	-1.1	0.071302	-1.1	0.0
487.58	0.118805	0.117750	-0.9	0.118785	-0.8	0.0
546.89	0.190680	0.188313	-1.2	0.190753	-1.3	0.0
661.91	0.325851	0.319402	-2.0	0.326263	-2.1	-0.1
776.71	0.424015	0.405968	-4.3	0.424212	-4.3	-0.0

FEL F-305, calibration transferred from FEL F-514

λ [nm]	$L_m(5/7/01)$	L_e	$\Delta(5/7/01)[\%]$	$L_m(5/8/01)$	$\Delta(5/8/01)[\%]$	Stabil. [%]
410.69	0.050367	0.0503774	0.0	0.050483	-0.2	-0.2
441.51	0.077666	0.0773179	-0.4	0.077725	-0.5	-0.1
487.58	0.127758	0.127239	-0.4	0.127826	-0.5	-0.1
546.89	0.202309	0.200748	-0.8	0.202471	-0.9	-0.1
661.91	0.339502	0.334519	-1.5	0.340016	-1.6	-0.2
776.71	0.437603	0.419382	-4.2	0.438044	-4.3	-0.1

SIMBIOS FEL F-474, calibrated by OL

λ [nm]	$L_m(5/7/01)$	L_e	$\Delta(5/7/01)[\%]$	$L_m(5/8/01)$	$\Delta(5/8/01)[\%]$	Stabil. [%]
410.69	0.044578	0.0452629	1.5	0.044502	1.7	0.2
441.51	0.069509	0.0703532	1.2	0.069353	1.4	0.2
487.58	0.115926	0.117585	1.4	0.115611	1.7	0.3
546.89	0.186261	0.188133	1.0	0.185723	1.3	0.3
661.91	0.318680	0.317654	-0.3	0.317808	-0.0	0.3
776.71	0.415740	0.401740	-3.4	0.414507	-3.1	0.3

Table 4.4: Radiances at UCSB. See Table 4.1 for explanation of symbols and abbreviations.

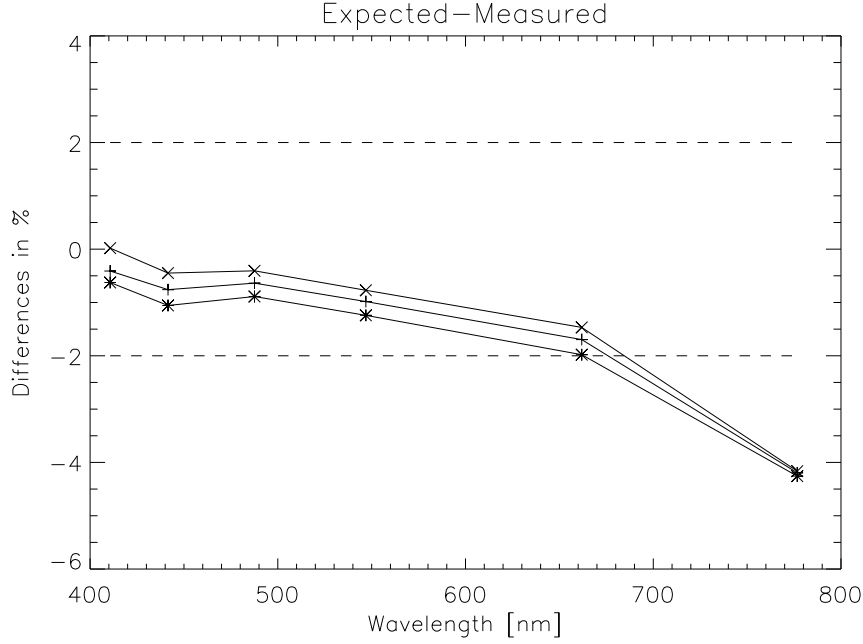


Figure 4.8: Difference of the expected radiance and the SXR-II measured radiance at UCSB. +: FEL 514, *: FEL 473, x: FEL 305, dashed line: UCSB estimated $k=1$ uncertainty.

differences involved the lamp drift tracked by the HOBI Labs transfer radiometer, whose uncertainty is estimated to be about 3 %.

4.3.7 NASA Code 920.1

For the first day of measurements, the expected radiances and the measured radiances agree very well within the combined uncertainties, see Fig. 4.10. The differences for channels 2 to 5 are less than 1 %. Although the difference at 411 nm is 3.8 %, this is almost in line with the estimated uncertainty for the Hardy sphere at that wavelength (2.9 %). This indicates a careful uncertainty estimation by NASA Code 920.1. However, such large uncertainties are problematic for the calibration of oceanographic radiometers (only atmospheric radiometers are calibrated at NASA Code 920.1).

The degradation of the SXR-II channel 1 discussed in section 2.3.2 has probably some effect on the comparisons at NASA Code 920.1. From Fig. 2.9 on page 14, we estimate that channel 1 has already degraded by about 0.5 % at the time of the Code 920.1 measurements. The uncertainty estimate of the SXR-II of 0.8 % may be too conservative for the channel 1 measurements at NASA Code 920.1.

At the second day, the differences of expected and measured radiances are very similar for SXR-II channels 1 to 3, see Table 4.6 or Fig. 4.10. But for SXR-II channels 5 and 6, the differences increase by more than 1 %. Another instrument is needed to decide whether the SXR-II or the NASA transfer radiometer OL 746 has shifted. Fortunately, there is an internal detector inside the Hardy sphere (see section 3.2.6). It can be seen from Table 4.7 that the differences between the two measurement days are consistent between OL 746 and internal monitor for the wavelengths 410 nm and 440 nm. But for wavelengths 640 nm and 840 nm the OL 746 is lower by 1.0 % at 640 nm and 1.1 % at 840 nm on the second day, whereas the Hardy internal monitor is about 0.25 % higher for those wavelengths on the second day. Thus there is an inconsistency between the internal monitor and the OL 746 of about 1.2 %, the same inconsistency as found between the SXR-II and the OL 746. Although the wavelengths are not exactly the same, the SXR-II and the internal monitor find very consistent changes from day 1 to day 2 at 410, 440, and 640 nm (compare the last columns of Tables 4.6 and 4.7).

Unfortunately, no hints were found during the processing of the OL 746 data which of the two measurements should be discarded. The comparison with the calibration of the SIMBIOS FEL 474 (see Table 4.6) shows better

Oriel 7-1259, calibrated by Oriel

λ [nm]	$L_m(5/10/01)$	L_e	$\Delta(5/10/01)[\%]$	$L_m(5/11/01)$	$\Delta(5/11/01)[\%]$	Stabil. [%]
410.69	0.244657	0.240436	-1.7	0.244847	-1.8	-0.1
441.51	0.367372	0.360538	-1.9	0.367287	-1.8	0.0
487.58	0.583896	0.576010	-1.4	0.583428	-1.3	0.1
546.89	0.890424	0.881427	-1.0	0.88962	-0.9	0.1
661.91	1.41032	1.40414	-0.4	1.41111	-0.5	-0.1
776.71	1.72435	1.70267	-1.3	1.72184	-1.1	0.1

Oriel 7-1244, calibrated by Oriel

λ [nm]	$L_m(5/10/01)$	L_e	$\Delta(5/10/01)[\%]$	$L_m(5/11/01)$	$\Delta(5/11/01)[\%]$	Stabil. [%]
410.69	0.227073	0.207305	-8.7	0.227169	-8.7	-0.0
441.51	0.343595	0.314702	-8.4	0.343385	-8.4	0.1
487.58	0.551177	0.510600	-7.4	0.549981	-7.2	0.2
546.89	0.847331	0.794032	-6.3	0.846088	-6.2	0.1
661.91	1.36143	1.29442	-4.9	1.36044	-4.9	0.1
776.71	1.68164	1.59457	-5.2	1.67638	-4.9	0.3

Oriel 7-1339, calibrated by Oriel

λ [nm]	$L_m(5/10/01)$	L_e	$\Delta(5/10/01)[\%]$	$L_m(5/11/01)$	$\Delta(5/11/01)[\%]$	Stabil. [%]
410.69	0.216811	0.19981	-7.8	0.217979	-8.3	-0.5
441.51	0.329436	0.303358	-7.9	0.330637	-8.3	-0.4
487.58	0.530119	0.492224	-7.1	0.531724	-7.4	-0.3
546.89	0.819264	0.765743	-6.5	0.820948	-6.7	-0.2
661.91	1.32666	1.25078	-5.7	1.33103	-6.0	-0.3
776.71	1.64932	1.54531	-6.3	1.65160	-6.4	-0.1

Table 4.5: Radiances at HOBI Labs. See Table 4.1 for explanation of symbols and abbreviations.

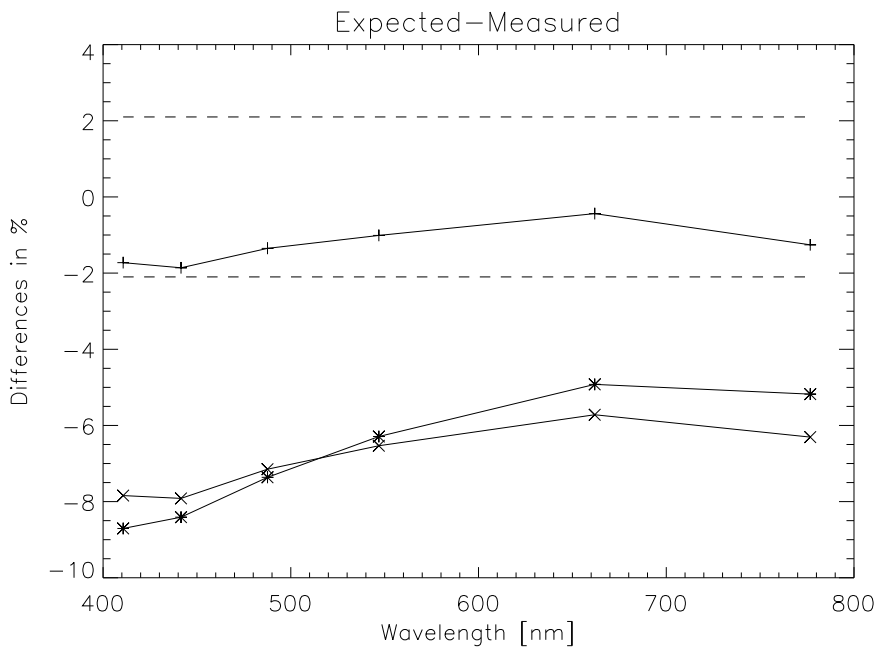


Figure 4.9: Difference of the expected radiance and the SXR-II measured radiance at HOBI Labs. +: ORIEL 7-1259, *: ORIEL 7-1244, x: ORIEL 7-1339. The dashed line shows the uncertainty estimate from HOBI Labs.

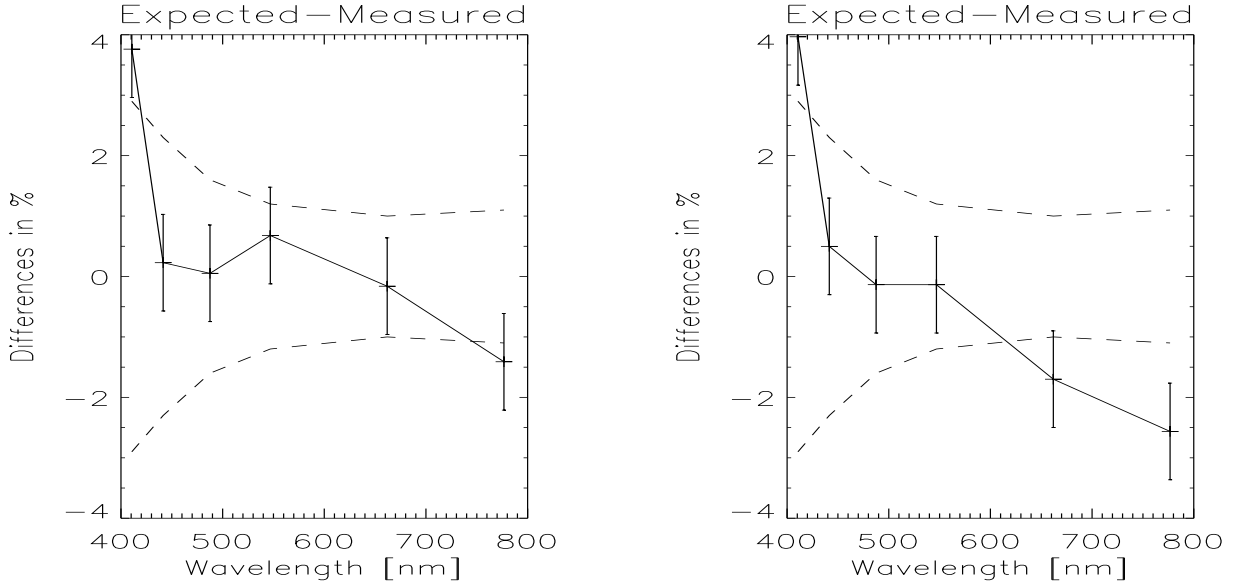


Figure 4.10: Difference of the expected radiance and the SXR-II measured radiance at NASA Code 920.1 on the first day of measurements (left plot) and on the second day (right plot). The vertical bars show the estimated SXR-II $k=1$ uncertainties. The dashed line shows the $k=1$ uncertainty for the sphere radiance provided by NASA Code 920.1.

Hardy Sphere, 6 lamps

λ [nm]	$L_m(6/18/1)$	$L_e(6/18/1)$	$\Delta(6/18/1)[\%]$	$L_m(6/19/1)$	$L_e(6/19/1)$	$\Delta(6/19/1)[\%]$	Stabil. [%]
410.69	3.73338	3.87384	3.8	3.76337	3.91264	4.0	-0.8
441.51	7.69026	7.70786	0.2	7.73149	7.77001	0.5	-0.5
487.58	15.0674	15.0753	0.1	15.0907	15.0703	0.1	-0.2
546.89	25.2058	25.3767	0.7	25.2542	25.2200	0.1	-0.2
661.91	40.6941	40.6287	-0.2	40.8343	40.1402	-1.7	-0.3
776.71	48.1221	47.4432	-1.4	48.1123	46.8788	-2.6	-0.0

Table 4.6: Radiances at NASA Code 920.1. See Table 4.1 for explanation of symbols and abbreviations.

agreement on the first day as well. Thus the main author of this study believes that the measurements of the OL 746 on the second day had shifted lower for certain wavelengths by about 1 %. As can be seen in Fig. 4.10, for channel 6 the difference is greater than the $k=1$ combined standard uncertainties. However, the results still agree within the $k=2$ combined standard uncertainties.

4.3.8 Satlantic

The comparison results (expected radiances minus measured radiances) for Satlantic are shown in Fig. 4.11. All three curves have a 'hook' at the left end of the spectrum. This confirms the drop in responsivity of the SXR-II channel 1 found with the SQM-II measurements, see section 2.3.2. If we would correct for this effect, the points at 411 nm in Fig. 4.11 would be 2 % lower, which would result in a difference almost continuously decreasing with increasing wavelength for all the standards measured at Satlantic.

The two primary standards calibrated by OL are both within the $k = 1$ combined standard uncertainties. But it can be seen that the two standards differ by about 2 %. A Satlantic radiometer, the OCR-200, measured the radiances right after the SXR-II. The same difference in radiances between the two standards was found when comparing the raw signals of the OCR-200 and the SXR-II, see forth and sixth column of Table 4.10. This difference was also found during measurements by Satlantic of the two standards prior to the SIMRIC-1.

The difference between expected and measured radiances for the NIST calibrated F-409 is a little higher than

Hardy Sphere, 6 lamps

λ [nm]	OL 746 [%]	FRMS during 746 mmt. [%]	FRMS during SXR-II mmt. [%]
410	-1.06	-1.40	-0.80
440	-0.94	-1.05	-0.52
640	0.96	-0.27	-0.19
840	1.09	-0.24	-0.44

Table 4.7: Stability of measured signals of NASA Code 920.1 instruments (transfer radiometer OL 746 and internal monitor FRMS), calculated as signal(6/18/01) minus signal(6/19/01).

SIMBIOS FEL F-474 measured by 746, calibrated by OL in 1997

λ [nm]	E_m (6/18/01)	E_e	Δ (6/18/01)[%]	E_m (6/19/01)	Δ (6/19/01)[%]	Stabil. [%]
400	1.9278	1.91	-0.93	1.871	2.04	3.04
450	3.9615	3.94	-0.55	3.862	1.98	2.58
500	6.6420	6.54	0.12	6.486	2.47	2.41
600	12.6202	12.7	0.63	12.417	2.23	1.64
700	17.5672	17.9	1.86	17.254	3.61	1.82
800	20.5651	21.0	2.07	20.173	3.94	1.94

Table 4.8: Irradiance of the SIMBIOS FEL F-474 for a distance of 50 cm, measured by the OL 746. Symbols and abbreviations are similar to Table 4.6, with radiance L replaced by irradiance E . Irradiance unit is $\mu\text{W}/(\text{cm}^2 \text{ nm})$. Expected irradiance E_e is from the OL 1997 calibration. Common wavelengths of OL calibration and 746 are shown.

for the OL standards, reaching up to 2.7 %. As this FEL had been calibrated in 1996, the validity of its calibration has expired since 1997. Still the difference is within the combined standard uncertainties.

All the results discussed so far refer to the first day of measurements. For the second day, there are several indications that the SXR-II was misaligned for several measurements, and that the FEL F-646 was unstable, see section 4.1. The SXR-II misalignment was discovered after comparing the results of the two days. The SXR-II was turned around its axis from the 12 o'clock position to the 1 o'clock position. Obviously one of the screws of the tripod holding the SXR-II had not been properly fastened. Unfortunately, it was not possible to determine which measurements of the second day were affected.

The voltage measured for the FEL F-646 had increased from its value on the previous day (115.2 Volts versus 114.5 Volts). The calibration protocols of Satlantic do not allow calibrations under these conditions. Because of the SXR-II misalignment and the F-646 instability, none of the measurements of the second day at Satlantic can be considered as reliable.

4.3.9 SIMBIOS FEL

This section compares the expected and the measured values for the SIMBIOS FEL F-474 measured at the respective laboratories. FEL F-474 was not shipped with the remaining SIMBIOS equipment, but carried in the hand luggage to avoid shocks during transport. F-474 was calibrated in 1997 by Optronics Laboratories. As the validity of the calibration has long expired, only the relative differences from one laboratory to another are discussed here. The interpolation from the OL calibration wavelengths to the SXR-II wavelengths was done by the main author of this report using the procedure described in [Walker et al., 1987], see section 4.5 below.

The relative differences (expected values minus measured values) for the F-474 are plotted in Fig. 4.12. Similar tendencies as for the differences of the laboratory-owned irradiance standards (see Figs. 4.2 and 4.3) can be seen: NRL, UCSB and Satlantic are similar in their spectral shape, Biospherical is about 1 % higher than the average of those three laboratories. This may indicate that the major source for the differences between the laboratories are not the calibrations of the lamps, but rather other sources (like e.g. plaque reflectance, effective distance correction, stray light). The results for UCSB show a similar difference at 777 nm as for their primary standard F-514, possibly caused by a stray light problem of the baffling material of the UCSB laboratory.

The F-474 could not be measured directly at NASA Code 920.1 with the SXR-II, thus in Fig. 4.12 the difference of irradiance of the OL calibration and the irradiance measured with the OL 746 are shown. These measurements show a different trend than the measurements of the three laboratories measured first (NRL, Biospherical, UCSB):

FEL F-646, calibrated by OL

λ [nm]	$L_m(9/5/01)$	L_e	$\Delta(9/5/01)[\%]$	$L_m(9/6/01)$	$\Delta(9/6/01)[\%]$	Stabil. [%]
410.69	(0.15278)	0.154099	(0.9)	(0.15455)	(-0.3)	-1.2
441.51	0.233175	0.233027	-0.1	0.235358	-1.0	-0.9
487.58	0.374515	0.374877	0.1	0.377994	-0.8	-0.9
546.89	0.574484	0.579800	1.0	0.579587	0.0	-0.9
661.91	0.927392	0.933789	0.7	0.934639	-0.1	-0.8
776.71	1.13476	1.15156	1.5	1.14309	0.7	-0.7

FEL F-662, calibrated by OL

λ [nm]	$L_m(9/5/01)$	L_e	$\Delta(9/5/01)[\%]$	$L_m(9/6/01)$	$\Delta(9/6/01)[\%]$	Stabil. [%]
410.69	(0.15274)	0.150779	(-1.3)	(0.15437)	(-2.3)	-1.1
441.51	0.233359	0.228620	-2.0	0.235314	-2.8	-0.8
487.58	0.375295	0.368087	-1.9	0.378654	-2.8	-0.9
546.89	0.576669	0.569951	-1.2	0.581694	-2.0	-0.9
661.91	0.933487	0.921780	-1.3	0.940821	-2.0	-0.8
776.71	1.14477	1.14111	-0.3	1.15660	-1.1	-0.8

FEL F-409, calibrated by NIST in 1996

λ [nm]	$L_m(9/5/01)$	L_e	$\Delta(9/5/01)[\%]$	$L_m(9/6/01)$	$\Delta(9/6/01)[\%]$	Stabil. [%]
410.69	(0.10037)	0.098678	(-1.7)	(0.10103)	(-2.3)	-0.7
441.51	0.158358	0.154160	-2.7	0.159083	-3.1	-0.5
487.58	0.265019	0.258689	-2.4	0.266210	-2.8	-0.4
546.89	0.424091	0.416265	-1.8	0.426083	-2.3	-0.5
661.91	0.726887	0.712348	-2.0	0.730191	-2.4	-0.5
776.71	0.925653	0.916354	-1.0	0.929704	-1.4	-0.4

SIMBIOS FEL F-474, calibrated by OL in 1997

λ [nm]	$L_m(9/5/01)$	L_e	$\Delta(9/5/01)[\%]$	$L_m(9/6/01)$	$\Delta(9/6/01)[\%]$	Stabil. [%]
410.69	(0.10510)	0.106340	(1.2)	(0.10511)	(1.2)	-0.0
441.51	0.165380	0.165843	0.3	0.165073	0.5	0.2
487.58	0.275759	0.277647	0.7	0.275212	0.9	0.2
546.89	0.439726	0.445320	1.3	0.438902	1.5	0.2
661.91	0.750018	0.753303	0.4	0.748303	0.7	0.2
776.71	0.951247	0.958767	0.8	0.948936	1.0	0.2

Table 4.9: Radiances at Satlantic. See Table 4.1 for explanation of symbols and abbreviations. The calibration of the SXR-II channel 1 (L_m at 410.69 nm) is unreliable due to suspected SXR-II instabilities (see section 2.3), thus the numbers are enclosed in brackets.

$\lambda(\text{OCR-200})$ [nm]	Stabil.(F-646) [%]	Stabil.(F-662) [%]	F-662 - F-646 [%]	$\lambda(\text{SXR-II})$	F-662 - F-646 [%]
399.8	-0.67	-0.10	-0.25	410.7	-0.02
490.8	-0.72	-0.02	0.13	487.6	0.21
590.2	-0.68	0.16	0.25	546.9	0.38
699.0	-0.61	0.11	0.11	661.9	0.65
780.0	-0.54	0.01	0.40	776.7	0.87

Table 4.10: Comparison of the Satlantic OCR-200 raw signals (background subtracted). The first column shows the center wavelengths of the OCR-200 channels. The second and third columns give the stability (signal(9/5/01) minus signal(9/6/01)) for the respective FEL, the forth column shows the difference between the OCR-200 signals for F-662 and F-646 on 9/5/01. The fifth column shows the wavelength of the closest SXR-II channel, the sixth column shows the difference of the SXR-II signals for F-662 and F-646 on 9/5/01.

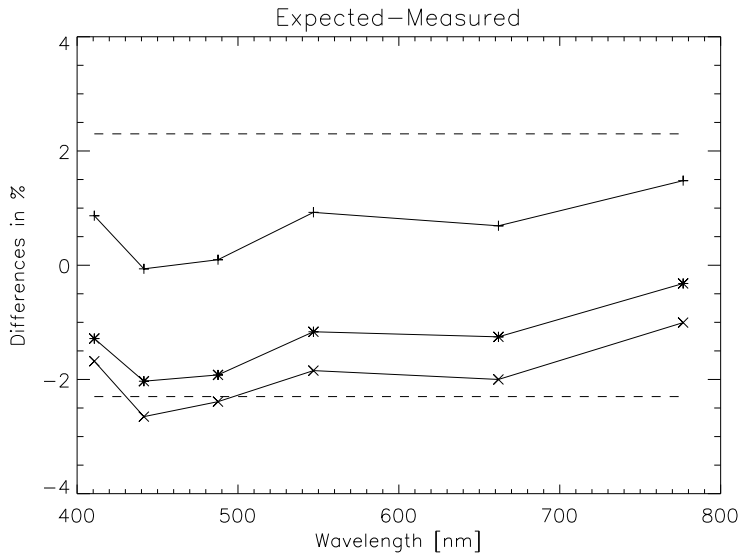


Figure 4.11: Difference of the expected radiance and the SXR-II measured radiance at Satlantic. +: FEL 646 (calibrated by OL), *: FEL 662 (calibrated by OL), x: FEL 409 (calibrated by NIST in 1997), dashed line: Satlantic $k=1$ uncertainty from [Hooker et al., 2002] (measured uncertainty).

whereas the differences for those laboratories decreases with wavelength from 490 to 777 nm, they increase for the OL 746, which was measured after the above laboratories. There is no spectral trend for the F-474 differences at Satlantic which was measured last.

4.4 Transfer from Primary to Secondary Standard

It is a common practice to transfer the irradiance scale from a primary standard to a secondary standard in order to minimize operating hours for the primary standard. If a secondary standard is used to calibrate radiometers, it is important to evaluate how well the transfer from the primary to the secondary standard was done. At Biospherical, one primary standard and one secondary standard were measured once each. If the transfer was perfect and the SXR-II measurements were exact, the differences between expected and SXR-II measured values would be the same for both primary and secondary standard. The difference between these differences is thus a measure of how well the calibration was transferred from the primary to the secondary standard. For Biospherical, the difference of the differences is 0.5 % or less (0.3 %, 0.0 %, -0.2 %, 0.0 %, 0.0 %, -0.5 % for channels 1 to 6, resp.); for NRL it is below 0.4 %; for UCSB it is below 0.4 % for FEL-305 and below 0.5 % for FEL-473. The intrinsic repeatability uncertainty for the SXR-II is 0.1 %, an estimated setup uncertainty of 0.3 % should be added quadratically. Thus it can be concluded that the calibration transfer from primary to secondary standard was done by these three laboratories with an accuracy of 0.5 % or better, which is highly satisfying.

4.5 Irradiance Interpolation

The calibration of the irradiance of the lamps is usually provided at discrete wavelengths. To obtain the irradiance at wavelengths in between the wavelengths where the calibration was done, the calibration data must be interpolated. There is a surprising variety in the methods used to interpolate the irradiance values. In [Walker et al., 1987], the NBS (now NIST) recommended to first fit

$$\ln(E_\lambda \cdot \lambda^5) = a + b/\lambda \quad (4.3)$$

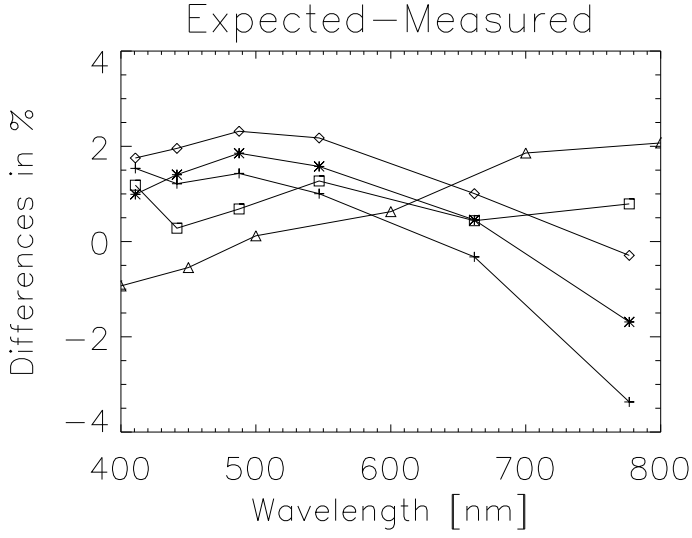


Figure 4.12: The differences of the expected radiances (using the OL calibration from September 1997) and the SXR-II measurements for the SIMBIOS FEL-474 of the respective laboratory. The symbols represent: stars - NRL, rhombs - Biospherical, triangles - GSFC, squares - Satlantic, plus signs - UCSB. Note that the GSFC measurements are not calculated from SXR-II measurements, but from 746 measurements.

where E_λ are the calibration irradiances at wavelength λ , and a and b are fitting coefficients. No weighting should be applied at this stage. After a and b have been determined, a polynomial of degree n is fitted:

$$E_\lambda = (A_0 + A_1 \cdot \lambda + \dots + A_n \cdot \lambda^n) \cdot \lambda^{-5} \cdot e^{a+b/\lambda} \quad (4.4)$$

using a weighting of $1/E_\lambda^2$. The spectral regions 250 nm to 400 nm and 350 nm to 1600 nm should be fitted separately. There is no indication in [Walker et al., 1987] on what degree should be chosen for the polynomial, a 5th order polynomial is most often used and was also chosen for this study (as in e.g. [Johnson et al., 1999]). For the wavelength range 400 to 800 nm, [Andor, 1998] reports excellent results using a 1st order polynomial. The uncertainty of values obtained for E_λ using eq. 4.4 is given in [Walker et al., 1987] as about 0.5 %, but there is no explanation whether this value must be combined with other measurement uncertainties, and if yes (which is likely) how to do this. In [Biggar, 1998], this uncertainty is added quadratically.

Figs. 4.13 to 4.15 compare the interpolations calculated by the main author of this study using the method of [Walker et al., 1987] with the interpolations calculated by those laboratories participating in the SIMRIC-1 that provided the original calibration reports for their FEL lamps (NRL, UCSB and HOBI Labs). It can be seen that usually the differences are about 0.6 % or less. Usually the laboratory interpolations are closer to the original calibration values than the interpolations with the [Walker et al., 1987] method. Although a unified approach to this important aspect of irradiance calibration interpretation is desirable, it is difficult to determine which approach is actually the best.

The polynomial correction is on the order of 2 %. This means that the irradiance of the lamps can be quite well described by a gray-body-like spectrum. [Huang et al., 2000] suggested to replace the polynomial by an empirical function that considers experimental findings on the lamp emissivity. This approach supposedly has the advantages of fewer fitting parameters, a single fit over the whole wavelength range, and a better quality of the fit (measured by the deviation of the fitted data from the input data).

4.6 BRF of Spectralon

Many Spectralon plaques used in this report (NRL, Biospherical, HOBI Labs) were calibrated by Labsphere in terms of directional-hemispherical reflectance at an 8° illumination zenith angle (symbol $R(8^\circ/h)$) in [Johnson et al., 1996],

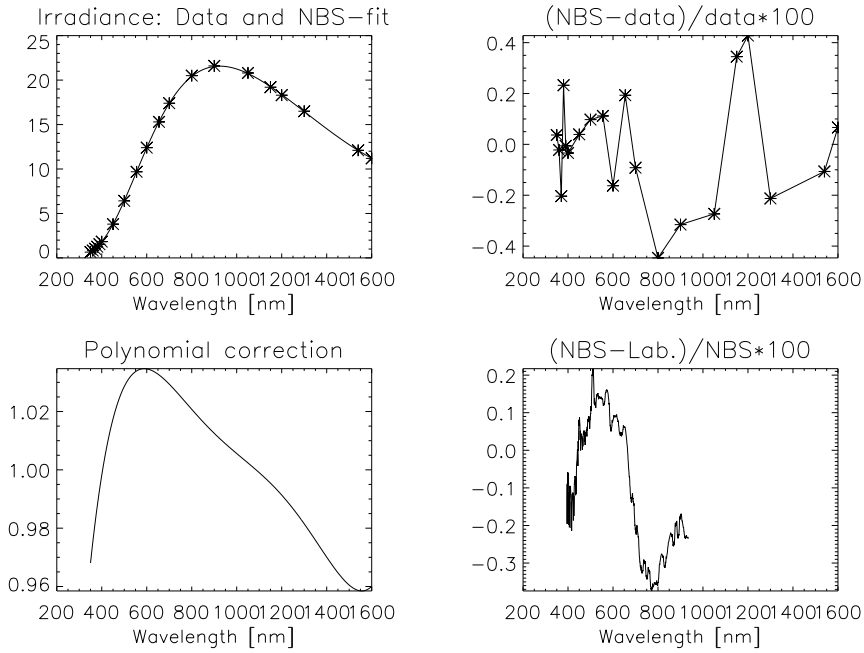


Figure 4.13: Irradiance interpolation comparison for F-400 from NRL. NRL uses Lagrange interpolation. The top left plot shows the calibration points as stars, the solid line is the fit with the NBS method, calculated by the main author of this study. The top right plot shows the differences in % for calibration points and the fitted curve as stars (solid line is for illustration purposes only). The lower left plot shows the polynomial fitted with the NBS method. The lower right plot shows the differences between the interpolated values calculated by the participating laboratories (in this case NRL) and the NBS method.

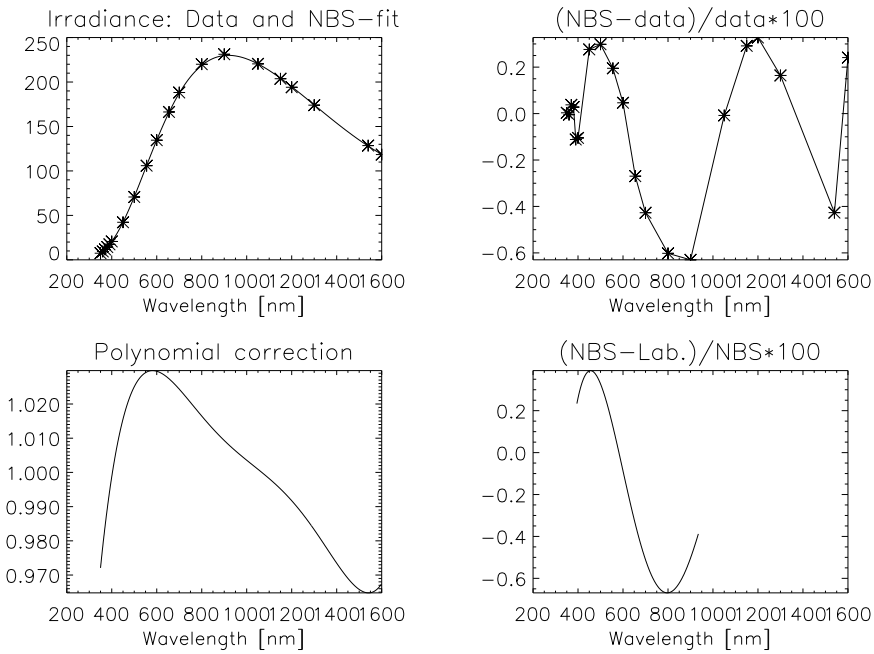


Figure 4.14: Irradiance interpolation comparison for F-514 from UCSB. UCSB uses Planck/polynomial-fitting with removal of outliers. See Fig. 4.13 for explanation of the plots.

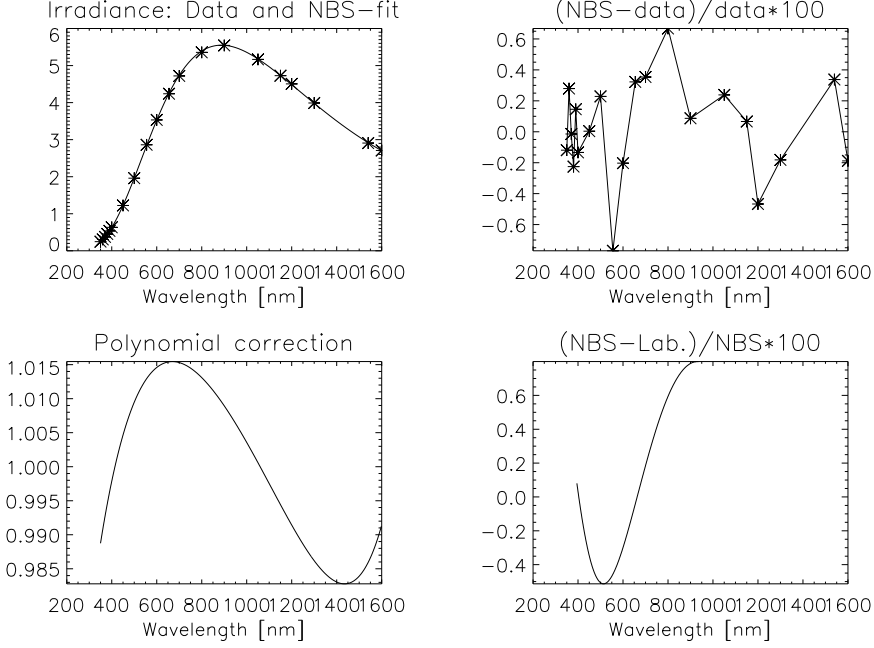


Figure 4.15: Irradiance interpolation comparison for 7-1259 from HOBI Labs. HOBI Labs uses ORIEL lamps (not FELs) and an ORIEL provided fitting function, that is similar to equation 4.4, but the polynomial is modified and there seems to be no separate fitting of the parameters a and b (eq. 4.3). See Fig. 4.13 for explanation of the plots.

symbol $\rho(\theta_i, \phi_i; 2\pi)$ in [Nicodemus et al., 1977] (Table 1 therein)). This quantity gives the ratio of the light reflected from the surface into any direction to the light incident from only one direction (in this case from 8°). However, the quantity needed to predict the reflected radiance for the geometrical setup in the laboratories is the bidirectional reflectance factor (BRF) for an incidence angle of 0° and a viewing angle of 45° (symbol $\rho(\theta_i, \phi_i; \theta_r, \phi_r)$ in [Nicodemus et al., 1977] (Table 2 therein), called directional/directional reflectance factor in [Johnson et al., 1996], with symbol $R(0^\circ/45^\circ)$). Labsphere refers to this quantity as $0^\circ/45^\circ$ spectral reflectance factor. Of the SIMRIC-1 participants, only UCSB and Satlantic have their plaque calibrated by Labsphere in terms of the BRF. In [Johnson et al., 1996], a conversion factor is presented to convert $R(8^\circ/h)$ to $R(0^\circ/45^\circ)$:

$$R(0^\circ/45^\circ) = 1.028 \cdot R(8^\circ/h) \quad (4.5)$$

This conversion factor should only be used if $R(0^\circ/45^\circ)$ cannot be determined reliably by other means. Although its order of magnitude is confirmed by the SIMRIC-1 measurements (see below), more research is needed to establish this relation on a firm basis. BRDF measurements of Spectralon reported in [Early et al., 2000] and [Johnson et al., 1999] (section 7.4.4 therein) agree well with the BRDF measurements of Spectralon in [Johnson et al., 1996], all of them showing a strong decrease of BRDF with increasing θ_v for $\theta_i = 0^\circ$.

The first confirmation for the necessity to use eq. 4.5 is that all the SXR-II measured values at NRL, Biospherical, and HOBI Labs' 7-1259 (these are all laboratories that use eq. 4.5) are higher than the predicted values from the primary standards, from 0 to up to 3 %. If eq. 4.5 is not used, the differences increase to between 3 and 6 %.

The second confirmation comes from the measurements of the NRL sphere. A monochromator first measured the FEL 400, and afterwards the sphere. The SXR-II measurements of the sphere are 1.4 to 2.4 % higher than the expected values. Note that the plaque is not involved in these measurements. The SXR-II measurements of the plaque illuminated by FEL F-400 are 1.1 to 3.1 % higher than the expected values. If eq. 4.5 is not used to calculate the expected values, the SXR-II measurements of the plaque are 3.9 to 5.9 % higher than the expected values. Thus using eq. 4.5 yields very consistent results, whereas not using eq. 4.5 would lead to strong inconsistencies.

In [Johnson et al., 1996], Spectralon reflectance factors are published for 0° illumination angle as a function of viewing angle θ_v . The reflectance factors at $\theta_v = 35^\circ$ are about 2 % higher than at $\theta_v = 45^\circ$. Accidentally, at HOBI Labs measurements with the SXR-II were taken at about $\theta_v = 35^\circ$ and $\theta_v = 45^\circ$ for the ORIEL lamp 7-1244. The

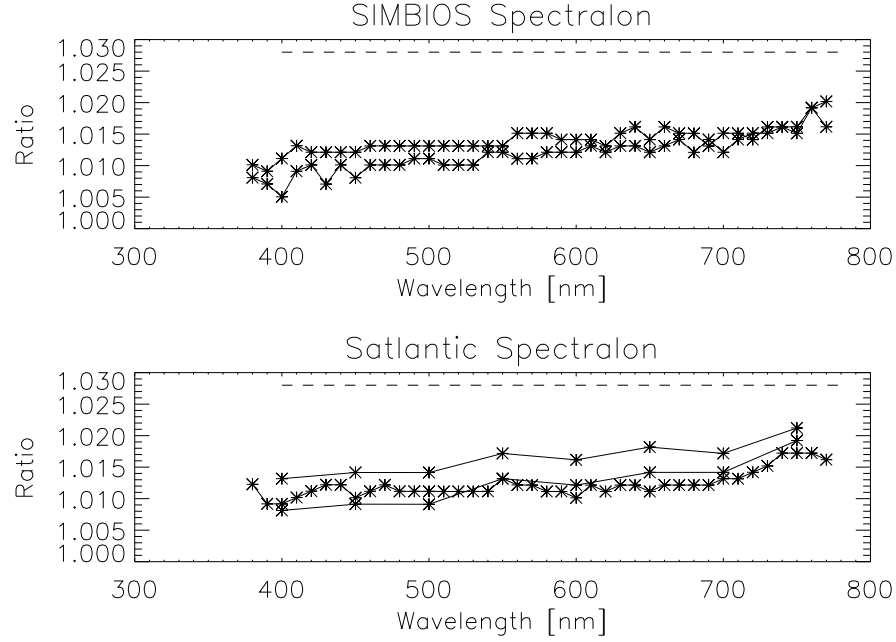


Figure 4.16: Ratios of the BRF $R(0^\circ/45^\circ)$ and the 8° /hemispherical Reflectance Factor from the Labsphere calibrations from August 2001 and September 2001 for the SIMBIOS Spectralon plaque (top). Both ratios increase with wavelength, the August ratio is about 0.002 higher than the September ratio. The lower plot shows the ratio for Spectralon plaques from Satlantic, calibrated by Labsphere in 1995, 1999 and 2001. They increase with wavelength as well, the magnitude of the ratios is also very similar to the SIMBIOS data. The data points are shown as stars, connected by lines.

measurements at the 6 wavelengths of the SXR-II at $\theta_v = 35^\circ$ are 2.1 to 2.3 % higher than at $\theta_v = 45^\circ$. This does not directly confirm eq. 4.5, but it agrees with the trends seen in the Spectralon plaques used in [Johnson et al., 1996].

It is very likely that eq. 4.5 contradicts calibrations performed by Labsphere. The SIMBIOS Project acquired a Spectralon plaque (SRT-99-120) from Labsphere and had it calibrated in August 2001, and again September 2001 after some minor defects from the surface had been removed. The calibrations were done for both the BRF $R(0^\circ/45^\circ)$ and the 8° /hemispherical Reflectance Factor. The ratio of these two quantities is shown in Fig. 4.16. It can be seen that the ratio is about 1.013, considerably less than the 1.028 from eq. 4.5. The lower plot in Fig. 4.16 shows the ratios for three Spectralon plaques of Satlantic, calibrated in 1995, 1999, and 2001, resp. The ratio of the Satlantic plaques is similar to the ratio of the SIMBIOS plaque. Both ratios increase with wavelength by about 1 % from 400 nm to 770 nm.

More research is necessary on the determination of the correct Bidirectional Reflectance Factors, especially on how to convert $R(8^\circ/\text{hemispherical})$ to $R(0^\circ/45^\circ)$. We do not discourage the usage of Spectralon plaques because of these problems. In effect, it is advantageous that only one kind of reflectance plaque is used, because this facilitates the investigation of improvements to the calibration protocols. We expect future editions of the Ocean Optics Protocols [Mueller and Fargion, 2002a] to address this issue.

4.7 Effective Distance Correction

Underwater radiometers are radiometrically very sensitive, thus the radiance reflected from a plaque illuminated by a 1000 W FEL at a distance of 50 cm is so bright that the radiance is much higher than the radiance levels at which the calibration is desired. This is a dilemma, because NIST calibrations are only valid for a distance of 50 cm and over an area 23 mm in diameter [Johnson et al., 1996]. Nonetheless, performing calibrations at distances greater than 50 cm is a common practice (e.g. in [Johnson et al., 1996], [Biggar, 1998]). Three of the SIMRIC-1 participants place the lamp at a distance greater than 50 cm from the plaque, 1.3 m at Satlantic, 2.952 m at Biospherical, and

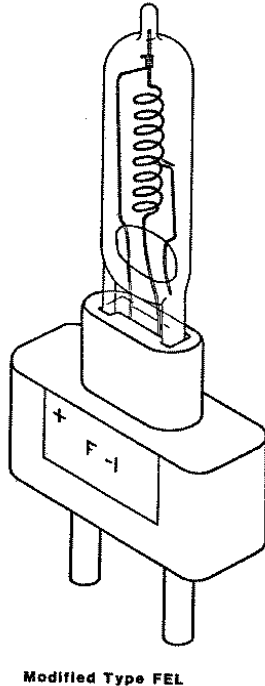


Figure 4.17: Sketch of a modified type bipost FEL lamp, taken from [Walker et al., 1987].

2 m at UCSB. The irradiances of the lamps are calibrated at a distance of 50 cm. The irradiance drops proportional to the inverse of the squared distance (d), thus the calibrated irradiance $E(d = 0.5m)$ must be scaled, e.g. at UCSB:

$$E(d = 2.0m) = \frac{(0.5m)^2}{(2.0m)^2} \cdot E(d = 0.5m) = 0.0625 \cdot E(d = 0.5m) \quad (4.6)$$

But during the calibration of the FEL lamp, the distance 50 cm was measured starting at the 'plane tangent to both posts' [Walker et al., 1987], not starting at the center of the lamp filament (see Fig. 4.17). The distance from the center of the lamp filament to the 'plane tangent to both posts' is 0.32 cm. Thus another way to do the scaling is given by [Biggar, 1998]:

$$E(d = 2.0032m) = \frac{(0.5032m)^2}{(2.0032m)^2} \cdot E(d = 0.5032m) = 0.0631005 \cdot E(d = 0.5m) \quad (4.7)$$

which gives a value for the scaled irradiance that is 0.95 % higher than the above value. This shows that it is clearly important whether this correction is used or not. There is disagreement in the scientific community whether this correction should be applied. None of the SIMRIC-1 participants uses this correction. Unpublished measurements at UCSB did not support the application of the correction. During [Johnson et al., 1999], the (original) SXR measured a plaque that was illuminated with distances between lamp and plaque of 150, 172 and 197 cm. These measurements do not support the application of the correction proposed by [Biggar, 1998], but the data do not show a clear pattern. Different reasons are cited for the failure of the correction, from straylight to the individual filament structure of each lamp. This suggests that it may be necessary for each laboratory to determine the needed correction for each bulb. But as the SIRREX 5 results show, the accuracy needed to perform these measurements may surpass the available capabilities. This is a severe problem, because NIST staff recommends to determine this correction for each individual bulb (Howard Yoon, pers. comm.).

For SIMRIC-1, predicted values using this correction would be in better agreement with the SXR-II measurements for UCSB and Satlantic laboratories (neither improvement nor deterioration for Biospherical). However, the combined uncertainties are too large to draw conclusions. The main author of this study believes that the

reasoning given in [Biggar, 1998] for applying the correction is sound and that the correction should be applied if no measurements are available that provide a better correction. This issue should be addressed in future editions of [Mueller and Fargion, 2002a].

A second point of concern with irradiance scaling is the spatial homogeneity of the illuminated plaque: the center of the plaque is expected to be brighter than points away from the center because the distance between plaque and FEL is shortest for the center of the plaque. This is not a problem for the SXR-II, because its FOV is quite small, thus the measured area on the plaque can be expected to be homogeneously illuminated. However, many underwater radiometers have a wide FOV. The problems associated with instrument shadow when installing the radiometer close to the plaque require the radiometer to be positioned a certain distance away from the plaque. This distance depends on the size of the radiometer. Large radiometers are used at NRL, Biospherical, UCSB, and Satlantic. The horizontal diameter of the area viewed by the radiometers is typically about 30 cm. In the case of UCSB (distance lamp-plaque of 2 m), irradiance scaling to a point 15 cm away from the center of the plaque leads to an irradiance value that is 0.6 % lower than at the center. Neither UCSB nor Biospherical correct for this decrease. NRL does correct for it when using the PHILLS radiometer, but its data could not be used for the SIMRIC-1, see section 3.2.1. Satlantic corrects for this effect. The effects of a nonhomogeneously illuminated plaque have not been investigated during the SIMRIC-1. This is a potential problem, because the SXR-II views an area with a horizontal diameter of only about 4.5 cm (vertical diameter: about 3 cm). Unfortunately, it seems unlikely that such investigations can be carried out in future SIMRICs, because thorough measurements of these effects are extremely time consuming. A small radiometer (that also has a small FOV) is used at HOBI Labs. This allows a small distance between plaque and radiometer. At a distance of 25 cm the viewed area has a horizontal diameter of about 2 cm.

Chapter 5

Conclusions

During the SIMRIC-1, the SXR-II measured the radiances produced for calibration purposes in seven different laboratories at six wavelengths from 411 nm to 777 nm. The differences between the SXR-II measured radiances and the radiances expected by the laboratories are typically about 2 %. As the k=1 uncertainties of the calibration radiances produced by the laboratories are typically about 2 % and the k=1 uncertainties of the SXR-II are about 0.8 %, the differences are well within the expected range. At HOBI Labs, two out of three irradiance standards were identified that showed differences of more than 5 %. These lamps were recalibrated by the manufacturer following the SIMRIC-1 measurements.

The measurements of the calibration radiances were repeated on the following day. On average, the SXR-II measured radiances on the second day differed from the first day by about 0.3 %. In two cases, larger variations from day to day were found, probably due to the transfer radiometer OL 746 at NASA Code 920.1 and lamp instabilities and SXR-II misalignments at Satlantic.

Many laboratories transfer the calibration from a primary standard to a secondary standard. The quality of the transfer was investigated at three laboratories (NRL, Biospherical, UCSB), with highly satisfying results (variations of less than 0.5 % were found). At Satlantic, only primary standards calibrated by Optronics Laboratories are used for calibration. Although this eliminates the uncertainty introduced by the calibration transfer, the variations between primary standards is surprisingly large (about 2 % for the two primary OL standards measured at Satlantic during the SIMRIC-1).

UCSB is the only laboratory that continually monitors the time series of the calibration coefficients of its transfer radiometer and has established a time record over several years. This is very beneficial in detecting lamp changes and adds a considerable amount of confidence to its calibration efforts. The SIMBIOS Project encourages all calibration laboratories to establish a similar time series if an appropriate radiometer is available.

The uncertainty introduced by the Labsphere Spectralon plaques is a difficult problem. The SIMBIOS Project suggests to include information on the handling of the plaque reflectance in all issued calibration reports. This would include the serial number of the plaque, the calibration date of the plaque reflectance, and information on the reflectance quantity used (in Labsphere's nomenclature: 0°/45° spectral reflectance factor, 0°/45° relative reflectance factor, 8°/hemispherical reflectance factor with or without using the SIRREX-4 conversion factor). Results from the SIMRIC-1 support the use of the SIRREX-4 conversion factor for converting 8°/hemispherical reflectance factors to 0°/45° spectral reflectance factors, but reflectance calibrations delivered by Labsphere suggest a conversion factor that is about 1 to 2 % smaller. Further research is necessary on this subject.

Furthermore, it would be useful to identify on each calibration report the NIST irradiance standard the calibration can ultimately be traced to. This information should include the number of the NIST FEL, its year of calibration and the year of the NIST irradiance scale. Also the FEL number and date of calibration of each secondary standard involved in the calibration chain should be documented.

The effective distance correction suggested by [Biggar, 1998] encounters considerable reluctance in the oceanographic community. None of the three laboratories that illuminate the plaque at a greater distance than the calibration distance of 50 cm employs this correction. The recommendation from NIST staff (Howard Yoon, personal communication) that each lab should determine the effective distance correction factor for their own lamps by themselves probably cannot be accomplished due to a lack of sufficiently precise equipment. More work is necessary to settle this issue.

NIST calibrates its irradiance standards only at certain wavelengths, thus an interpolation between these wavelengths is necessary to obtain the irradiance at the wavelength of the measurement channels of the radiometer. A variety of methods exists for this interpolation, with variations between these methods of up to 0.6 %. The uncertainty reported for the method of [Walker et al., 1987] is 0.5 %. This uncertainty could be reduced if the calibrations were provided with a better wavelength sampling, e.g. at 10 nm intervals.

The concept of monitoring the stability of the SXR-II channels with monthly measurements of the SQM-II was applied with success: the SXR-II/SQM-II measurements confirm the assumption that the change between the two SXR-II calibrations on SIRCUS from December 2000 and December 2001 evolved linearly to within ± 0.5 % for channels 2 to 6, a temporary degradation of channel 1 of about 2 % was detected. The degradation of the SXR-II channel 1 seems to be a continuous drift that started in April 2001 and ended in August 2001, not a single event due to shipping. We do not know how to prevent this drift. Thus for future round-robbins, further comparisons at NIST between the yearly calibrations on SIRCUS are planned. The responsivity of the SXR-II changed between 0.3 % (channel 6) and 1.6 % (channel 2) from December 2000 to December 2001.

Acknowledgments

The authors want to thank B. Carol Johnson, Steve Brown and Howard Yoon from the NIST, Gaithersburg, Maryland, and Christophe Pietras from the SIMBIOS Project for their support and advice. Also thanks to Jim Butler and Stan Hooker from NASA (Code 920.1 and Code 970.2, resp.) for several important comments. This work was funded by the SIMBIOS Project.

Appendix A

SXR-II FOV and SQM-II Footprint

The Field of View (FOV) of a radiometer determines the area from which light is collected. The FOV is often given as an angle, so that the viewed area can be easily calculated knowing the distance between radiometer and target, where it is usually assumed that the rays coincide inside the radiometer. A more exact method for presenting the FOV is as a spatial responsivity function $h(x, z)$ that gives the responsivity for certain coordinates (x, z) on the area perpendicular to the viewing direction. The center of the area is at a distance y from the radiometer. $h(x, z)$ of the original SXR was determined by [Johnson et al., 1998a] by varying the x and z coordinates of a point-like light source. Such a setup was not available at the SIMBIOS optical laboratory, thus a simpler (and less accurate) method was used: the SQM-II was used as a light source, but most of the light was blocked by a movable device except for a small square hole in the center. The x-coordinate of the small square was varied by pushing the device on a rail to the desired position (printed on the rail), the z-coordinate (height) was varied by adding or removing building blocks to the two supporting legs of the rail. Building blocks with a height of 0.97 cm were used, thus 0.97 cm was also chosen as sampling interval on the x-axis to obtain a symmetric sampling pattern. The edges of the square hole had a length of 0.97 cm as well.

Obviously this method needs a spatially homogeneous light field from the SQM-II. As this is not given (Satlantic measured variances of several % in the SQM footprint), the SQM-II footprint was measured as well, in order to correct the SXR-II FOV measurements. The same movable device was used as described above to block all the light except at the center of the device, but this time the x and z position of the SXR-II were moved synchronously with the x and z position of the center of the movable device. Thus the center of the movable device always stayed in the center of the FOV of the SXR-II. The SXR-II was moved manually as well, using a lab jack to obtain the needed height, and sliding the lab jack on aluminum plates to obtain the needed x position. Once the correct positions of light blocker and SXR-II were set, measurements were taken with the SXR-II. The whole procedure takes some time (75 minutes for the 55 measurements shown in Fig. A.1 and 70 minutes for the 46 measurement points shown in Fig. A.2) and should only be applied for determining the footprint of relatively small areas with low spatial resolution.

The SQM-II HiBank footprint was measured over an area of 9 cm width and 8 cm height (see Fig. A.1 for omitted positions). The SXR-II measured the SQM-II without the 9 cm aperture (i.e. the shadow collar of the SQM-II was removed). The intensity is highest in the center of the aperture. At a distance of 2 cm from the center, the intensity has dropped by about 2 %, at a distance of 4 cm from the center by about 5 %.

Fig.A.2 shows the SXR-II FOV. The SXR-II handle was on top (north position). Note the clockwise rotation of the maximum (except for channel 4) with increasing channel, probably due to the clockwise arrangement of channels inside the SXR-II. This clockwise rotation of the maximum can also be seen in the FOV measurements of the original SXR. However, the measurements of the FOV of the SXR-II show a much better radial symmetry than the measurements of the original SXR in [Johnson et al., 1998a].

Fig. A.3 (left plot) shows the responsivity per area as a function of distance d from the center. It was calculated by summarizing the measurements at distances from the center between $d - \Delta d$ and $d + \Delta d$ and dividing by the respective area $\pi \cdot (d + \Delta d)^2 - \pi \cdot (d - \Delta d)^2$. To obtain smooth curves, the measured values were interpolated from the measured 9.7 mm grid to a 1 mm grid. The responsivity drops to about 0.01 % at a distance of 4 cm from the center (relative to the maximum value at the center).

Neglecting contributions outside of a centered circular area with an 8 cm diameter and assuming that the

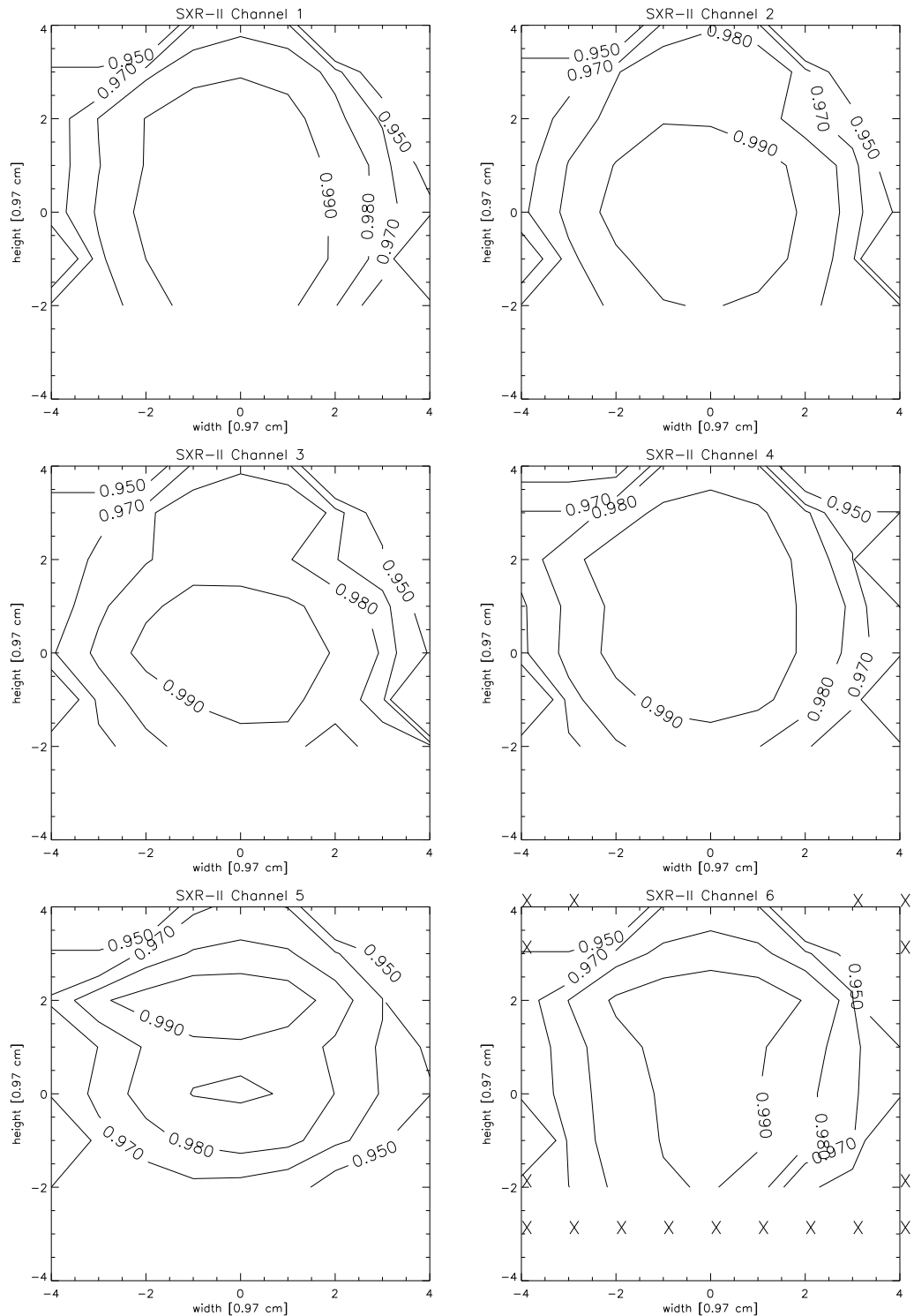


Figure A.1: Contour plots of the footprint of the SQM-II HiBank. The lower left corner of the crosses in the plot for channel 6 mark positions where no measurements were taken (for all channels). Shown are the SXR-II signals after background correction, normalized to the maximum value of each channel.

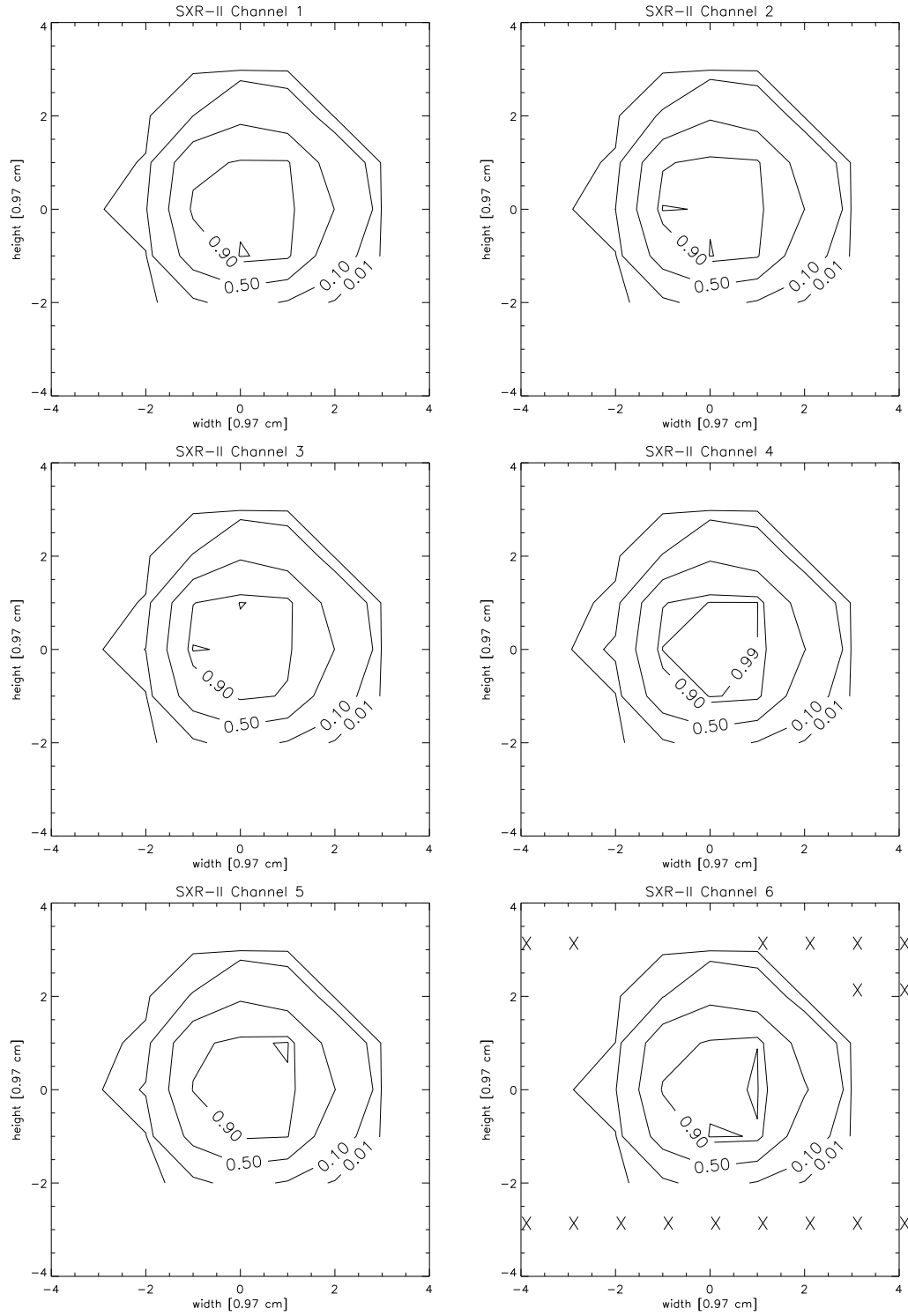


Figure A.2: Contour plots of the FOV of the SXR-II. The lower left corner of the crosses in the plot for channel 6 mark positions where no measurements were taken (for all channels). Shown are the ratios of the SXR-II FOV measurements and the SQM-II footprint measurements (Fig. A.1), normalized to the maximum value of each channel. Inside the 0.90 contour line the 0.99 contour line is shown. In case there are two 0.99 contour lines, it is likely that the actual maximum is in between the two contour lines, but was not directly measured due to the coarse spatial resolution of the measurements.

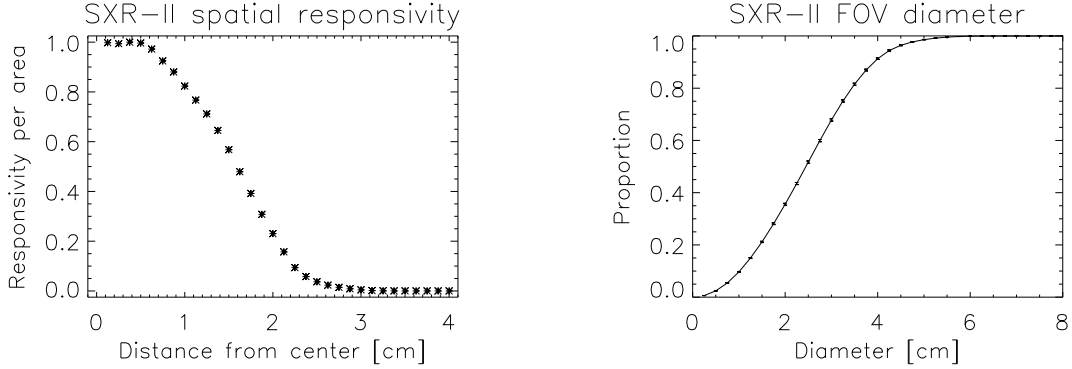


Figure A.3: Plot on the left: Responsivity of the SXR-II per area as a function of the distance from the center, normalized to the maximum value, averaged over all 6 channels. Note that the constant values from 0 to 0.5 cm may be an artifact of the spatial resolution of the measurements. Plot on the right: Size of the FOV of the SXR-II. The plot shows the signal produced by centered circular areas as a function of their diameter, normalized to the centered circular area with a diameter of 8 cm. These values were calculated by dividing the sum of the interpolated values inside the circle given from the respective diameter by the total sum and averaged over all 6 channels.

Channel	1	2	3	4	5	6
k_a (SXR)	0.9957	0.9985	0.9988	0.9976	0.9950	0.9899
k_a (SXR-II)	0.9975	0.9977	0.9971	0.9983	0.998200	0.9934
Δ [%]	0.2	-0.1	-0.2	0.1	0.3	0.4

Table A.1: Spatial correction factors k_a for the original SXR and for the SXR-II, both for measurements of the NASA Code 920.1 Hardy sphere. The difference Δ between the two is about 0.2 % averaged over all 6 channels.

illumination is spatially homogeneous, 91.3 % of the signal is produced from a centered circular area with a diameter of 4 cm, about 98.5 % of the signal is produced from a circular area with a diameter of 5 cm, and 99.9 % from a circular area with a diameter of 6 cm, see Fig. A.3 (right plot). This dependence is also called 'size-of-source' effect [Walker et al., 1987].

For SIMRIC-1, on-axis-cavity measurements are subtracted from the SXR-II signal measurements to account for this size-of-source effect, see section 3.3. In [Johnson et al., 1998a], correction factors k_a for the size-of-source effect for the original SXR (calculated from the measured spatial responsivity) are given for measurements at the GSFC Hardy sphere for two lens focal settings of the original SXR, 0.85 m and 1.13 m. Table A.1 reports these values averaged over the two settings. If no on-axis cavity measurements are available, the signal measurements should be multiplied by k_a . The on-axis-cavity measurements of SIMRIC-1 at the GSFC Hardy sphere with the SXR-II allow the calculation of this correction factor. They are shown in Table A.1 as well. It can be seen that the values are quite similar for both instruments.

Appendix B

SIMRIC-1 Participants

The SIMRIC-1 participants are listed below in alphabetical order:

Peter Abel, NASA Goddard Space Flight Center, Code 920.1
Greenbelt Rd, Greenbelt, MD 20771
Tel: 301 614 5943, peter.abel.1@gsfc.nasa.gov

Robert Barnes, SAIC / SIMBIOS, Goddard Space Flight Center, Code 970.1
Greenbelt Rd, Greenbelt, MD 20771
Tel: 301 286 0501, rbarnes@seawifs.gsfc.nasa.gov

John Cooper, Raytheon Information Technology and Science Services
NASA Goddard Space Flight Center Code 920.1
Greenbelt Rd, Greenbelt, MD 20771
Tel: 301 284 5949, john.w.cooper.1@gsfc.nasa.gov

Curtiss Davis, Naval Research Laboratory
Optical Sensing Section, Code 7212
4555 Overlook Avenue, SW, Washington, DC 20375
Tel: 202 767 9269, davis@rsd.nrl.navy.mil

Michael Godin, HOBI Labs
(Hydro-Optics, Biology & Instrumentation Laboratories)
P.O. Box 859
Moss Landing, CA 95039
Tel: 831 884 9409 x 12, Godin@hobilabs.com

David Goebel, Biospherical Instruments Inc.
5340 Riley St, San Diego, CA 92110
Tel: 619 686 1888 x 176, daveg@biospherical.com

Giulietta Fargion, SAIC / SIMBIOS, Goddard Space Flight Center Code 970.1
Greenbelt Rd, Greenbelt, MD 20771
Tel: 301 286 0744, gfargion@simbios.gsfc.nasa.gov

Robert Frouin, Scripps Institution of Oceanography
University of California, San Diego
8810 La Jolla Shores Drive, La Jolla, CA 92037
Tel: 858 534 6243, rfrouin@ucsd.edu

Daniel Korwan, Naval Research Laboratory
Optical Sensing Section, Code 7212
4555 Overlook Avenue, SW, Washington, DC 20375
Tel: 202 404 1391, korwan@poamc.nrl.navy.mil

Robert Maffione, HOBI Labs
(Hydro-Optics, Biology & Instrumentation Laboratories)
P.O. Box 859
Moss Landing, CA 95039
Tel: 831 684 2970, Maffione@hobilabs.com

Charles McClain, Office for Global Carbon Studies
NASA Goddard Space Flight Center Code 971
Greenbelt Rd, Greenbelt, MD 20771
Tel: 301 286 0758, chuck@seawifs.gsfc.nasa.gov

Scott McLean, Satlantic
Richmond Terminal, Pier 9, 3481 North Marginal Road
Halifax, Nova Scotia, Canada, B3K 5X8
Telephone: 902 492 4780, scott@satlantic.com

Gerhard Meister, Futuretech / SIMBIOS, Goddard Space Flight Center Code 970.1
Greenbelt Rd, Greenbelt, MD 20771
Tel: 301 286 0758, meister@simbios.gsfc.nasa.gov

David Menzies, The Institute for Computational Earth System Science (ICESS)
University of California at Santa Barbara (UCSB), Santa Barbara, CA 93106-3060
Tel: 805 893 8496, davem@ices.s.ucs.edu

Antoine Poteau, Scripps Institution of Oceanography
8810 La Jolla Shores Drive, La Jolla, CA 92037
Tel: 858 822 1416, poteau@genius.ucsd.edu

James Robertson, Biospherical Instruments Inc.
5340 Riley St, San Diego, CA 92110
Tel: 619 686 1888, robertson@biospherical.com

Jennifer Sherman, Satlantic
Richmond Terminal, Pier 9, 3481 North Marginal Road
Halifax, Nova Scotia, Canada, B3K 5X8
Telephone: 902 492 4780, jennifer@satlantic.com

Bibliography

- [Andor, 1998] Andor, G. (1998). Approximation of spectral irradiance of standard lamps. *Metrologia*, 35:427–429.
- [Barnes et al., 2001] Barnes, R., Clark, D., Esaias, W., Fargion, G., Feldman, G., and McClain, C. (2001). Development of a consistent multi-sensor global ocean color time series. In *Proceedings of the International Workshop on Geo-Spatial Knowledge Processing for Natural Resource Management*. Varese, Italy, University of Insubria.
- [Barnes et al., 1998] Barnes, W., Pagano, T., and Salomonson, V. (1998). Prelaunch characteristics of the moderate resolution imaging spectroradiometer (modis) on eos-am1. *IEEE Transactions on Geoscience and Remote Sensing*, 36(4):1088–1100.
- [Biggar, 1998] Biggar, S. (1998). Calibration of a visible and near-infrared portable transfer radiometer. *Metrologica*, 35:701–706.
- [Brown et al., 2000] Brown, S., Eppeldauer, G., and Lykke, K. (2000). Nist facility for spectral irradiance and radiance responsivity calibrations with uniform sources. *Metrologia*, 37:579–582.
- [Clark et al., 2002] Clark, D., Feinholz, M., Yarbrough, M., Johnson, B., Brown, S., Kim, Y., and Barnes, R. (2002). Overview of the radiometric calibration of moby. In *Proceedings of SPIE 4483*, pages 64–76.
- [DAAC, 2001] DAAC (2001). Pathfinder advanced very high resolution radiometer (avhrr) land (pal) data. http://daac.gsfc.nasa.gov/CAMPAIGN_DOCS/LAND_BIO/GLBDST_Data.html.
- [Early et al., 2000] Early, E., Barnes, P., Johnson, B., Butler, J., Bruegge, C., Biggar, S., Spyak, P., and Pavlov, M. (2000). Bidirectional reflectance round-robin in support of the earth observing system program. *American Meteorological Society*, pages 1077–1091.
- [Fargion and McClain, 2001] Fargion, G. and McClain, C., editors (2001). *SIMBIOS Project 2000 Annual Report*. NASA/TM-2001-209976. NASA, Goddard Space Flight Center, Greenbelt, Maryland 20771.
- [Fargion and McClain, 2002] Fargion, G. and McClain, C., editors (2002). *SIMBIOS Project 2001 Annual Report*. NASA/TM-2002-210005. NASA, Goddard Space Flight Center, Greenbelt, Maryland 20771.
- [Harrison et al., 2000] Harrison, N., Woolliams, E., and Fox, N. (2000). Evaluation of spectral irradiance transfer standards. *Metrologia*, 37:453–456.
- [Hooker, 2000] Hooker, S. (2000). Stability monitoring of field radiometers using portable sources. In Fargion, G. and Mueller, J., editors, *Ocean Optics Protocols for Satellite Ocean Color Sensor Validation, Revision 2*, NASA/TM-2000-209966. NASA, Goddard Space Flight Center, Greenbelt, Maryland 20771.
- [Hooker and Aiken, 1998] Hooker, S. and Aiken, J. (1998). Calibration evaluation and radiometric testing of field radiometers with the seawifs quality monitor (sqm). *Journal of Atmospheric and Oceanic Technology*, 15:995–1007.
- [Hooker et al., 2002] Hooker, S., Zibordi, G., McLean, S., Sherman, J., Small, Lazin, G., and Brown, J. (2002). The seventh seawifs intercalibration round-robin experiment (sirrex-7), march 1999. In Hooker, S. and Firestone, E., editors, *SeaWiFS Postlaunch Technical Report Series*, volume 17 of *NASA Technical Memorandum 206892*. NASA, Goddard Space Flight Center, Greenbelt, Maryland 20771.

- [Huang et al., 2000] Huang, L., Cebula, R., and Hilsenrath, E. (2000). New procedure for interpolating nist fel lamp irradiances. *American Meteorological Society*, pages 1077–1091.
- [Johnson et al., 2000] Johnson, B., Brown, S., and Yoon, H. (2000). Radiometric calibration history of visible and near-infrared portable radiometers. *Metrologia*, 37:423–426.
- [Johnson et al., 1996] Johnson, B., Bruce, S., Early, E., Houston, J., O'Brian, T., Thompson, A., Hooker, S., and J.L.Mueller (1996). The forth seawifs intercalibration round-robin experiment (sirrex-4), may 1995. In Hooker, S. and Firestone, E., editors, *SeaWiFS Technical Report Series*, volume 37 of *NASA Technical Memorandum 104566*. NASA, Goddard Space Flight Center, Greenbelt, Maryland 20771.
- [Johnson et al., 1998a] Johnson, B., Fowler, J., and Cromer, C. (1998a). The seawifs transfer radiometer (sxr). In Hooker, S. and Firestone, E., editors, *SeaWiFS Postlaunch Technical Report Series*, volume 1 of *NASA Technical Memorandum 1998-206892*. NASA, Goddard Space Flight Center, Greenbelt, Maryland 20771.
- [Johnson et al., 1998b] Johnson, B., Shaw, P.-S., Hooker, S., and Lynch, D. (1998b). Radiometric and engineering performance of the seawifs quality monitor (sqm): A portable light source for field radiometers. *Journal of Atmospheric and Oceanic Technology*, 15:1008–1022.
- [Johnson et al., 1999] Johnson, B., Yoon, H., Bruce, S., Shaw, P.-S., Thompson, A., Hooker, S., Barnes, R., R.E.Eplee, J., Maritorena, S., and J.L.Mueller (1999). The fifth seawifs intercalibration round-robin experiment (sirrex-5), march 1999. In Hooker, S. and Firestone, E., editors, *SeaWiFS Postlaunch Technical Report Series*, volume 7 of *NASA Technical Memorandum 206892*. NASA, Goddard Space Flight Center, Greenbelt, Maryland 20771.
- [Markham et al., 1998] Markham, B., Schafer, J., Jr, F. W., Dabney, P., and Barker, J. (1998). Monitoring large aperture spherical integrating sphere sources with a portable radiometer during satellite instrument calibration. *Metrologia*, 35:643–648.
- [McClain and Fargion, 1999a] McClain, C. and Fargion, G., editors (1999a). *SIMBIOS Project 1998 Annual Report*. NASA/TM-1999-208645. NASA, Goddard Space Flight Center, Greenbelt, Maryland 20771.
- [McClain and Fargion, 1999b] McClain, C. and Fargion, G., editors (1999b). *SIMBIOS Project 1999 Annual Report*. NASA/TM-1999-209486. NASA, Goddard Space Flight Center, Greenbelt, Maryland 20771.
- [Mueller, 1992] Mueller, J. (1992). The first seawifs intercalibration round-robin experiment (sirrex-1), july 1992. In Hooker, S. and Firestone, E., editors, *SeaWiFS Technical Report Series*, volume 14 of *NASA Technical Memorandum 104566*. NASA, Goddard Space Flight Center, Greenbelt, Maryland 20771.
- [Mueller, 2000] Mueller, J. (2000). Instrument performance specifications. In Fargion, G. and Mueller, J., editors, *Ocean Optics Protocols for Satellite Ocean Color Sensor Validation, Revision 2*, NASA/TM-2000-209966. NASA, Goddard Space Flight Center, Greenbelt, Maryland 20771.
- [Mueller and Fargion, 2002a] Mueller, J. and Fargion, G., editors (2002a). *Ocean Optics Protocols For Satellite Ocean Color Sensor Validation, Revision 3, Part I*. NASA/TM-2002-210004/Rev3-Vol1. NASA, Goddard Space Flight Center, Greenbelt, Maryland 20771.
- [Mueller and Fargion, 2002b] Mueller, J. and Fargion, G., editors (2002b). *Ocean Optics Protocols For Satellite Ocean Color Sensor Validation, Revision 3, Part II*. NASA/TM-2002-210004/Rev3-Vol1. NASA, Goddard Space Flight Center, Greenbelt, Maryland 20771.
- [Mueller et al., 1993] Mueller, J., Johnson, B., Cromer, C., Cooper, J., McLean, J., Hooker, S., and Westphal, T. (1993). The second seawifs intercalibration round-robin experiment (sirrex-2), june 1993. In Hooker, S. and Firestone, E., editors, *SeaWiFS Technical Report Series*, volume 16 of *NASA Technical Memorandum 104566*. NASA, Goddard Space Flight Center, Greenbelt, Maryland 20771.
- [Mueller et al., 1996] Mueller, J., Johnson, B., Cromer, C., Hooker, S., McLean, J., and Biggar, S. (1996). The third seawifs intercalibration round-robin experiment (sirrex-3), september 1994. In Hooker, S. and Firestone, E., editors, *SeaWiFS Technical Report Series*, volume 34 of *NASA Technical Memorandum 104566*. NASA, Goddard Space Flight Center, Greenbelt, Maryland 20771.

[NASA-Code-920.1, 2001] NASA-Code-920.1 (2001). Procedures for radiance calibration of a radiometric source. <http://spectral/docs/proc/radcalprocs.pdf>.

[Nicodemus et al., 1977] Nicodemus, F., Richmond, J., Hsia, J., , Ginsberg, I., and Lamperis, T. (1977). Geometric considerations and nomenclature for reflectance. Monogram 160:52, US Department of Commerce, National Bureau of Standards.

[O'Brien et al., 2000] O'Brien, M., Menzies, D., Siegel, D., and Smith, R. (2000). Seawifs postlaunch technical report series. In Hooker, S. and Firestone, E., editors, *SeaWiFS Postlaunch Calibration and Validation Analyses, Part 3*, volume 11 of *NASA/TM-2000-206892*, chapter 4. NASA, Goddard Space Flight Center, Greenbelt, Maryland 20771.

[Riley and Bailey, 1998] Riley, T. and Bailey, S. (1998). The sixth seawifs/simbios intercalibration round-robin experiment (sirrex-6), august-december 1997. In Hooker, S. and Firestone, E., editors, *SeaWiFS Technical Report Series*, NASA Technical Memorandum 1998-206878. NASA, Goddard Space Flight Center, Greenbelt, Maryland 20771.

[Stock et al., 2000] Stock, K., Raatz, H.-H., Sperfeld, P., Metzdorf, J., Kuebarsepp, T., Kaerhae, P., Ikonen, E., and Liedquist, L. (2000). Detector-stabilized fel lamps as transfer standards in an international comparison of spectral irradiance. *Metrologia*, 37:441–444.

[Walker et al., 1987] Walker, J., Saunders, R., Jackson, J., and McSparron, D. (1987). Spectral irradiance calibration. In Hooker, S. and Firestone, E., editors, *NBS Special Publication*, volume 250-20 of *NBS Measurement Services*. US Department of Commerce, National Bureau of Standards, Gaithersburg, Maryland 20899.

[Werdell et al., 2000] Werdell, P., Bailey, S., and Fargion, G. (2000). Seabass, data protocols and policy. In Fargion, G. and Mueller, J., editors, *Ocean Optics Protocols for Satellite Ocean Color Sensor Validation, Revision 2*, NASA/TM-2000-209966. NASA, Goddard Space Flight Center, Greenbelt, Maryland 20771.

[Yoon et al., 2002] Yoon, H., Gibson, C., and Barnes, P. (2002). The realization of the nist detector-based spectral irradiance scale. *Applied Optics*, submitted.

REPORT DOCUMENTATION PAGE			Form Approved OMB No. 0704-0188
<p>Public reporting burden for this collection of information is estimated to average 1 hour per response, including the time for reviewing instructions, searching existing data sources, gathering and maintaining the data needed, and completing and reviewing the collection of information. Send comments regarding this burden estimate or any other aspect of this collection of information, including suggestions for reducing this burden, to Washington Headquarters Services, Directorate for Information Operations and Reports, 1215 Jefferson Davis Highway, Suite 1204, Arlington, VA 22202-4302, and to the Office of Management and Budget, Paperwork Reduction Project (0704-0188), Washington, DC 20503.</p>			
1. AGENCY USE ONLY (Leave blank)	2. REPORT DATE	3. REPORT TYPE AND DATES COVERED	
	March 2002	Technical Memorandum	
4. TITLE AND SUBTITLE		5. FUNDING NUMBERS	
The First SIMBIOS Radiometric Intercomparison (SIMRIC-1), April–September 2001		970	
6. AUTHOR(S)		8. PERFORMING ORGANIZATION REPORT NUMBER	
Gerhard Meister, Peter Abel, Charles McClain, Robert Barnes, Giulietta Fargion, John Cooper, Curtiss Davis, Daniel Korwan, Mike Godin, Robert Maffione, David Goebel, James Robertson, Robert Frouin, Antoine Poteau, Scott McLean, Jennifer Sherman, and David Menzies		2002-01353-0	
7. PERFORMING ORGANIZATION NAME(S) AND ADDRESS (ES)		10. SPONSORING / MONITORING AGENCY REPORT NUMBER	
Laboratory for Hydrospheric Processes Goddard Space Flight Center Greenbelt, Maryland 20771		TM—2002–210006	
9. SPONSORING / MONITORING AGENCY NAME(S) AND ADDRESS (ES)		11. SUPPLEMENTARY NOTES	
National Aeronautics and Space Administration Washington, DC 20546-0001		G. Meister, Futuretech Corp., Greenbelt, Md; R. Barnes, G. Fargion, SAIC, Greenbelt, Md; J. Cooper, Raytheon Information Tech. and Science Serv., Lanham, Md; C. Davis, D. Korwan, Naval Res. Lab., Wash., D.C.; M. Godin, R. Maffione, HOBI Labs, Watsonville, Calif; D. Goebel, J. Robertson, Biospherical Instr. Inc., San Diego, Calif; R. Frouin, A. Poteau, Scripps Inst. of Oceanography, Univ. of California, San Diego, Calif; S. McLean, J. Sherman, Satlantic Inc., Halifax, Canada; D. Menzies, Inst. for Computational Earth System Science, Univ. of California, Santa Barbara, Calif.	
12a. DISTRIBUTION / AVAILABILITY STATEMENT		12b. DISTRIBUTION CODE	
Unclassified–Unlimited Subject Category: 48 Report available from the NASA Center for AeroSpace Information, 7121 Standard Drive, Hanover, MD 21076-1320. (301) 621-0390.			
13. ABSTRACT (Maximum 200 words)			
<p>This report describes the first SIMBIOS (Sensor Intercomparison and Merger for Biological and Interdisciplinary Oceanic Studies) Radiometric Intercomparison (SIMRIC-1). The purpose of the SIMRIC-1 is to ensure a common radiometric scale of the calibration facilities that are engaged in calibrating in situ radiometers used for ocean color related research and to document the calibration procedures and protocols. SIMBIOS staff visited the seven participating laboratories for at least two days each. The SeaWiFS Transfer Radiometer SXR-II measured the calibration radiances produced in the laboratories. The measured radiances were compared with the radiances expected by the laboratories. Typically, the measured radiances were higher than the expected radiances by 0 to 2%. This level of agreement is satisfactory. Several issues were identified, where the calibration protocols need to be improved, especially the reflectance calibration of the reference plaques and the distance correction when using the irradiance standards at distances greater than the 50 cm. The responsivity of the SXR-II changed between 0.3% (channel 6) and 1.6% (channel 2) from December 2000 to December 2001. Monitoring the SXR-II with a portable light source showed a linear drift of the calibration, except for channel 1, where a 2% drop occurred in summer.</p>			
14. SUBJECT TERMS		15. NUMBER OF PAGES	
SIMBIOS, oceanography, intercalibration, round-robin, SIMRIC, plaque reflectance, irradiance standards, spectral radiance, sphere sources, radiometric calibration, radiometric stability.		60	
16. PRICE CODE			
17. SECURITY CLASSIFICATION OF REPORT	18. SECURITY CLASSIFICATION OF THIS PAGE	19. SECURITY CLASSIFICATION OF ABSTRACT	20. LIMITATION OF ABSTRACT
Unclassified	Unclassified	Unclassified	UL